National Library of Canada
Bibliothèque nationale du Canada

Canadian Theses Service
Service des thèses canadiennes

Ottawa, Canada
K1A 0N4

NOTICE

The quality of this microform is heavily dependent upon the quality of the original thesis submitted for microfilming. Every effort has been made to ensure the highest quality of reproduction possible.

If pages are missing, contact the university which granted the degree.

Some pages may have indistinct print especially if the original pages were typed with a poor typewriter ribbon or if the university sent us an inferior photocopy.

Reproduction in full or in part of this microform is governed by the Canadian Copyright Act, R.S.C. 1970, c. C-30, and subsequent amendments.

AVIS

La qualité de cette microforme dépend grandement de la qualité de la thèse soumise au microfilmage. Nous avons tout fait pour assurer une qualité supérieure de reproduction.

S'il manque des pages, veuillez communiquer avec l'université qui a conféré le grade.

La qualité d'impression de certaines pages peut laisser à désirer, surtout si les pages originales ont été dactylographiées à l'aide d'un ruban usé ou si l'université nous a fait parvenir une photocopie de qualité inférieure.

La reproduction, même partielle, de cette microforme est soumise à la Loi canadienne sur le droit d'auteur, SRC 1970, c. C-30, et ses amendements subséquents.

NL-339 (r. 88/04) c

Canada

Analysis of Semiconductor Laser Nonlinearity

by

Tapan K. Biswas, B.Sc.Eng.

A thesis submitted to the
School of Graduate Studies and Research
in partial fulfillment of the requirements
for the degree

Master of Applied Science

Ottawa-Carleton Institute for Electrical Engineering
Department of Electrical Engineering
Faculty of Engineering
University of Ottawa
April 1991

© Tapan Kanti Biswas, Ottawa, Canada, 1991

National Library of Canada
Bibliothèque nationale du Canada

Canadian Theses Service
Service des thèses canadiennes

Ottawa, Canada
K1A 0N4

The author has granted an irrevocable non-exclusive licence allowing the National Library of Canada to reproduce, loan, distribute or sell copies of his/her thesis by any means and in any form or format, making this thesis available to interested persons.

The author retains ownership of the copyright in his/her thesis. Neither the thesis nor substantial extracts from it may be printed or otherwise reproduced without his/her permission.

L'auteur a accordé une licence irrévocable et non exclusive permettant à la Bibliothèque nationale du Canada de reproduire, prêter, distribuer ou vendre des copies de sa thèse de quelque manière et sous quelque forme que ce soit pour mettre des exemplaires de cette thèse à la disposition des personnes intéressées.

L'auteur conserve la propriété du droit d'auteur qui protège sa thèse. Ni la thèse ni des extraits substantiels de celle-ci ne doivent être imprimés ou autrement reproduits sans son autorisation.

ISBN 0-315-68015-6

Canada

UNIVERSITÉ D'OTTAWA
UNIVERSITY OF OTTAWA

Abstract

Semiconductor lasers are the main sources of light in fiber optic transmissions. They have a very wide bandwidth which makes them very attractive as components in broadband communication systems. This wide bandwidth permits subcarrier multiplexing to be used which is attractive for multichannel(TV) distribution on fibers. However, nonlinearities of the laser introduce distortion in the optical output which considerably degrades the system performance especially in the case of analog signal transmission. In this thesis a theoretical model of laser nonlinearity is analysed and the intermodulation noise is calculated. The large-signal-model of the laser rate equations is used in the analysis. An output-to-input approach is used to obtain a general system equation for the laser and then Volterra series expansion is applied to the system equation to obtain system transfer functions. First, the nth-order Volterra transfer functions, $G_n(\omega_1, ..., \omega_n)$, from output to input are calculated. Then, based on harmonic balance the forward Volterra transfer functions, $F_n(\omega_1, ..., \omega_n)$, are calculated from $G_n(\omega_1, ..., \omega_n)$, and these $F_n(\omega_1, ..., \omega_n)$, are used to model the frequency dependent form input-to-output nonlinearities of the laser. The theoretical models for second harmonic($2HD$), third harmonic ($3HD$) and third-order intermodulation(IMD) distortions are expressed in terms of signal frequency, optical modulation depth and laser parameters. Using the Mircea-Sinnreich equations, intermodulation spectra are computed. Harmonic distortions and third-order intermodulation distortion for various carrier (C) levels have been computed and variations of $2HD/C$, $3HD/C$ and IMD/C with frequency and D.C. bias are shown graphically. This system analysis are compared with previously published [15], [16], [17] results and experiments and a good agreement is found.

0.1 Acknowledgement

I would like to express my sincere appreciation to my thesis supervisor Dr. W.F.McGee, who first directed me to the field of fiber-optic communication. I am very thankful to him for his guidance and encouragement during the preparation of this thesis and for the time he spent in correcting the thesis.

I respectfully remember my late father S. K. Biswas who passed away immediately after I left my country for Canada. With his memory in my mind I thank all of my family members for their patience and sacrifice during the period of my study here. My uncle Mr. R. Chowdhury is gratefully acknowledged for his cooperation in the beginning of my program.

Special thanks to Dr. M. Kavehrad of our Department. His financial support allowed me to complete this work. My thanks to Dr. P. Galko for his help in LATEX.

I would also like to thank all of my graduate student friends of B-408.

This work has been supported by the Telecommunication Research Institute of Ontario (TRIO) by the Photonics Network project of Prof. M. Kavehrad and by Bell-Northern Research (BNR) and Natural Sciences and Engineering Research Council (NSERC) through the Industrial Research Chair program.

Contents

List of Figures

Chapter 1

INTRODUCTION

1.1 Introduction

Subcarrier multiplexing (SCM) is an important approach to the design of broadband optical communication systems. Significant progress has been made recently in the research on high capacity SCM systems [1], [2], [3], [4], [5]. This technology is greatly facilitated by the development of optoelectronic devices, specially by the development of high-speed semiconductor laser diodes [5]. Recently laser bandwidths up to 22 GHz for Febry-perot lasers and 13 GHz for distributed feedback(DFB) lasers have been obtained[1]. This large bandwidth of the laser is very suited in broadband fiber optic transmission. Fiber has a very low loss of about 0.5 dB/km [6], [7] and single-mode fiber technology offers a very high transmission bandwidth at reasonable cost. Today's fiber construction and installation technology is mature [8]. All these attractive features make SCM very popular for multichannel transmission. Experimentally, 120 frequency-modulated video channels, and 20 100-Mb/sec FSK digital video channels have been transmitted with single-mode fiber [1].

In SCM a large number of modulated microwave carriers are combined in the frequency domain in the transmitter. The composite signal is then used to intensity modulate the light from a high-speed laser diode. The light signal is transmitted over a span of fiber and at the receiving end the signal is detected with a high-speed photodiode. The resulting electrical signal is then amplified and the baseband signal is recovered with conventional microwave

techniques. This transmission technique is called subcarrier multiplexing because the primary carrier is the optical carrier at 10^{14} Hz while the multiplexed microwave carriers at 1-10 GHz are the subcarriers[1]. Fig 1 shows the block diagram representation of a SCM system.

The main advantage of SCM is the possibility of offering different services without synchronization or co-ordination (since every service is carried by different RF carriers) and the simplicity [5]. Another advantage is that by using commercially available components and low-frequency well-developed microwave technology, a baseband signal and microwave signals can be readily multiplexed and demultiplexed.

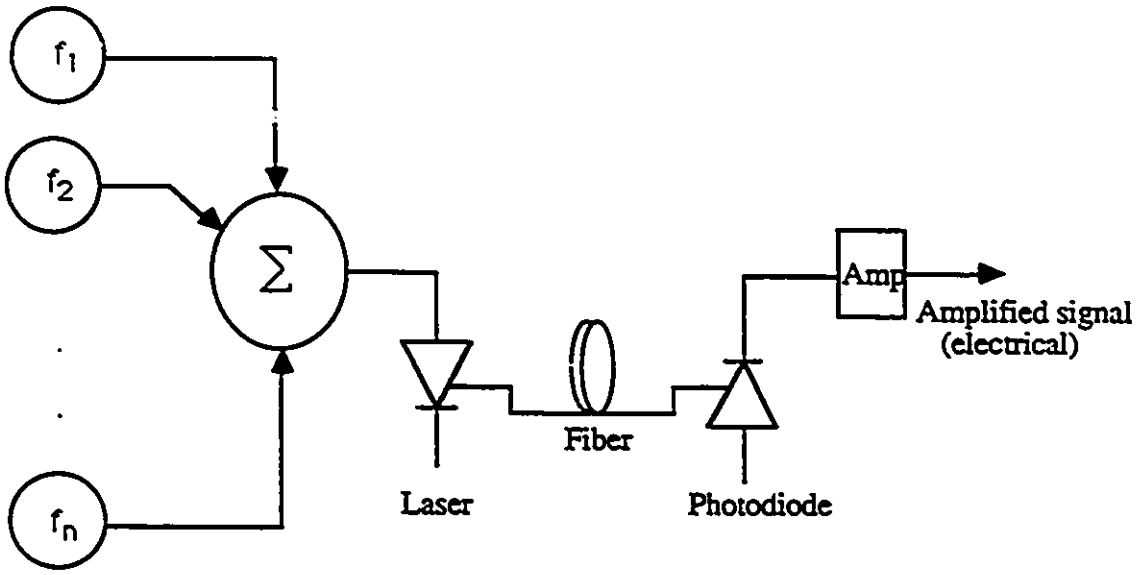

Fig. 1. Block diagram of a subcarrier multiplexing system

Today's telephone companies are using fiber-based transmission extensively for long distance and interoffice trunk lines [9] and this technology is becoming more and more popular in other fields of communications. Both analog and digital signals can be simultaneously

transmitted in SCM system. There are a large number of applications where analog fiber optic transmission scheme is suitable. Among these, one of the most common applications is the analog transmission of video signals through fiber[2], [8], [10], [11]. The multichannel AM-VSB signal, used in present CATV system, can be upgraded (more channels) using fiber-based SCM transmission.

The principal components of a fiber optic system for either analog or digital signals are the optical source(laser, LED), the optical channel(fiber) and the optical receiver(photodetector). To achieve a reliable and secure communication it is necessary that all these components within the transmission system are compatible so that their individual performance, as far as possible, enhances rather than degrades the overall system performance. Single-mode fiber is free from intermodal dispersion and can be considered as reliable optical channel.

In the point-to-point optical link from transmitter to receiver there are a few noise sources that limit the system performance. These are relative intensity noise of the laser, shot noise of photodetector and thermal noise from the electronic preamplifier. All these noise components can be measured at the output of a preamplifier with current gain G. The signal power per ohm of load resistance at the output of preamplifier is[2]

$$P_{sig} = \frac{(mGI_p)^2}{2}$$

Where I_p is the received photocurrent and m is the optical modulation depth. Relative intensity noise (RIN) of the laser has been discussed extensively in the literature [3], [4], [8], [12]. The intensity fluctuations are caused by statistical nature of photon generation and electron-hole recombination within the laser cavity. RIN is defined [3] as the ratio of the square of intensity fluctuations Δq to the square of the average light intensity Q_o as:

$$RIN = \frac{<\Delta q^2>}{Q_o^2}$$

RIN is proportional to the transmitted power and since it experiences the same link attenuation as does the signal, the carrier-to-noise ratio due to RIN is constant[8]. Noise

spectral density due to RIN in A^2/Hz is given by[2]

$$S_{RIN}(f) = \{\eta G I_p \sqrt{(RIN)}\}^2$$

Where η is the coupling loss between the laser and the detector. The second source of noise is the shot noise. It originates in the photodetector during the photon-electron conversion process. It is proportional to the received optical power. Therefore, a 1-dB change in received optical power results in a 1-dB change in the CNR[8]. The noise spectral density due to shot noise is[2]

$$S_s(f) = 2eI_pG^2$$

Where e is the electronic charge and I_p is the detected photocurrent. The third source of noise is the thermal noise from the preamplifier. It can be described by an equivalent input noise current i_T (typically 10 pA/$(Hz)^{\frac{1}{2}}$) and the spectral density due to i_T is[2]

$$S_T(f) = (i_T G)^2$$

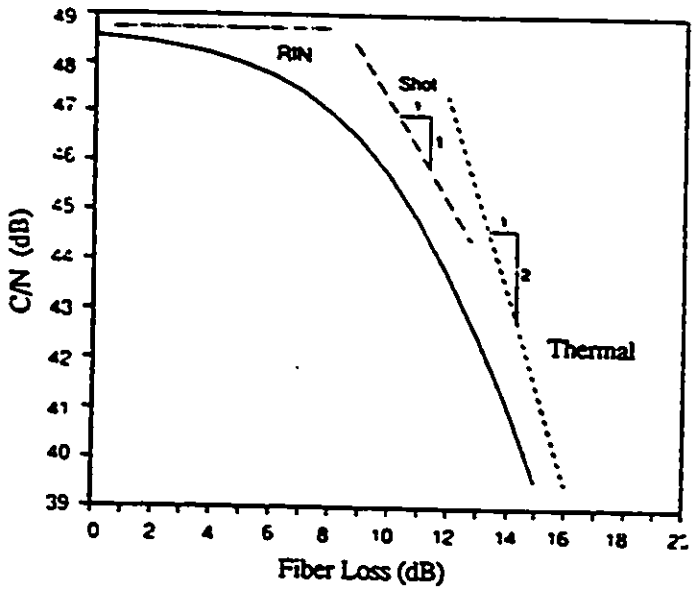

Fig. 2. Carrier-to-noise ratio (due to RIN, shot and thermal noise) as a function of fiber loss in a CATV system.[8]

Thermal noise is independent of received optical power and depends on the load resistance and the noise figure of the amplifier. Therefore, for a given load resistor and at a given temperature it is constant. This results, for a 1-dB change in received optical power, in a 2-dB change in CNR[8]. The plot showing the CNR as a function of fiber loss[8] is shown in Fig 2.

In addition to the above noise sources, in SCM systems, another dominant source of degradation is the nonlinearity of the laser diode, the optical source. Although in many communication applications where analog signals are transmitted, certain levels of amplitude and phase distortion can be tolerated, this is not the case in SCM systems where a high degree of linearity is required in order to minimize interference between individual channels caused by the generation of intermodulation products. One of the main considerations of analog fiber-optic TV transmission is the signal quality(high SNR) and therefore, linearity of laser light-current characteristic is very important. To obtain high SNR a large signal modulation of the laser is necessary. However, nonlinearities of the laser introduce distortions in the output light which, in turn, create harmonic and intermodulation noise affecting the system performance seriously when signal level is high. For lasers with relatively linear light-current characteristics, nonlinear distortion is very little when modulated at low frequencies (below a few tens of MHz). However, as the modulation frequency increases, harmonic distortion increases very rapidly with frequency and the second and third harmonic distortions can no longer be ignored. In multichannel transmission the other factor of concern is the intermodulation noise. Therefore, laser nonlinearities are subject to much work in order to understand how they originate, how they depend on laser parameters and how their effects can be modeled to predict system performance. The goal of our work is to analyze the nonlinearity of semiconductor lasers.

1.2 Organization of the Thesis

Chapter 2 of this thesis introduces the laser diode and its behavior. Here we begin our discussion with the optical sources used in fiber optic communication and give an introductory discussion on the laser diode and its operation. A few other topics relating to the laser like optical feedback in the laser cavity and laser osciilation, laser input-output characteristic, the injection laser and its suitability in fiber optic communication and the effect of temperature are also discussed in this chapter.

In chapter 3, we focus our discussion on the transient behavior of semiconductor lasers. Starting with the well-known rate equations of the laser, we then discuss the dynamic response of the laser. Following that, an output-to-input approach is developed which gives a very general system equation, which in turn, is helpful in deriving the various order output-to-input transfer functions of the laser. To reduce the complexity of analysis and for finding a simpl analytical model for the nonlinearity of the laser, we then develope a simplified analytical technique which is based on a few assumptions.

An introductory discussion with the Volterra series is given in chapter 4. Here it has been shown how Volterra series can be useful for the analysis of nonlinear systems. The output-to-input Volterra transfer functions, G_n, are calculated in the following section and then the calculation of forward Volterra transfer functions, H_n, with the technique inverse-method, are shown.

In chapter 5, we focus on the nonlinearity problem of the laser diodes and we discuss the different aspects of the nonlinear behavior of semiconductor lasers. Then with Volterra series and Volterra transfer functions we develop the models for harmonic and intermodulation distortions. Intermodulation distortion based on simplified analysis is also developed in this chapter which, in turn, gives a clear idea of how it differs from previous model. Following that, we discuss the intermodulation spectra of the laser. In this chapter we show the system results which are calculated based on computer program. The comparison of our results with previously published theoretical, simulation and experimental results are also

shown graphically.

Chapter 6 summarizes all the aspects and results of the thesis and gives suggestions for further research.

1.3 Review of Related Work

With the increasing interest and need for broadband fiber optic transmission, laser non-linearities have been subject of work from the very beginning. Researchers have studied this problem experimentally. Simulation based on large-signal-model rate equations and theoretical analysis have also been done. In this section we will discuss some previous literature which are quite related to our work.

Earlier investigators showed that in the light-current characteristic of the laser there are kinks [13] which affect the emission characteristic of the laser. In the vicinity of a kink, the optical power can even decrease as the current increases. Laser with kinks has characteristic as shown in Fig 3. Kinks result from a number of reasons such as lack of carrier confinement,

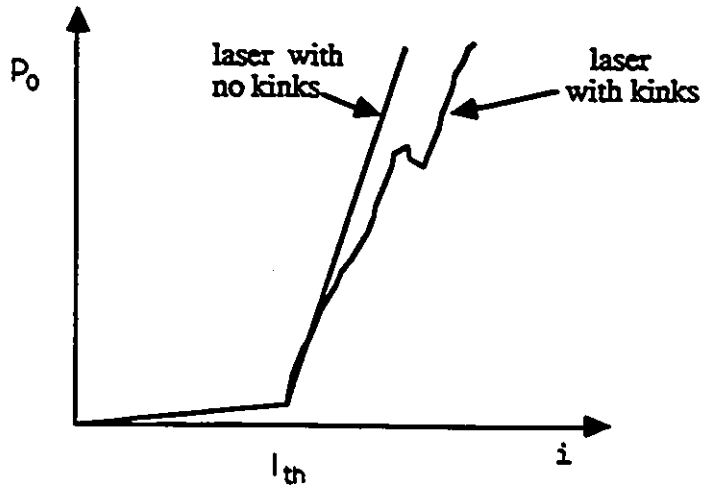

Fig. 3. Laser characteristic with and without kinks. P_o is the optical output power, i is the drive current and I_{th} is the threshold current.

wide active region, defects within the crystal structure, mode hopping, etc. The effect of kinks can be reduced or eliminated by reducing the strip width of the laser. This provides optical confinement in the horizontal plane and therefore improves linearity. Further improvement in the research made it possible that, kinks can be eliminated from the emission characteristics of laser. But there are still instabilities present when the laser is modulated. In 1980, Kristian Stubkjaer and Magnus Danielsen[13] investigated the harmonic distortions of GaAlAs laser diode for various structures. The nth harmonic distortion(R_{nf}) is the magnitude of frequency component appeared in the output of a system at a frequency nf which is n times the input frequency f. Their experiment shows that relative second harmonic and third harmonic distortion($R_{2f/f}, R_{3f/f}$) reach minimum levels of -38 and -50 dB respectively for a laser with strip width of 20 μm and distortion increases slowly at higher bias current. Measurements of $R_{2f/f}$ and $R_{3f/f}$ for lasers with stripe widths from 2.6 to 20μm indicated a correlation between minimum harmonic distortion and strip widths. The best results were obtained for the strip widths less than 6 μm. For these lasers, the minimum levels for $R_{2f/f}$ were about -50 dB and those for $R_{3f/f}$ were -60 to -70 dB for output signals of 4 mW. However, in our work we did not deal with device structure and size, instead we tried to find a theoretical model for the nonlinearities of the laser.

Distortions properties were also investigated [13] for transverse junction lasers, whose build-in carrier confinement should improve the intensity of emitted light. For an output signal of 4 mW and with modulation frequency of 60 MHz, the lowest values for $R_{2f/f}$ and $R_{3f/f}$ were found in the range of -52 to -60 dB and -60 to -70 dB, respectively [13]. It is true that feedback to the laser from an external cavity(e.g., fibers, mirrors, connectors, etc.) induces instabilities. The authors showed that second harmonic distortion is more sensitive to feedback than third harmonic distortion. They have also investigated the intermodulation distortion and compared the second- and third-order products with second and third harmonics and showed that when biased well above threshold and modulated at frequencies far below the relaxation oscillation frequency, the lasers behave as simple nonlinearities without

memory and concluded that measurements of harmonic distortion are sufficient for characterization of the laser nonlinearities and more complicated measurements of intermodulation products (intermodulation products are the frequency components appeared at the output of a nonlinear system because of the interference between different carriers) can be avoided. However, in multichannel transmission where the information bearing signals from different channels are transmitted by a number of well separated carriers, the intermodulation products can not be avoided.

In 1984, K. Y. Lau and A. Yariv [14] investigated the intermodulation(IM) distortion in a directly modulated semiconductor injection laser. They have shown that for multichannel transmission the second and third harmonic distortions generated by the signals in the channel are of little concern. The relevant quantity of concern is the third-order intermodulation product of the laser transmitter. Because when the input to the device are a number of carriers with different frequencies, the device nonlinearity introduces frequency components at the output which are the sum and difference of input frequencies. These frequency components fall within the bandwidth of the transmitted channels and thus undesirable. Lau and Yariv have studied the IM characteristics of high-speed laser diodes and conducted an experiment by modulating the lasers with two sinusoidal signals 20 MHz apart and observed the various sum, difference and harmonic frequencies. It was found that (1) at low frequencies (a few hundred MHz) all the lasers tested exhibit very low IM products of below -60 dB (relative to the signal amplitude) even at an optical modulation depth(OMD) of approaching 100 percent, (2) the second harmonic of the modulation signals increase roughly as the square of the OMD while the IMD product increase as the cube of the OMD. As we will see in chapter 5, our results are in excellent agreements with the above two conclusions.

The first detailed theoretical analysis for the laser nonlinear distortion has been done by T.E.Darcie et. al. [15] in 1985. They have extended the analysis of ref [14] to include the additional distortion terms and damping due to gain compression of the active region. They presented a theory for the prediction of nonlinear distortion of the laser and also measured the distortions for a variety of lasers and observed that for a given relaxation oscillation

frequency f_r (it is the frequency at which a resonance peak appears in the transfer function) and optical modulation depth(OMD), all the lasers measured generate approximately the same levels of distortions. We have performed a similar theoretical analysis for the laser nonlinearity using a Volterra series approach. Since we will use Darcie's expressions for comparison with our results later, we like to write them here. These expressions for the second harmonic, the third harmonic and the third-order intermodulation distortion are given by

$$\frac{2HD}{C} = OMD\frac{f_1^2}{f_r^2 g(2f_1)} \tag{1.1}$$

$$\frac{3HD}{C} = \frac{3}{2}(OMD)^2\frac{(\frac{f_1}{f_r})^4 + \frac{1}{2}(\frac{f_1}{f_r})^2}{g(2f_1)g(3f_1)} \tag{1.2}$$

$$\frac{IMD}{C} = \frac{1}{2}(OMD)^2\frac{[\{(\frac{f_1}{f_r})^4 - \frac{1}{2}(\frac{f_1}{f_r})^2\}^2 + (\frac{2\pi\tau_p f_1^2}{f_r^2})^2]^{\frac{1}{2}}}{g(f_1)g(2f_1)} \tag{1.3}$$

and

$$g(f_1) = [\{(\frac{f_1}{f_r})^2 - 1\}^2 + (\frac{2\pi\epsilon f_1}{g})^2]^{\frac{1}{2}} \tag{1.4}$$

where ϵ is the gain compression damping coefficient, τ_p is the photon lifetime and g is the optical gain coefficient, $2HD$, $3HD$ and IMD are the second harmonic, third harmonic and two tone third-order intermodulation distortions, respectively. C is the amplitude of fundamental carrier. f_1 is the carrier frequency. We will again discuss these terms later when we discuss the rate equations of the laser.

In 1986, A. Czylwik [17] performed similar nonlinearity analysis applying Volterra series to the rate equations. We will discuss his analysis in the comparison later in chapter 5.

To obtain a better understanding of the device nonlinearities, W.I.Way [16] has performed a simulation and experimental work based on the large-signal-model rate equations, in 1987. He used a high-speed GaAlAs single-mode laser diode (Ortel SL-620) and measured the two-tone intermodulation products. The results show that the IMD product is lower when the laser is biased at a high current level($\simeq 2.5I_{th}$) and is higher when the laser is biased at a low current level($\simeq 1.25I_{th}$). We will also show Way's simulation and experimental results later (in chapter 5) for comparison.

Our colleague P. Neusy [35] has conducted similar analysis with computer simulation. He carried out his simulation by developing a computer model of the laser and using software simulator package BOSS.

Nonlinear systems with memory (e.g., semiconductor laser) can not be solved by linear system analysis techniques. For such systems Volterra series expansion is very appropriate because it includes both system nonlinearity and its memory property. The Volterra kernels can be derived from the system equation and the nonlinearities can be calculated analytically. However, there is a strict limitation in the practical application of Volterra series. The systems with weak nonlinearities can be analyzed using Volterra series so that only a few Volterra kernels need to be considered. For strong nonlinear systems, calculation of higher-order Volterra kernels becomes almost impossible. In the case of semiconductor laser only weak nonlinearity exists and therefore, Volterra series analysis is an attractive approach.

Theoretical analysis is very important in the design of communication systems. However, in the previous perturbation technique[14],[15] the details of the analysis were not given. The gain compression term ϵ was not included in Lau and Yariv's[14] work which is an important laser parameter for nonlinearity analysis. Also their results are not clear dimensionally. Although Darcie[15] used the same rate equations as we did (which include the parameter ϵ), he just gave the expressions for $2HD$, $3HD$ and IMD without explaining any analytical steps. Czylwik's [17] analysis is based on the rate equations which do not contain the

important gain compression parameter ϵ and intermodulation distortion was not considered in that analysis. Therefore, for the system designers it is not possible to follow through any theoretical method of analysing the system performance until now. In this thesis we give a detailed analytical method and derive Volterra transfer functions for the laser. These transfer functions are used throughout the analysis. Once the transfer functions are known, these can be used by any system designer to analyze the overall system performance. But in the time domain perturbation analysis either the Volterra kernels or the Volterra transfer functions are not specified.

Chapter 2

THE LASER

In this chapter we give an introductory discussion on light sources, mainly the laser diode. This is for the understanding of the laser operation, light generating mechanism in the laser, its necessity and use in broadband fiber optic transmission. All the contents of this chapter are taken from the literature [18], [19], [20] and [21].

2.1 An Introduction to the Laser Diode

The optical source is often considered to be the active component in an optical fiber communication. Its function is to convert electrical energy in the form of current into optical energy in the form of light in an efficient manner so that the optical output can be effectively coupled into the optical fiber. There are three types of light source available which are

(a) wideband 'continuous spectra' sources (incandescent lamps),
(b) monochromatic incoherent sources (light emitting diodes or LEDs), and
(c) monochromatic coherent sources (lasers).

In a coherent source, the optical energy produced in the cavity has spatial coherence which means the emitted photons are in phase and the optical output beam is highly directional. In the incoherent LED the emitted photons have random phases, the output radiation has a broad spectral width and the radiation is not as directed. In the early stages of optical

fiber communication the most powerful narrowband coherent light sources were necessary due to severe attenuation and dispersion in the fibers. Therefore, gas lasers (helium-neon) were utilized initially. However, the development of the semiconductor injection laser and the LED, together with the substantial improvement in the properties of optical fiber, makes these two devices very attractive as light source in fiber optic communications. The major requirements for an optical source are

(1) A size and configuration compatible with launching light into an optical fiber.
(2) Emit light at wavelengths where the fiber has low losses and low dispersion and where the detectors are efficient.
(3) Very narrow spectral bandwidth (linewidth) in order to minimize dispersion in the fiber.
(4) Linear to minimize distortion.
(5) Couple sufficient optical power to overcome attenuation in the fiber plus additional losses and leave adequate power to drive the detector.
(6) Must be capable of maintaining a stable output.

To a large extent the semiconductor lasers and the LEDs fulfill these major requirements. LEDs are generally low power devices and are able to couple lower optical power into the fiber (of the order of microwatt) and they have smaller modulation bandwidth than laser. Unlike the LEDs, the laser has a high gain due to stimulated emission and more output power(several mW) can be coupled to the fiber. In the early stage of optical communication, light sources were designed to operate between 0.8 and 0.9 μm. These early systems, utilized multimode step index fibers, LED or lasers. Because of smaller bandwidth and low coupling power, the LED was not suitable for long distance wideband transmission. The semiconductor lasers became more popular because of their superior performance (bandwidth, power and transmission distance). After the recent development of single-mode fibers, which offer extremely low dispersion, single-mode laser diodes became very important as optical sources. These single-mode systems are suited to extra wideband, very long-haul applications and are

currently used for long distance telecommunications. On the other hand, LED has many spatial modes which cannot be readily focused and coupled into single-mode fiber.

In 1962, the first GaAs semiconductor laser operating at low temperature was reported[19]. These devices are based on *pn* junctions of a single semiconductor, and therefore, were called homojunction lasers. At present the injection laser diodes are used extensively as single-mode light source and tend to find more use as a device in single-mode fiber systems. Most semiconductor lasers use the double heterostructure design, in which the active region is sandwiched between two adjoining semiconductor materials with different band-gap energies. This design serves to confine the electorns to a narrow region and achieves a high carrier density. They have adequate output power for a wide range of applications and their optical power output can be directly modulated by varying the input current to the device. The light emitting region consists of a *pn* junction constructed of direct-band-gap III-V semiconductor materials.

To achieve efficient generation of light from semiconductor, firstly a suitable energy level is necessary so that electrons can be excited from some initial energy state to some higher energy state. Secondly the excitation mechanism for elevating the electrons to higher energy state should be efficient. The excited electrons must eventually return to their initial energy levels. In doing so, they lose energy which appear as quanta of light called photons.

2.2 Absorption and Emission of Radiation

The interaction of light with matter takes place in discrete particles called photons. The quantum theory says that the electron in atoms exists only in certain discrete energy states such that absorption and emission of light causes them to make a transition from one discrete energy state to another. The frequency of absorbed or emitted radiation f is related to the difference in energy E between the higher energy state E_2 and the ground energy state E_1 by the expression:

$$E = E_2 - E_1 = hf$$

where $h = 6.626X10^{-34}$ Joule-sec is Planck's constant. Laser action is the result of three key processes which are photon absorption, spontaneous emission and stimulated emission. These three processes can be represented by the simple two-state energy diagram of Fig 4. Normally the system is in the ground state. When a photon of energy $E_2 - E_1$ is incident on the system, an electron in state E_1 can absorb the photon energy and be excited to state E_2. Since this is an unstable state, the electron shortly returns to the ground state thereby emitting a photon of energy hf. When the atom is initially in the higher energy state E_2 and makes a transition to lower energy state E_1, the emission can occur in two ways:
(a) by spontaneous emission in which the atom returns to the lower state in an entirely random manner, (b) by stimulated emission when a photon having an energy equal to the energy difference between the two states $(E_2 - E_1)$ interacts with the electron in the upper energy state, the electron is immediately stimulated to drop to the ground state and give off a photon of energy hf. This photon is in phase with the incident photon.

The random nature of the spontaneous emission process in semiconductors results in incoherent radiation. This is the basic mechanism for light generation in LED. However, it is the stimulated emission which gives the laser its special properties as an optical source. In fact, coherent radiation is obtained with the laser.

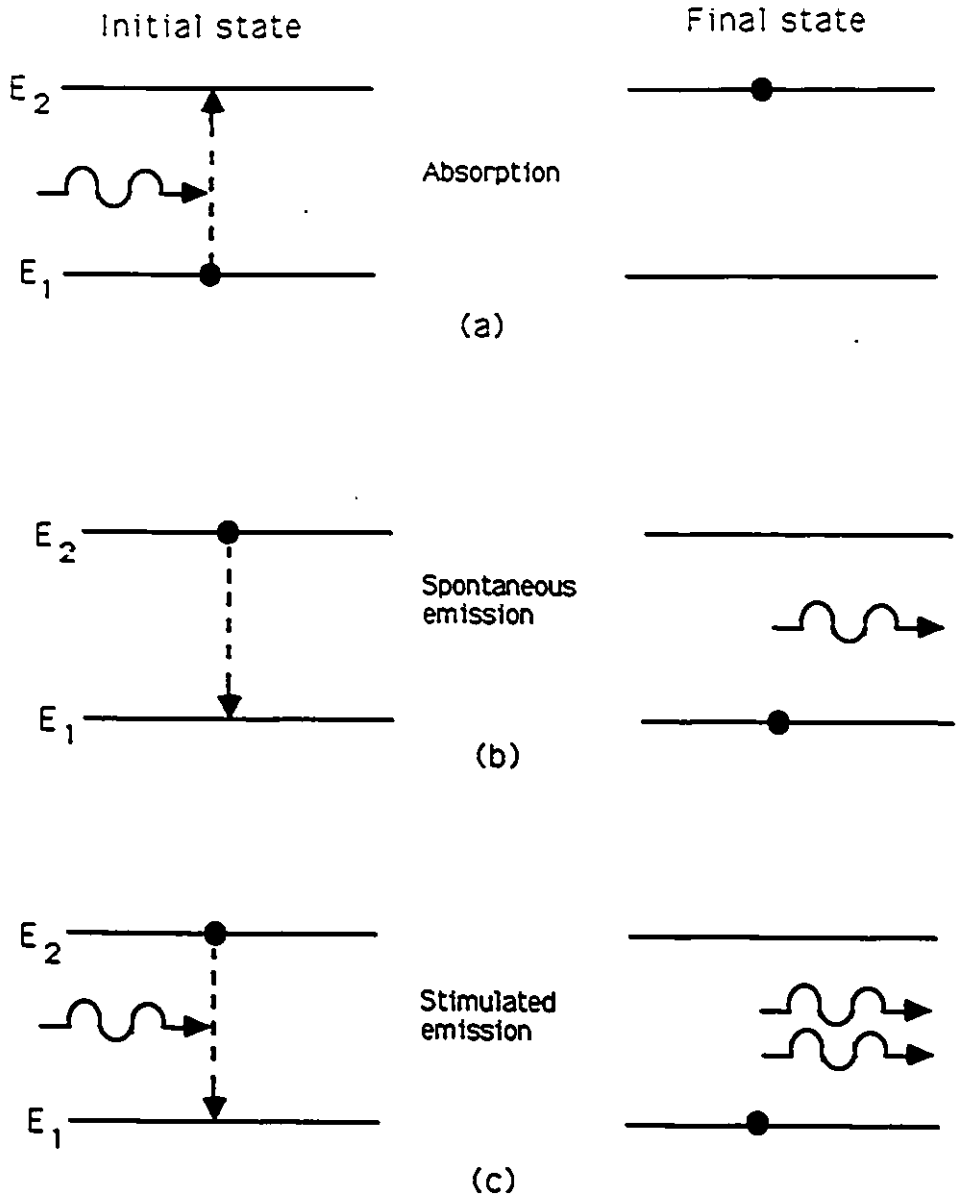

Fig. 4. The energy state diagram showing the three key transition processes involved in laser action, (a) absorption, (b) spontaneous emission and (c) stimulated emission, the incident photons are shown on the left of each diagram and the emitted photons are shown on the right, the black dot indicates the state of electron before and after a transition takes place[18].

In thermal equilibrium the density of the excited electrons is very small. Most photons incident on the system will therefore be absorbed, so that stimulated emission is essentially negligible. Stimulated emission exceeds absorption only if the population of the excited state is greater than the population of the ground state. This condition is known as *population inversion*. Since this is not an equilibrium condition, population inversion is achieved by various "pumping" techniques. In the case of a semiconductor laser, population inversion is accomplished by injecting electrons into the material at the device contacts to fill the lower energy states of the conduction band.

2.3 Optical Feedback and Laser Oscillation

Stimulated emission in semiconductor lasers arises from optical transitions between distributions of energy states in the valance and conduction bands. When a photon collides with an electron in the excited energy state, this causes the stimulated emission of a second photon and then these photons release two more. Continuation of this process effectively creates avalanche multiplication, and the electromagnetic waves associated with these photons are

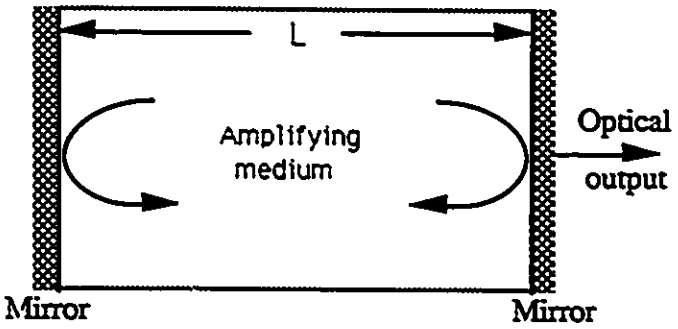

Fig. 5. The semiconductor laser diode structure with reflecting mirrors at two ends of the cavity[18].

in phase and thus amplified coherent emission is obtained. To achieve this action it is necessary to contain photons within the laser medium and maintain the condition for coherence. This is accomplished by forming mirrors at either end of the amplifying medium. This is shown in Fig 5. The optical cavity formed is analogous to an oscillator as it provides feedback

of the photons by reflection at the mirrors at both ends of the cavity. Hence the optical signal is fed back many times whilst receiving amplification as it passes through the medium. Although the amplification of the signal from a single pass through the medium is quite small, after multiple passes the net gain can be large. Furthermore, if one of the mirrors is made partially transmitting, useful radiation may escape from the cavity. A stable output is obtained when the optical gain is exactly matched by the losses in the amplifying medium. The major losses result from factors such as absorption and scattering in the medium and at the mirrors etc.

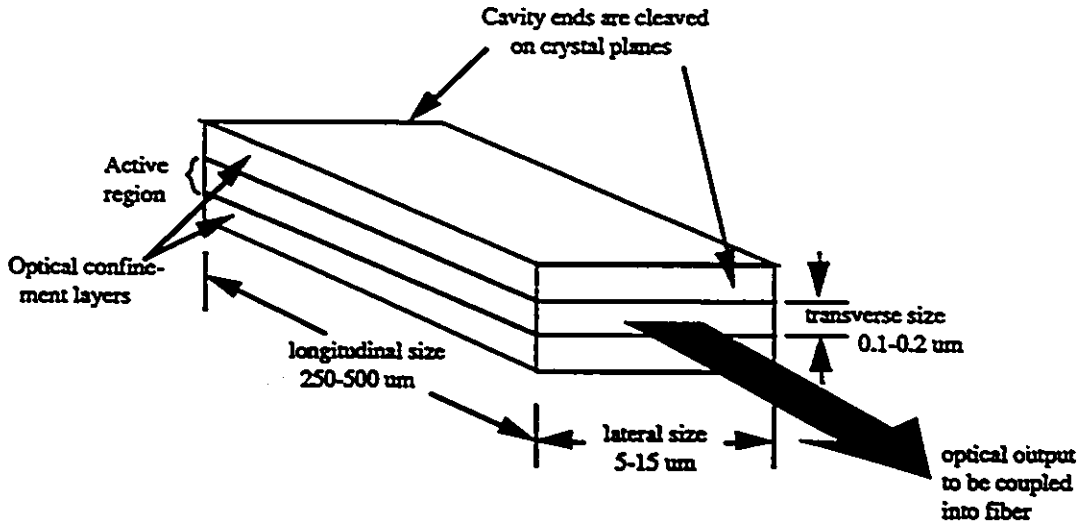

Fig. 6. Fabry-Perot resonator cavity for a laser diode[21].

This radiation in the laser diode is generated within a Fabry-Perot resonator cavity as shown in Fig 6. The sizes of this cavity are approximately 250-500 μm long, 5-15 μm wide and 0.1-0.2 μm thick. These dimensions are commercially referred to as the longitudinal, lateral and transverse dimensions of the cavity. The two reflecting mirrors are directed toward each other to enclose the cavity. The mirror facets are constructed by making two parallel cleaves along natural cleavage planes of the semiconductor crystal. In distributed feedback (DFB) lasers, the cleaved facets are not required for optical feedback. The fabrication of this device is similar to the Fabry-Perot types, except that the lasing action is obtained from Bragg

reflectors (gratings) or periodic variations of the refractive index.

2.4 Semiconductor Injection Laser

For optical fiber communication, the light sources used almost extensively are semiconductor lasers. This is because stimulated emission is encouraged in the semiconductor which gives the injection laser several major advantages over other lasers. However, lasers come in many forms with dimensions ranging from the size of a grain of salt to one that will occupy an entire room[21]. The lasing medium can be a gas, a liquid, a crystal or a semiconductor. The main advantages of semiconductor injection lasers are:

(a) High radiance due to the amplifying effect of stimulated emission. Injection lasers will generally supply milliwatts of optical output power.
(b) Narrow linewidth of the order of 1 nm or less which is useful in minimizing the effects of material dispersion in the fiber.
(c) Modulation capabilities which at present extended up into the several gigahertz range and will be improved upon.
(d) Good spatial coherence which allows the output to be focused by a lens into a spot which has greater intensity than the dispersed unfocused emission.
(e) Its size and configuration is very suitable to lunch optical output into the fiber effectively.

These advantages, of the injection laser led to the development of the device in the 1970s. These early devices used basic homojunction structure which had a high threshold current density due to their lack of carrier confinement and proved inefficient light sources. Later, improved carrier confinement and thus lower threshold current densities were achieved using heterojunction structures. The double heterojunction injection laser fabricated from a lattice matched III-V alloy provided both carrier and optical confinement on both sides of the *pn* junction giving the injection laser a greatly enhanced performance. This enables

these devices with the appropriate heat sinking to be operated in a continuous wave (CW) mode.

The optical output versus current characteristic for a semiconductor injection laser is shown in Fig 7. In the region below threshold (I_{th}) the optical output is very low which is due to the spontaneous emission in the cavity. However, above the threshold, the light output increases substantially for small increases in current through the device. This corresponds to the region of stimulated emission when the device is acting as an amplifier of light. The threshold current I_{th} is conveniently defined by extrapolation of lasing region of the power-current curve as shown in Fig 7. At high power outputs the slope of the curve decreases because of junction heating.

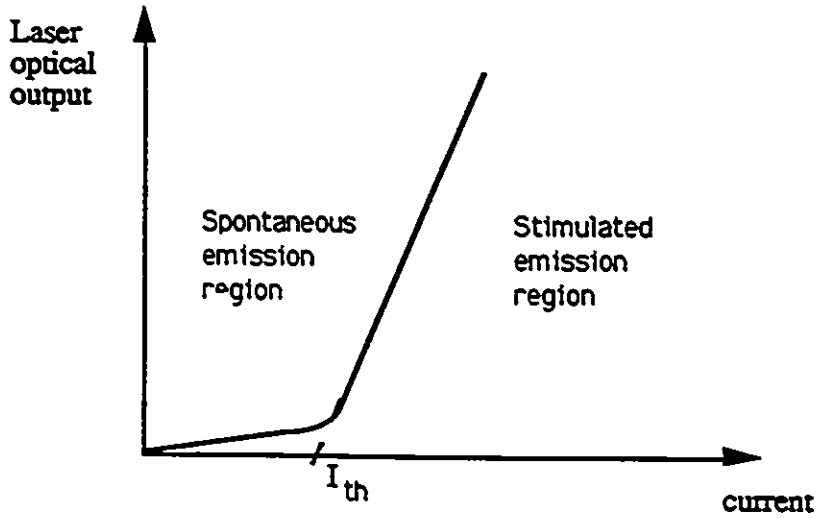

Fig. 7. Optical output (power) versus current characteristic for a semiconductor injection laser diode.

2.4.1 Efficiency

The operational efficiency of the semiconductor lasers are defined in a number of ways. A useful definition is that of differential quantum efficiency η_D which is the ratio of the increase in photon output rate for a given number of injected electrons. This is defined by

$$\eta_D = \frac{dP_e/hf}{dI/e} \tag{2.1}$$

Where P_e is the optical power emitted from the device, I is the current, e is the electronic charge and hf is the photon energy. η_D gives a measure of the rate of change of the optical output power with current and hence defines the slope of the output characteristic. For a CW semiconductor laser it is usually in the range 40-60 percent[18].

The internal efficiency is defined as

$$\eta_i = \frac{number\ of\ photons\ produced\ in\ the\ laser\ cavity}{number\ of\ injected\ electrons} \tag{2.2}$$

This is in the range 50-100 percent. It is related to the external differential quantum efficiency by the relation

$$\eta_D = \eta_i[\frac{1}{1 + (2\alpha L/ln(1/R_1R_2))}] \tag{2.3}$$

The total quantum efficiency η_T is defined as

$$\begin{aligned} \eta_T &= \frac{total\ number\ of\ output\ photons}{total\ number\ of\ injected\ electrons} \\ &= \frac{P_e/hf}{I/e} \end{aligned} \tag{2.4}$$

In the region above threshold η_T is related to η_D as

$$\eta_T = \eta_D(1 - \frac{I_{th}}{I}) \tag{2.5}$$

2.5 Effects of Temperature

In the application of laser diodes an important factor of consideration is the temperature dependence of the threshold current $I_{th}(T)$. This parameter increases with temperature in

all types of semiconductor lasers because of various complex temperature-dependent factors. The complexity of these factors prevents the formulation of a single equation holding for all devices and temperature ranges. However, the temperature variation of I_{th} can be approximated by the empirical relation

$$I_{th}(T) = I_z e^{T/T_o} \tag{2.6}$$

where T_o is a measure of the relative temperature intensitivity and I_z is a constant. For a conventional stripe-geometry laser diode T_o is typically 120 to 165°C in the vicinity of room temperature. A typical curve is shown in Fig 8. Smaller dependence of I_{th} on temperature has been obtained for GaAlAs quantum-well heterostructure lasers[21]. For these lasers T_o can be as high as 437°C. Variation of lasing threshold can also change as the laser ages. If a constant optical output power is to be maintained as the temperature of the laser changes or the laser ages, it is necessary to adjust the dc bias current .

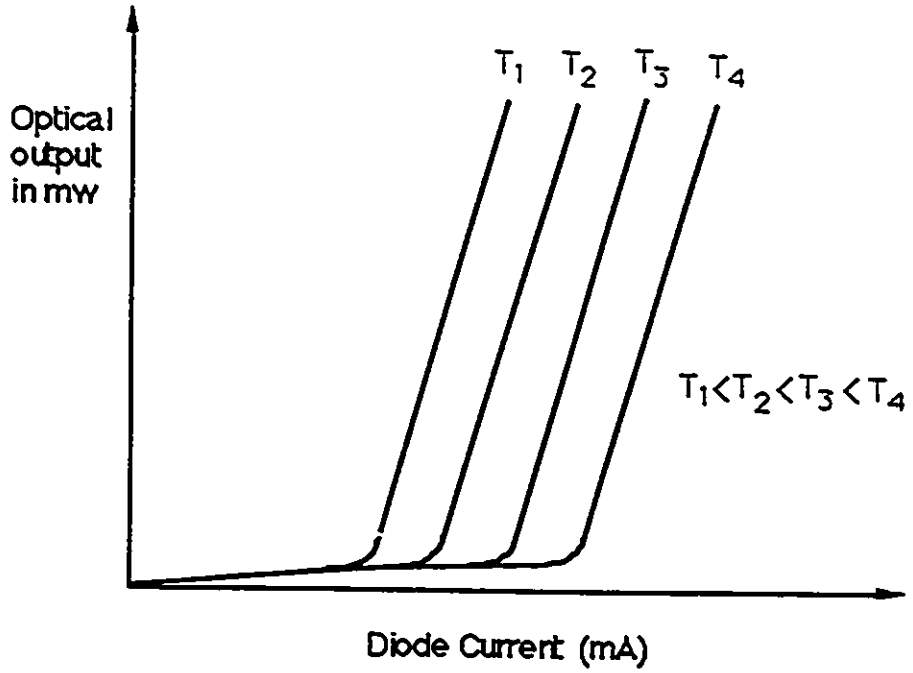

Fig. 8. Temperature dependent behavior of the laser optical output power as a function of bias current.

Chapter 3

LASER TRANSIENT PHENOMENA

In the previous chapter we have described the laser diode. The actual analysis for the modeling of laser nonlinear distortion starts from this chapter. Since the rate equations of the laser are the basis of our analysis we will start our discussion with them.

3.1 The Rate Equations

The transient behavior of the semiconductor laser is completely characterized by the coupled single-mode rate equations. These are appropriate for laser diodes under the following assumptions[22]:(a) the laser is operating in a single-mode above threshold, (b) an ideal cavity with homogeneous population inversion and (c) the gain coefficient is a linear function of the injected carrier density N above a minimal value N_o. A large-signal-model of these equations was first introduced by Tucker[23], who has introduced a parameter ϵ, which is called the optical-field-dependent gain compression term. These equations are

$$\frac{dN}{dt} = \frac{I_a}{V'} - \frac{N}{\tau_{sp}} - g(N - N_o)(1 - \epsilon Q)Q \tag{3.1}$$

$$\frac{dQ}{dt} = \Gamma g(N - N_o)(1 - \epsilon Q)Q - \frac{Q}{\tau_p} + \Gamma\beta\frac{N}{\tau_{sp}} \tag{3.2}$$

where N is the electron density averaged over the volume of active region, I_a is the current injected to the active region, V' is the volume of the active region times electronic charge, τ_{sp} is the spontaneous recombination lifetime of the carriers, g is the optical gain coefficient, Q is the photon density, Γ is the optical confinement factor given by the ratio of the volume of the active region to the model volume, τ_p is the photon lifetime, β is the probability that a photon is emitted spontaneously into the lasing mode.

The term $\frac{dN}{dt}$ in equation (3.1) is the rate of change of carrier density, the terms on the right-hand side are the rate of carrier injection into the active region, carrier decrease due to spontaneous emission and carrier decrease due to stimulated emission, respectively. In equation (3.2) the term on the left-hand side is the rate of change of photon density. The first term on the right-hand side is the rate increase due to stimulated photon emission, the second term is the rate of loss of photon by radiation and absorption and the last term is the fractional increase of photon due to spontaneous emission into the lasing mode. The combined phenomena of current injection and photon emission as described by the above equations can be schematically represented by Fig 9 [24]. The term $gN(1-\epsilon Q)Q$ is the stimulated emission and the term $gN_o(1-\epsilon Q)Q$ is the stimulated absorption.

The parameter Γ is less than unity which means that not all the emitted photons are confined to the active region, a fraction are lost in the cavity. N_o is the minimum electron density at which $g = 0$ and above which stimulated emission starts i.e., $g > 0$. Therefore, for lasing action it is necessary that $N > N_o$. For undoped GaAs, a nominal current density of 4000 A/cm^2-μm is needed to obtain a lasing optical gain coefficient greater than zero at 300^{o}K and an approximate estimate of N_o can be obtained by the relation[15]

$$N_o = \frac{I_a \tau_{sp}}{V'} \tag{3.3}$$

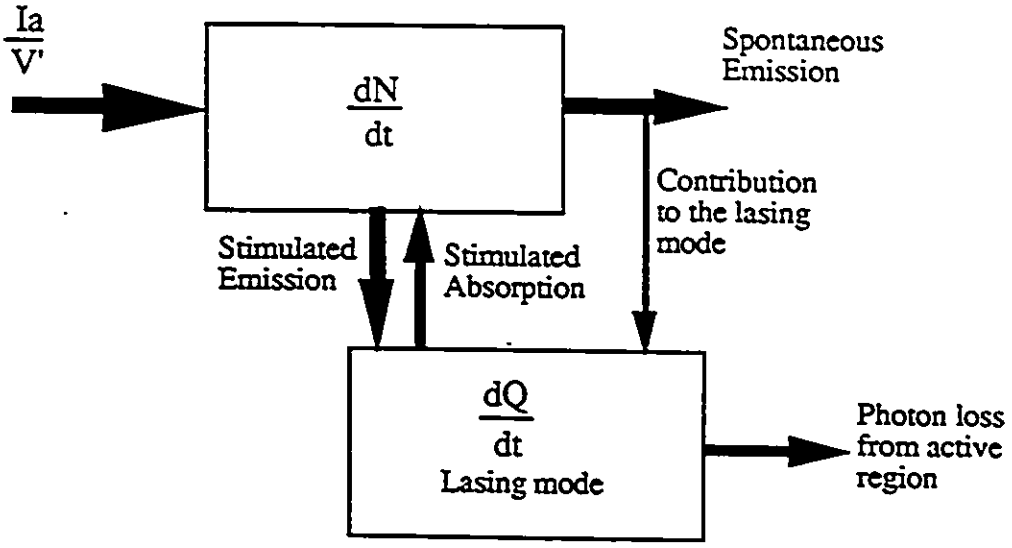

Fig. 9. Changes in electron and photon population in the light generation of a laser diode as given by the rate equations [24].

3.2 Dynamic Response

The dynamic behavior of the semiconductor laser is very critical especially when it is used in wideband optical fiber communications. This dynamic behavior is illustrated in Fig 10. When the laser is turned on with a current pulse, a transient occurs because of time required for the electron and photon populations to come into equilibrium[18]. This results in a switch-on delay often followed by a high frequency (of the order of 10 GHz) damped oscillations known as relaxation oscillations. This oscillation characteristic depends on the diode current, the spontaneous carrier lifetime, photon lifetime, gain nonlinearities, device structure and due to some other reasons. The switch on delay t_d may last for 0.5 nsec and the relaxation oscillation for perhaps twice that period. At data rates above 100 Mbits/sec this behavior can produce a serious deterioration in the pulse shape[18]. The switch on delay may be reduced by biasing the laser near threshold.

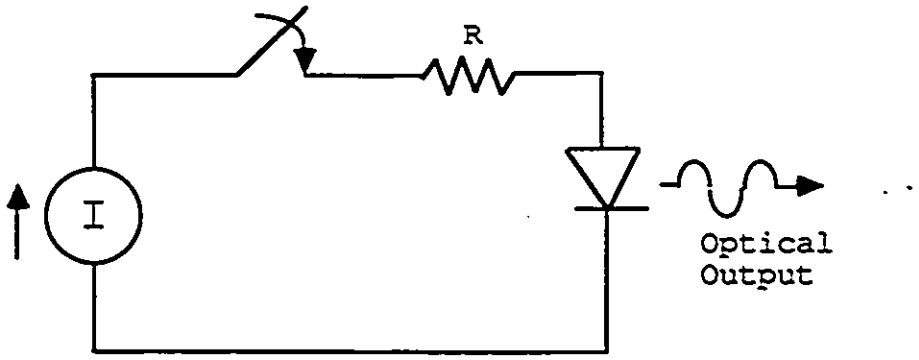

(a)

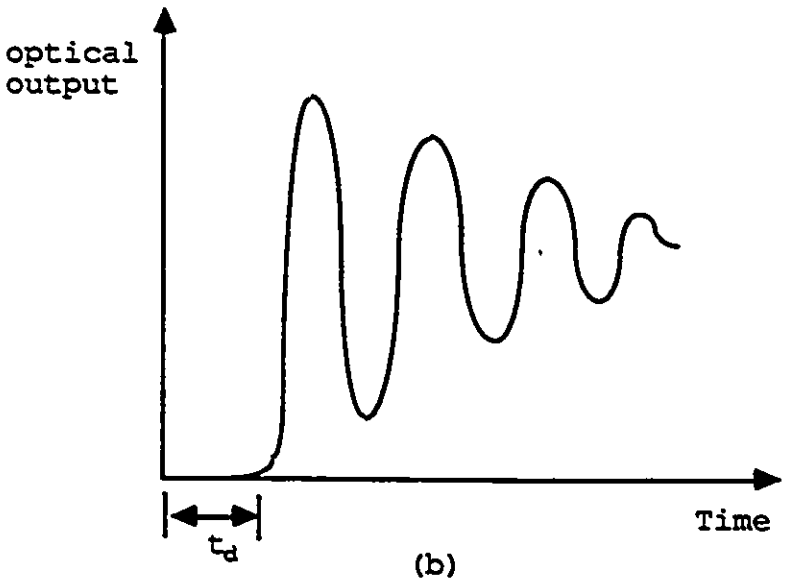

(b)

Fig. 10. (a) Simple diode circuit with a registor in series with the diode, (b) Transient behavior of an injection laser showing the switch on delay and relaxation oscillations[18].

However, the damping of the relaxation oscillations is less near threshold. Since lasers with strong damping have superior distortion characteristics, high resonance frequencies are desirable[15]. This can be achieved by biasing the laser well above threshold. As we will see later, a resonant condition appears in the system transfer function at some driving frequency which corresponds to the relaxation oscillation frequency and this resonance peak moves to higher frequencies as the bias level is increased. From the small signal analysis, the relaxation oscillation frequency f_r can be expressed by[25]

$$f_r \simeq \frac{1}{2\pi}(\frac{gQ_o}{\tau_p})^{\frac{1}{2}} \tag{3.4}$$

where Q_o is the steady state photon density.

3.3 Output-to-Input Approach

In the analysis of laser nonlinear distortion it is very difficult to accurately solve the rate equations for the output(photon density Q) as a function of the input(current I_a). However, an output-to-input approach can be applied to solve the rate equations which, in turn, helps in finding an accurate theoretical nonlinear model for the laser. In this approach we may consider the input as a function of the output. We assume the output photon density (Q) to be known and we can determine the carrier density (N) as a function of output(Q) using equation (3.2). Then the input current required to obtain this output can be determined from equation (3.1). With the procedure described above, the following equation can be obtained from equations (3.1) and (3.2) [26]. The derivation is shown in Appendix A.

$$\begin{aligned}\frac{I_a}{V'} &= \frac{N_o}{\tau_{sp}} + [\frac{1}{\tau_{sp}} + g(1-\epsilon Q)Q]\frac{[\frac{dQ}{dt} + \frac{Q}{\tau_p} - \frac{\Gamma\beta N_o}{\tau_{sp}}]}{[\Gamma g(1-\epsilon Q)Q + \frac{\Gamma\beta}{\tau_{sp}}]} \\ &\quad + \frac{d}{dt}\{[\frac{dQ}{dt} + \frac{Q}{\tau_p} - \frac{\Gamma\beta N_o}{\tau_{sp}}]/[\Gamma g(1-\epsilon Q)Q + \frac{\Gamma\beta}{\tau_{sp}}]\}\end{aligned} \tag{3.5}$$

The advantage of this approach is that the Volterra transfer functions from output-to-input can be easily calculated and an accurate nonlinear system model can be obtained from the transfer functions.

For the analysis let the steady-state value of photon density be Q_o and d.c. bias current be I_o. Then Q and I_a can be expressed as the sum of steady-state and time varying quantities. Therefore,

$$Q = Q_o + q(t)$$

and

$$I_a = I_o + i(t)$$

In equation (3.5) the denominator terms are very complicated. To reduce this complexity and for the interest of analysis we expand these terms with Taylor series. This expansion gives an equation (Appendix-B) where the drive current $i(t)$ of the laser is expressed in terms of photon density $q(t)$. Thus,

$$\begin{aligned} i(t) &= A + \{Dq(t) + Eq'(t) + Fq''(t)\} - \{Lq^2(t) + Mq(t)q'(t) \\ &\quad + Nq(t)q''(t) + Nq'^2(t)\} + \{Rq^3(t) + Sq^2(t)q'(t) \\ &\quad + 2Gq(t)q'^2(t) + Gq^2(t)q''(t)\} - \ldots\ldots + \ldots\ldots \end{aligned} \tag{3.6}$$

Where A, D, E, F, L, M, N, R, S and G are expressed in terms of the laser parameters and steady state photon density. In equation (3.6), $i(t)$ is the sum of d.c. component, linear terms, second-order terms, third-order terms and so on. $q'(t)$ and $q''(t)$ represents the first and second derivatives of $q(t)$, respectively. Here, the drive current is expressed in terms of the powers of photon density. From the equation it is seen that the second- through higher-order terms contain derivatives. This means that distortion is dependent on frequency. In our analysis we have considered terms up to the third-order.

3.3.1 Simplified Analysis

Equation (3.5) gives an accurate analysis of the device performance. However, the analysis is greatly simplified and we can obtain almost the same result if we make a few assumptions. The spontaneous emission factor β is a very small quantity and it has a very insignificant contribution to the photon density. This term can be omitted. The carrier lifetime is of the order of nsec which is almost 10^3 times bigger than the photon lifetime. Our analysis showed that if we set $\tau_{sp} = \infty$ and $\beta = 0$ it has a little effect in the distortion calculation in comparison with the exact analysis. However, we must consider the effect of threshold current ($\frac{N_o}{\tau_{sp}}$ can not be ignored, but it can be considered equals $\frac{I_{th}}{V'}$). The following equation results from (3.5) after these assumptions have been made.

$$\frac{I_o - I_{th}}{V'} = \frac{1}{\Gamma}\frac{dQ}{dt} + \frac{Q}{\Gamma\tau_p} + \frac{d}{dt}\frac{(\frac{dQ}{dt} + \frac{Q}{\tau_p})}{\Gamma g(1 - \epsilon Q)Q} \tag{3.7}$$

If we compare equation (3.5) and (3.7) we see that equation (3.7) is much simpler to analyze. From (3.7) the steady state photon density is

$$Q_o = \frac{\Gamma\tau_p(I_o - I_{th})}{V'} \tag{3.8}$$

In a similar manner as equation (3.5) we have expanded equation (3.7) by Taylor series and derived the equation for laser drive current i(t) (Appexdix B, equation (B.20)) which is

$$\begin{aligned} i(t) \;=\; & A_1 + \{D_1 q(t) + E_1 q'(t) + F_1 q''(t)\} - \{M_1 q(t)q'(t) + N_1 q(t)q''(t) \\ & N_1 q'^2(t)\} + \{S_1 q^2(t)q'(t) + 2G_1 q(t)q'^2(t) + G_1 q^2(t)q''(t)\} - \ldots + \ldots \end{aligned} \tag{3.9}$$

The constants A_1, D_1, E_1, F_1, M_1, N_1, S_1 and G_1 are expressed, in a similar way as in the case of equation (3.6), in terms of the laser parameters and steady state photon density. Equations (3.6) and (3.9) are similar except in (3.9) $R = 0$, $L = 0$. The set of constants A,

D, E, F, ... in equation (3.6)(which are given by equation (B.13)) are replaced with the set of constants A_1, D_1, E_1, F_1, ... in equation(3.9) (which are given by equation (B.21)).

Chapter 4

VOLTERRA SERIES

4.1 An Introduction to Volterra Series

The Volterra series is a power series with memory which expresses the output of a nonlinear system in "powers" of the input. This series is particularly useful in calculating distortions in communication systems. Wiener, first in 1942, had introduced this series into nonlinear circuit analysis. He had analyzed the response of a series *RLC* circuit with a nonlinear resistor to a white Gaussian excitation. After then many reports and papers have dealt with this subject. Some researchers have used Volterra series for analyzing transistor distortions [27], nonlinear differential equations and integrodifferential equations [28], distortions in satellite links [29], etc. Since the laser dynamic behavior is characterized by the set of coupled rate equations (differential equations) therefore, we can apply Volterra series to the rate equations for the analysis of laser nonlinear behavior. If $y(t)$ is the output function of a nonlinear system and $x(t)$ is the input function then the relation between output and input can be expressed in terms of the Volterra series in the form[30]

$$y(t) = \sum_{n=1}^{\infty} \frac{1}{n!} \int_{-\infty}^{\infty} \cdots \int_{-\infty}^{\infty} g_n(u_1 ... u_n) \prod_{l=1}^{n} x(t - u_l) du_1 ... du_n \tag{4.1}$$

in which for $n = 1, 2, 3, ...$

$g_n(u_1 ... u_n) = 0$ for any $u_j < 0$, j=1,2,.....,n

This functional form was studied by the mathematician Vito Volterra and in recognition of his mathematical contributions, the series is called the Volterra series and the function

$g_n(u_1...u_n)$ is called the nth-order Volterra kernel of the system. For example, $g_1(u_1)$ is the first-order Volterra kernel, $g_2(u_1, u_2)$ is the second-order Volterra kernel and so on. $g_1(u_1)$ is the familiar impulse response of a linear system. The higher-order kernels can be viewed as higher-order impulse responses which serve to characterize the various-orders of nonlinearity [31]. If we have a linear time invariant system then the output input relation can also be expressed by the first order kernel $g_1(u_1)$. In that case the second- through higher-order kernels are zero.

The n-dimensional Fourier transform of $g_n(u_1...u_n)$ is

$$G_n(\omega_1, ..., \omega_n) = \int_{-\infty}^{\infty} ... \int_{-\infty}^{\infty} g_n(u_1...u_n) e^{-j(\omega_1 u_1 + ... + \omega_n u_n)} du_1...du_n \qquad (4.2)$$

which is very important in our analysis. In the above equation $\omega_i = 2\pi f_i$ and G_0 is zero because Volterra series starts with $n = 1$. $G_1(\omega_1)$ is the familiar transfer function of the linear system. Thus the transfer function of the nth-order Volterra kernel, $G_n(\omega_1, ..., \omega_n)$, is seen to be analogous to an nth-order transfer function and is called the nth-order Volterra transfer function[30].

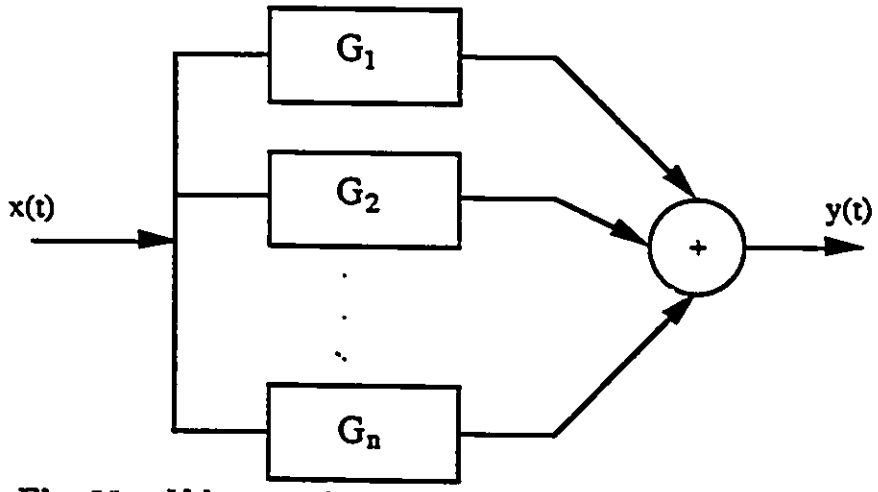

Fig. 11. Volterra series representation of a nonlinear system.

A nonlinear system, whose input-output relation is characterized by the Volterra series, can also be represented by transfer functions as shown in Fig 11. If the system is linear only the linear transfer function $G_1(\omega_1)$ exists, all other G_n's for n=2 and higher are essentially zero. In the figure, $y(t)$ is the sum of outputs from all the boxes. Since G_1 is the linear transfer function, therefore, nonlinearities come from all other G_ns for $n = 2$ and higher.

In order to have a better understanding, we can also express equation (4.1) with the operator notation as [31]

$$y(t) = \mathrm{B}_1[x(t)] + \mathrm{B}_2[x(t)] + \mathrm{B}_3[x(t)] + ... + \mathrm{B}_n[x(t)] + ... \tag{4.3}$$

$$y(t) = y_1(t) + y_2(t) + y_3(t) + ... + y_n(t) + ... \tag{4.4}$$

where

$$\mathrm{B}_n[x(t)] = \frac{1}{n!}\int_{-\infty}^{\infty} ... \int_{-\infty}^{\infty} g_n(u_1...u_n)x(t-u_1)...x(t-u_n)du_1...du_n \tag{4.5}$$

and

$$y_n(t) = \mathrm{B}_n[x(t)] \tag{4.6}$$

B_n is known as the nth order Volterra operator. For $n = 1$ we have $y_1(t) = \mathrm{B}_1[x(t)]$ and for $x(t) = e^{j\omega_1 t}$, the response is

$$\begin{aligned} y_1(t) &= \int_{-\infty}^{\infty} g_1(u_1)e^{j\omega_1(t-u_1)}du_1 \\ &= e^{j\omega_1 t}\int_{-\infty}^{\infty} g_1(u_1)e^{-j\omega_1 u_1}du_1 \\ &= G_1(\omega_1)e^{j\omega_1 t} \end{aligned} \tag{4.7}$$

Thus, $y_1(t)$ is the output of the upper box in Fig 11.

4.2 Output-to-Input Volterra Transfer Functions

So far we have discussed the Volterra series. Now, for the characterization of a nonlinear system by Volterra series we need to know either the Volterra kernels or the Volterra transfer functions of the system. Such kernels or transfer functions can be obtained from system

equations. For the case of the laser we have a set of rate equations. Therefore, we can apply Volterra series to the laser rate equations. But direct application of this series to the rate equations is very difficult because of the pattern of equations. This also can be seen from equation (3.6) which is derived from the rate equations. If we compare equation (3.6) with the Volterra equation (4.1) we can see that equation (3.6) does not fall under the normal form of Volterra equation. Although the kernels can be obtained from equation (3.6), the calculation in the time domain is very difficult. However, in the frequency domain the nth-order Volterra transfer functions, G_n, can be obtained easily from the system equation (3.6) by the harmonic-input method [31]. This method relies on the fact that a harmonic input must result in a harmonic output when (4.1) holds. Thus, when the input to the system $x(t)$ is the sum of sinusoids

$$x(t) = e^{j\omega_1 t} + e^{j\omega_2 t} + e^{j\omega_3 t} + ... + e^{j\omega_n t} \tag{4.8}$$

where $\omega_i = 2\pi f_i$, for $i = 1, 2, ..., n$, G_n is defined by [30]

$$\begin{aligned} G_n(\omega_1, ..., \omega_n) \;=\; & [Coefficient\ of\ the\ e^{j(\omega_1 + ... + \omega_n)t} \\ & term\ in\ the\ expansion\ of\ \ y(t)] \end{aligned} \tag{4.9}$$

The above method enables us to compute the transfer functions of the system. Now in our system equation (3.6), $i(t)$ corresponds to the output $y(t)$ of (4.1) and $q(t)$ corresponds to the input $x(t)$. For the calculation of linear transfer function $G_1(\omega_1)$ we assume the photon density be a single sinusoid i.e. $q(t) = e^{j\omega_1 t}$. Substituting this value of $q(t)$ in (3.6) we obtain $G_1(\omega_1)$ as

$$G_1(\omega_1) \;=\; [Coefficient\ of\ the\ e^{j\omega_1 t}\ term\ in\ the\ expansion\ of\ \ i(t)] \tag{4.10}$$

When we set $q(t)$ as the sum of two sinusoids at frequencies ω_1 and ω_2 i.e. $q(t) = e^{j\omega_1 t} + e^{j\omega_2 t}$, we obtain the second order transfer function $G_2(\omega_1, \omega_2)$ which is the coefficient of $e^{j(\omega_1+\omega_2)t}$ in the expansion of $i(t)$. Similarly with $q(t) = e^{j\omega_1 t} + e^{j\omega_2 t} + e^{j\omega_3 t}$ and taking the coefficient of $e^{j(\omega_1+\omega_2+\omega_3)t}$ we get the third order transfer function $G_3(\omega_1, \omega_2, \omega_3)$. These G's are (Appendix C)

$$G_1(\omega_1) = -F\omega_1^2 + jE\omega_1 + D \tag{4.11}$$

$$G_2(\omega_1, \omega_2) = N(\omega_1 + \omega_2)^2 - jM(\omega_1 + \omega_2) - 2L \tag{4.12}$$

$$G_3(\omega_1, \omega_2, \omega_3) = -2G(\omega_1 + \omega_2 + \omega_3)^2 + j2S(\omega_1 + \omega_2 + \omega_3) + 6R \tag{4.13}$$

In the similar way we can compute the higher-order transfer functions. However, the labor of computing higher-order terms increases rapidly as n increases. Fortunately, in the study of communication systems it is often possible to neglect terms higher than the third-order. Actually the input to the laser is the current and the output is the light which is the photon density $q(t)$. But in equation (3.6) and hence, in the calculation of G's we have assumed the photon density $q(t)$ as the input to the system and $i(t)$ as the output. Therefore, the transfer functions calculated above are the output-to-input transfer functions of the laser.

4.3 Forward Transfer Functions

In actual system modeling we require the input-to-output forward Volterra transfer functions of the system. Such transfer functions, which we call $H_n(\omega_1, ..., \omega_n)$, can be obtained from $G_n(\omega_1, ..., \omega_n)$ using the nth-order inverse and the harmonic-balance method[31]. This method says, when the inverse H_n is connected in tandem with G_n, results in a system in which the first-order Volterra kernel is a unit impulse and the second- through the nth-order kernels are zero[31]. We now consider Fig 12 for the calculation of linear transfer function $H_1(\omega_1)$.

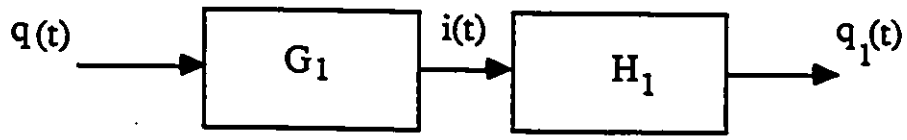

Fig. 12. Two linear systems connected in tandem, H_1 is the inverse of G_1.

The input-output relation of the system G_1 can be written as

$$i(\omega_1) = G_1(\omega_1)q(\omega_1)$$

The output of the system H_1 is

$$\begin{aligned} q_1(\omega_1) &= H_1(\omega_1)i(\omega_1) \\ &= H_1(\omega_1)G_1(\omega_1)q(\omega_1) \end{aligned} \tag{4.14}$$

If $H_1(\omega_1)$ is the inverse of $G_1(\omega_1)$ then according to the inverse theory we should have $q_1(\omega_1) = q(\omega_1)$ [31]. This condition is satisfied only when

$$H_1(\omega_1)G_1(\omega_1) = 1$$

From which the linear H is

$$H_1(\omega_1) = \frac{1}{G_1(\omega_1)} \tag{4.15}$$

Now, we determine the second-order forward transfer function $H_2(\omega_1, \omega_2)$. We consider Fig 13 which is the combination of two second order-systems connected in tandem.

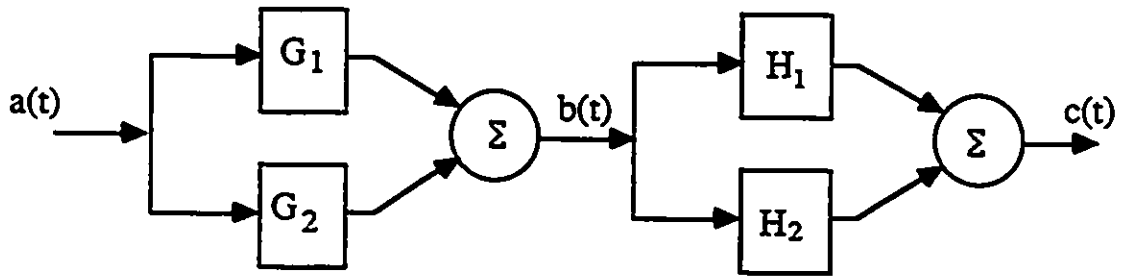

Fig. 13. Two second-order systems connected in tandem

The first system consisting of output-to-input transfer functions G_1, G_2 and the second system consists of the forward transfer functions H_1 and H_2, where H_2 is the second-order

forward transfer function. Let the input to the whole system be the sum of two sinusoids i.e.,

$$a(t) = e^{j\omega_1 t} + e^{j\omega_2 t} \tag{4.16}$$

The output of the first system be therefore,

$$b(t) = G_1(\omega_1)e^{j\omega_1 t} + G_1(\omega_2)e^{j\omega_2 t} + G_2(\omega_1, \omega_2)e^{j(\omega_1+\omega_2)t} \tag{4.17}$$

And the total output of the entire system is

$$\begin{aligned} c(t) \;=\; & H_1(\omega_1)G_1(\omega_1)e^{j\omega_1 t} + H_1(\omega_2)G_1(\omega_2)e^{j\omega_2 t} + H_1(\omega_1+\omega_2)G_2(\omega_1,\omega_2)e^{j(\omega_1+\omega_2)t} \\ & + H_2(\omega_1,\omega_2)G_1(\omega_1)G_1(\omega_2)e^{j(\omega_1+\omega_2)t} + H_2(\omega_1,\omega_1+\omega_2)G_1(\omega_1)G_2(\omega_1,\omega_2)e^{j(2\omega_1+\omega_2)t} \\ & H_2(\omega_2,\omega_1+\omega_2)G_1(\omega_2)G_2(\omega_1,\omega_2)e^{j(\omega_1+2\omega_2)t} \end{aligned} \tag{4.18}$$

If Q represents the total system then $c(t) = Q[a(t)]$ which is equal to zero according to the inverse theory[31]. Now using this relation and equating the coefficients of $e^{j(\omega_1+\omega_2)t}$ from both sides of equation (4.18) we have

$$H_1(\omega_1+\omega_2)G_2(\omega_1,\omega_2) + H_2(\omega_1,\omega_2)G_1(\omega_1)G_1(\omega_2) = 0 \tag{4.19}$$

Therefore,

$$H_2(\omega_1,\omega_2) = -\frac{G_2(\omega_1,\omega_2)}{G_1(\omega_1)G_1(\omega_2)G_1(\omega_1+\omega_2)} \tag{4.20}$$

In a similar manner as above we can calculate H_3. For this we consider the Fig 14. The input to the system is the sum of three sinusoids i.e., $a_1(t) = e^{j\omega_1 t} + e^{j\omega_2 t} + e^{j\omega_3 t}$. The steps are as follows,

$$\begin{aligned} b_1(t) \;=\; & G_1(\omega_1)e^{j\omega_1 t} + G_1(\omega_2)e^{j\omega_2 t} + G_1(\omega_3)e^{j\omega_3 t} + G_2(\omega_1,\omega_2)e^{j(\omega_1+\omega_2)t} \\ & G_2(\omega_1,\omega_3)e^{j(\omega_1+\omega_3)t} + G_2(\omega_2,\omega_3)e^{j(\omega_2+\omega_3)t} + G_3(\omega_1,\omega_2,\omega_3)e^{j(\omega_1+\omega_2+\omega_3)t} \end{aligned} \tag{4.21}$$

The output $c_1(t)$ is zero. Equating the coefficients of $e^{j(\omega_1+\omega_2+\omega_3)t}$ from $c_1(t)$ we get

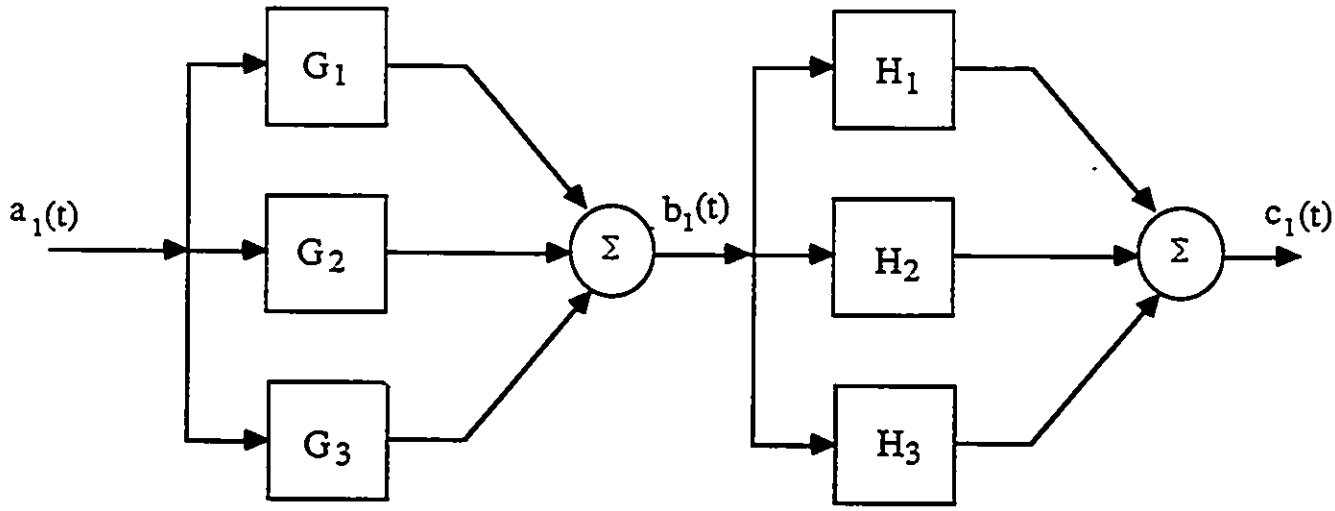

Fig. 14. Two third-order systems connected in tandem

$$H_1(\omega_1+\omega_2+\omega_3)G_3(\omega_1,\omega_2,\omega_3)+H_2(\omega_1,\omega_2+\omega_3)G_1(\omega_1)G_2(\omega_2,\omega_3)$$
$$+H_2(\omega_2,\omega_1+\omega_3)G_1(\omega_2)G_2(\omega_1,\omega_3)+H_2(\omega_3,\omega_1+\omega_2)G_1(\omega_3)G_2(\omega_1,\omega_2)$$
$$+H_3(\omega_1,\omega_2,\omega_3)G_1(\omega_1)G_1(\omega_2)G_1(\omega_3)=0 \qquad (4.22)$$

Using equations (4.15) and (4.20) the above equation becomes

$$\frac{G_3(\omega_1,\omega_2,\omega_3)}{G_1(\omega_1+\omega_2+\omega_3)}-\frac{G_1(\omega_1)G_2(\omega_2,\omega_3)G_2(\omega_1,\omega_2+\omega_3)}{G_1(\omega_1+\omega_2+\omega_3)G_1(\omega_1)G_1(\omega_2+\omega_3)}$$
$$-\frac{G_1(\omega_2)G_2(\omega_1,\omega_3)G_2(\omega_2,\omega_1+\omega_3)}{G_1(\omega_1+\omega_2+\omega_3)G_1(\omega_2)G_1(\omega_1+\omega_3)}-\frac{G_1(\omega_3)G_2(\omega_1,\omega_2)G_2(\omega_3,\omega_1+\omega_2)}{G_1(\omega_1+\omega_2+\omega_3)G_1(\omega_3)G_1(\omega_1+\omega_2)}$$
$$+H_3(\omega_1,\omega_2,\omega_3)G_1(\omega_1)G_1(\omega_2)G_1(\omega_3)=0 \qquad (4.23)$$

Therefore,

$$H_3(\omega_1,\omega_2,\omega_3) = -\frac{1}{G_1(\omega_1+\omega_2+\omega_3)G_1(\omega_1)G_1(\omega_2)G_1(\omega_3)}\Big[G_3(\omega_1,\omega_2,\omega_3)-$$
$$\frac{G_2(\omega_2,\omega_3)G_2(\omega_1,\omega_2+\omega_3)}{G_1(\omega_2+\omega_3)}-\frac{G_2(\omega_1,\omega_3)G_2(\omega_2,\omega_1+\omega_3)}{G_1(\omega_1+\omega_3)}$$
$$-\frac{G_2(\omega_1,\omega_2)G_2(\omega_3,\omega_1+\omega_2)}{G_1(\omega_1+\omega_2)}\Big] \qquad (4.24)$$

Thus, the first three forward Volterra transfer functions are calculated from the output-to-input transfer functions using the inverse technique. As we can see in the above analysis, all these H's are expressed in terms of G's and since the G's are expressible in terms of the laser parameters therefore, H's are expressed in terms of laser parameters.

Chapter 5

NONLINEAR DISTORTION

5.1 Nonlinearity in Semiconductor Lasers

As we have discussed before, the large bandwidth of the laser makes it very attractive for broadband distribution. But it is considered to be a major source of degradation in the fiber-optic system. The two sources of degradations are nonlinearity and noise. In analog multichannel transmission one of the main considerations is the signal quality i.e., high Signal-to-Noise ratio (SNR). Therefore, linearity of the laser light-current characteristic is very important because nonlinearity of the laser introduces distortion in the optical output which has a serious effect in the system performance. When a high signal level is used to modulate the laser, the generation of harmonic and intermodulation distortion becomes more serious. Therefore, analysis of nonlinearity is very important.

In communication systems it is the usual practice to characterize the nonlinearity in terms of memoryless approximations. However, in the case of the laser such an approximation can not be used to analyze the nonlinearity because the laser input-output involves memory. Therefore, a more accurate model for the device characteristics must be considered. In this respect, Volterra series can be used to model the frequency-dependent nonlinear behavior of the laser.

The relative intensity noise (RIN) of the laser causes intensity fluctuations of the output

light which arises due to the stochastic nature of the photon-generating process in the laser cavity. It is dependent on the d.c. bias of the laser. RIN may be calculated from the rate equations including the Langevin noise terms[1], [12] using the techniques of this thesis. However, in our work we have considered only the first source of degradation, the nonlinearity. This nonlinearity can be seen from the rate equations where the stimulated emission term, $g(N-N_o)(1-\epsilon Q)Q$, is the nonlinear coupling of electron and photon densities. It may be more clear to observe the nonlinearity if we recall equation (3.5)

$$\begin{aligned}\frac{I_a}{V'} &= \frac{N_o}{\tau_{sp}} + [\frac{1}{\tau_{sp}} + g(1-\epsilon Q)Q]\frac{[\frac{dQ}{dt} + \frac{Q}{\tau_p} - \frac{\Gamma\beta N_o}{\tau_{sp}}]}{[\Gamma g(1-\epsilon Q)Q + \frac{\Gamma\beta}{\tau_{sp}}]} \\ &\quad + \frac{d}{dt}\{[\frac{dQ}{dt} + \frac{Q}{\tau_p} - \frac{\Gamma\beta N_o}{\tau_{sp}}]/[\Gamma g(1-\epsilon Q)Q + \frac{\Gamma\beta}{\tau_{sp}}]\} \end{aligned} \tag{5.1}$$

where the relation between input current I_a and output light Q is clearly nonlinear.

In the analog application of the laser, a time varying electrical signal is used to modulate directly a laser diode about a bias current point as shown in Fig 15. Without any input signal, the optical power output is P_o and when a signal $a(t)$ is applied, the optical output power $P(t)$ is

$$P(t) = P_o[1 + ra(t)] \tag{5.2}$$

Here r is the electrical modulation depth which is defined by[21]

$$r = \frac{I}{I_o - I_{th}} \tag{5.3}$$

I is the peak amplitude of the signal about bias current point, I_o is the bias current and I_{th} is the threshold current of the device. To prevent excessive distortion in the output signal, the modulation must be confined to the linear-region of the curve. If I is greater than $(I_o - I_{th})$, which means if r is greater than 100 percent, the lower portion of the curve

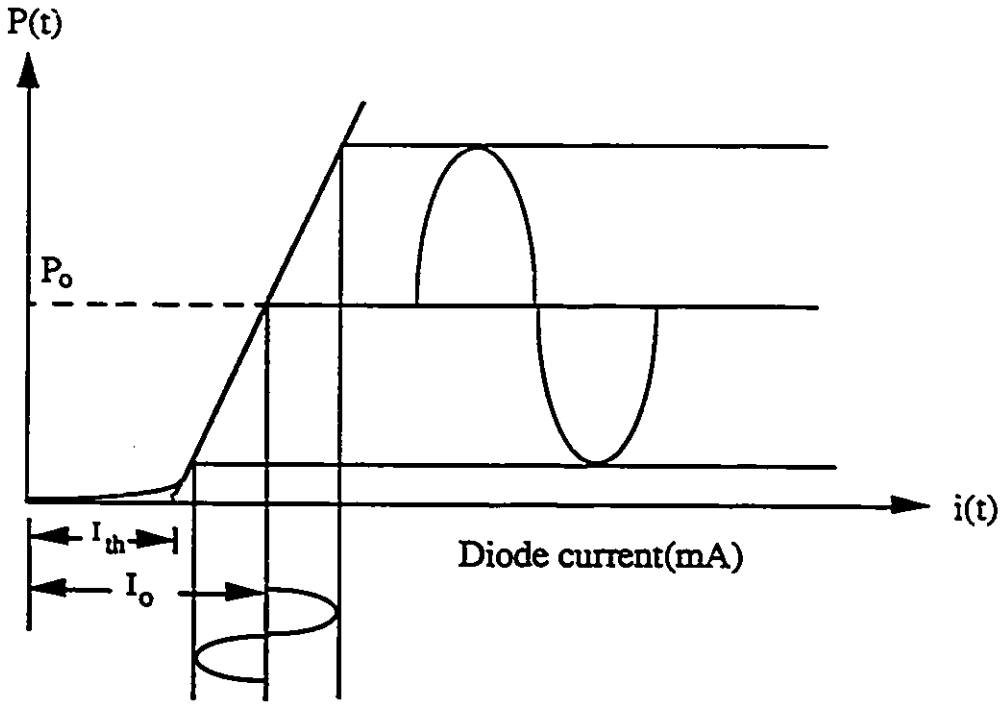

Fig. 15. Schematic of amplitude modulaticn range for analog modulation of laser diode.

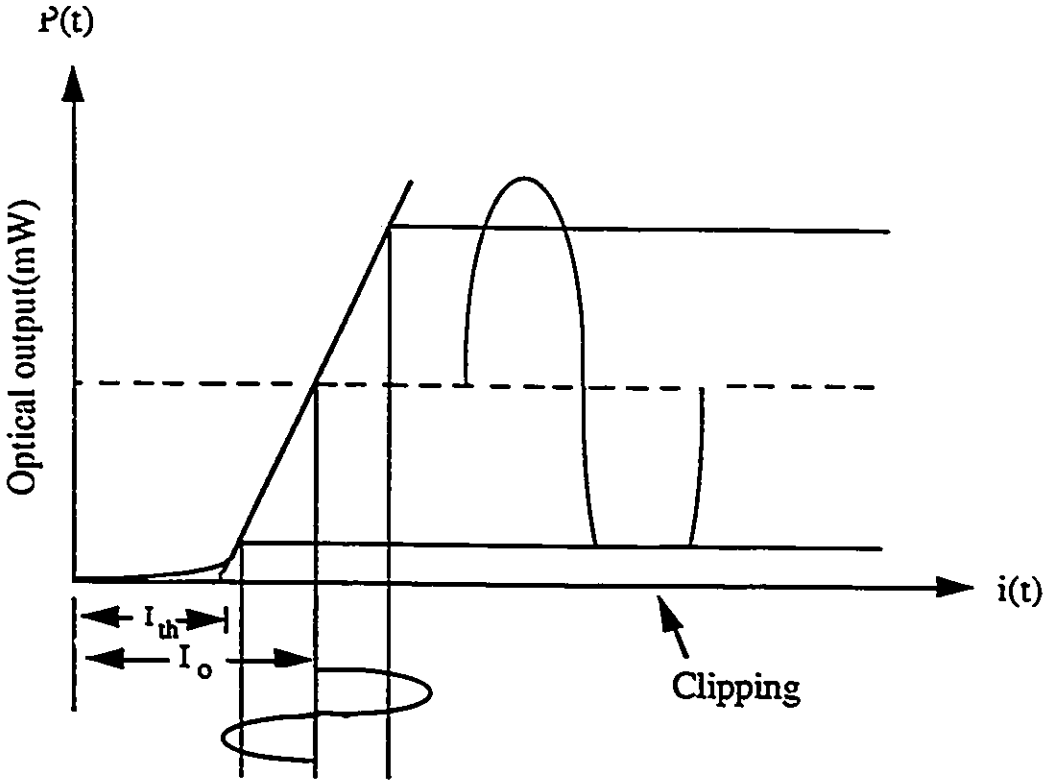

Fig. 16. Clipping in the optical output of a laser diode.

gets cut-off and severe distortion will result because of clipping. This is shown in Fig 16. In multichannel transmission, the composite signal is the sum of the signals from all the channels. When all these signals add, the phases are random and careful attention is necessary so that the resulting signal amplitude never becomes greater than $(I_o - I_{th})$. In that case a suitable bias current operating point should be chosen. In other words, the modulation depth should be adjusted so that no clipping results.

5.2 Harmonic and Intermodulation Distortions

In analog applications any device nonlinearities create frequency components in the output signal that were not present in the input signal. Two important nonlinear effects are harmonic and intermodulation distortions. When the signal input to a nonlinear device (e.g. laser) is a simple sinusoid

$$i(t) = I\ cos\omega t \tag{5.4}$$

the output will be of the form

$$q(t) = Q_o + C\ cos\omega t + 2HD\ cos2\omega t + 3HD\ cos3\omega t + ... \tag{5.5}$$

That is, the output signal will consist of a component at the input frequency ω plus spurious components at zero frequency, at the second harmonic frequency 2ω, at the third harmonic frequency 3ω and so on. Q_o is the d.c. component, C, $2HD$, $3HD$ etc. are the magnitudes of fundamental, second harmonic distortion, third harmonic distortion etc. respectively. This effect is known as harmonic distortion. The amount of nth-order distortion in decibels is given by

$$nth - order\ harmonic\ distortion\ = 20\ log\ \frac{nHD}{C} \tag{5.6}$$

When the input signal to the device consists of more than one sinusoid, then in addition to the harmonic distortions, the sum and difference frequencies give rise to the intermodulation distortions(IMD). To see the effect of IMD let the input to the device be sum of two

sinusoids with equal amplitudes

$$i(t) = I\ cos\omega_1 t + I\ cos\omega_2 t \tag{5.7}$$

The output signal will then be[21]

$$q(t) = \sum_{m,n} B_{mn} cos(m\omega_1 + n\omega_2)t \tag{5.8}$$

where m and $n = 0, 1, -1, 2, -2, 3, -3, ...$

This signal includes all the harmonics of ω_1 and ω_2 plus cross-product terms such as $\omega_2 - \omega_1$, $\omega_2 + \omega_1$, $\omega_2 - 2\omega_1$, $\omega_2 + 2\omega_1$, etc. The sum of the absolute values of the coefficients m and n determines the order of the intermodulation distortion[21]. For example, the second-order intermodulation products are at $\omega_1 + \omega_2$ and $\omega_1 - \omega_2$ with amplitude B_{11}, the third-order intermodulation products are at $2\omega_1 - \omega_2$, $2\omega_1 + \omega_2$, $2\omega_2 - \omega_1$ and $2\omega_2 + \omega_1$ with amplitudes B_{21} and B_{12}, and so on. Harmonic distortion are present wherever either $m \neq 0$ and $n = 0$ or when $m = 0$ and $n \neq 0$.

In general, the odd-order intermodulation products having $m = (n + 1)$ *or* $(n - 1)$ (such as $2\omega_1 - \omega_2$, $2\omega_2 - \omega_1$, $3\omega_1 - 2\omega_2$, etc.) are the most troublesome since they may fall within the bandwidth of the channel. Of these only the third-order terms are usually important since the amplitudes of the higher-order terms tend to be insignificant. In the case of the laser we are interested in calculating the second harmonic distortion, the third harmonic distortion and the third-order intermodulation distortion at $2\omega_1 - \omega_2$. For this, we consider the input current to the laser is the same as equation (5.7). Instead of B_{21}, we call the third-order intermodulation distortion IMD. Then we can model the output of the laser by

$$q(t) \ = \ Q_o + C\ cos\omega_1 t + 2HD\ cos2\omega_1 t + 3HD\ cos3\omega_1 t + IMD\ cos(2\omega_1 - \omega_2)t + ... \tag{5.9}$$

where $2HD$ and $3HD$ are the second harmonic and third harmonic distortions accumulated at $2\omega_1$ and $3\omega_1$ respectively due to the carrier at ω_1 (i.e., due to the input $I\ cos\omega_1 t$).

IMD is the magnitude of the intermodulation distortion accumulated at $2\omega_1 - \omega_2$ due to the interaction of both the input frequencies within the nonlinear device. In order to see the effect of these distortions on the system performance we need to express all these C, $2HD$, $3HD$ and IMD in terms of laser parameters. Therefore, we can proceed for the detailed calculation.

5.3 Analysis of Harmonic Distortions

The calculation of Volterra transfer functions for the laser was discussed in the previous chapter. Here, for the calculation of distortion we can use these transfer functions. With a sinusoidal signal $i(t) = I\ cos\omega t$ as the input to the laser and using the linear forward Volterra transfer function $H_1(\omega)$ we have calculated the response of the linear system in Appendix D which is

$$q_1(t) = I|H_1(\omega)|cos[\omega t + \theta(\omega)] \tag{5.10}$$

Comparing this with the linear term, $C\ cos\omega t$, on the right-hand side of equation (5.9), which is the response of the linear system, we have

$$C = I|H_1(\omega)| \tag{5.11}$$

If we observe equation (5.10), we can draw a few conclusions. For a sinusoidal input with frequency ω the response of a linear system also is a sinusoid with frequency ω. However, the output sinusoid is shifted in phase by an amount $\theta(\omega)$ and changed in amplitude by a factor $|H_1(\omega)|$ which is called the system gain. This gain is also a function of input frequency ω. Recalling equations (4.11) and (4.15) we find

$$|H_1(\omega)| = \frac{1}{|(-F\omega^2 + jE\omega + D)|} \tag{5.12}$$

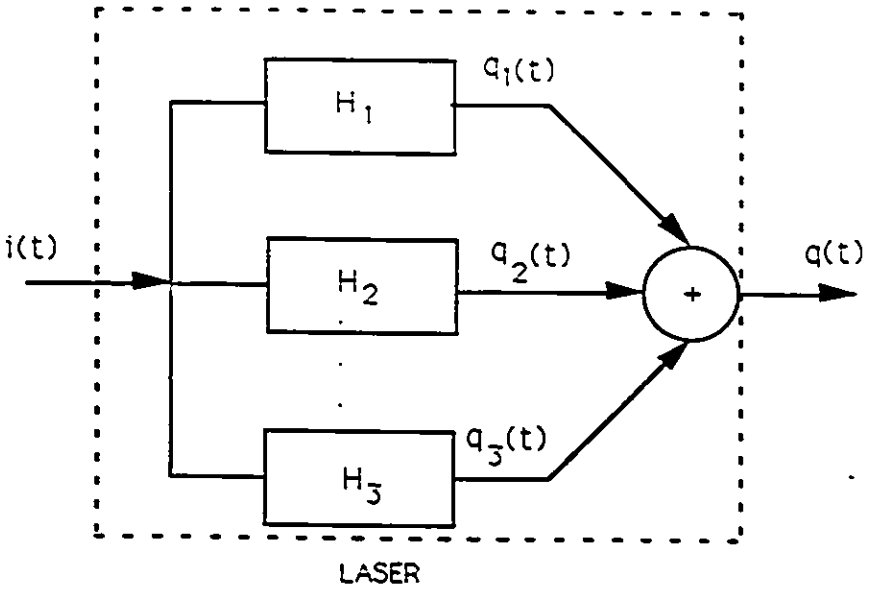

Fig. 17. A simple third order system representing the Laser.

Now, we like to see how the system gain varies with frequency and bias current. For this we will use a GaAlAs single-mode, Ortel SL-620, laser diode. The parameters of this device as given by Way [16] are listed in Table 5.1. We have plotted equation (5.12) for three different bias currents in Fig 18. In the plot, however, we have

Description	Parameters	Values	Units
Threshold current at room temp.	I_{th}	21	mA
Volume of active region times electronic charge	V'	1.44 X10^{-35}	m^3-coulomb
Photon lifetime	τ_p	2	psec
Spontaneous recombination lifetime of electron	τ_{sp}	3.72	nsec
transparent carrier density	N_o	4.6 X10^{24}	m^{-3}
Optical gain coefficient	g	1 X10^{-12}	m^3/sec
Optical confinement coefficient	Γ	0.646	unitless
Spontaneous emission coefficient	β	10^{-3}	unitless
Gain compression parameter	ϵ	3.8 X10^{-23}	m^3
Lasing wavelength	λ	0.835	μm

Table 5.1: Parameters for an Ortel SL-620 laser diode.

normalized the gain with respect to D, which is a constant and is independent of frequency. From the figure we can see the effect of bias current on the frequency response. At lower bias current there is a sharp resonance peak and this peak broadens and weakens as the bias current increases. At bias current of 36.75 mA this peak has almost disappeared.

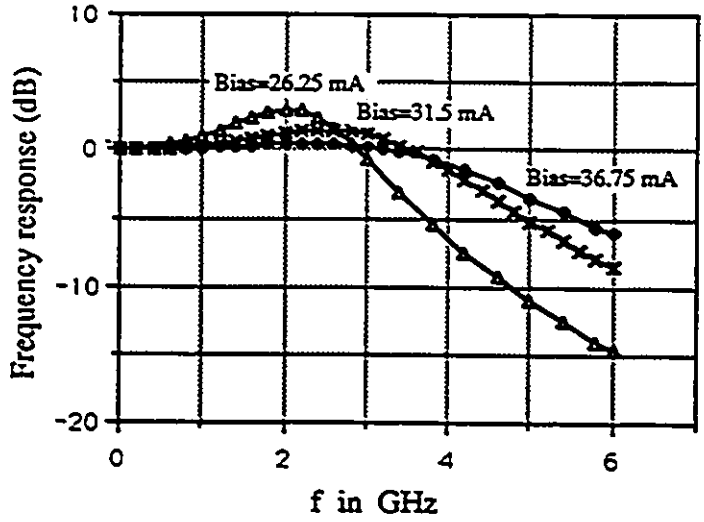

Fig. 18. Calculated frquency response, $|H_1(\omega)|$, for different bias current levels.

In the large-signal-model rate equations as given in equations (3.1) and (3.2) the term ϵ is the gain compression term. To see the effect of gain compression on laser frequency response we have plotted $H_1(\omega)$ for two different bias currents which are shown in Fig 19 and Fig 20. In both cases it is seen that if the gain compression is neglected i.e. $\epsilon = 0$, the resonance peak height raises to a very high value (15 dB for bias = 26.25 mA and 19 dB for bias = 31.5 mA). Such gain characteristics are not found in practice. We have also shown the Gain curve using Darcie's[15] expression (1.4) for $\epsilon = 3.8X10^{-23}$. Although there is a slight difference observed between our theoretical curve and Darcie's curve, our analysis gives the exact gain characteristic for the device. Darcie's expression is based on some assumptions and if we make these assumptions as discussed in section 3.3.1 and neglect the small product

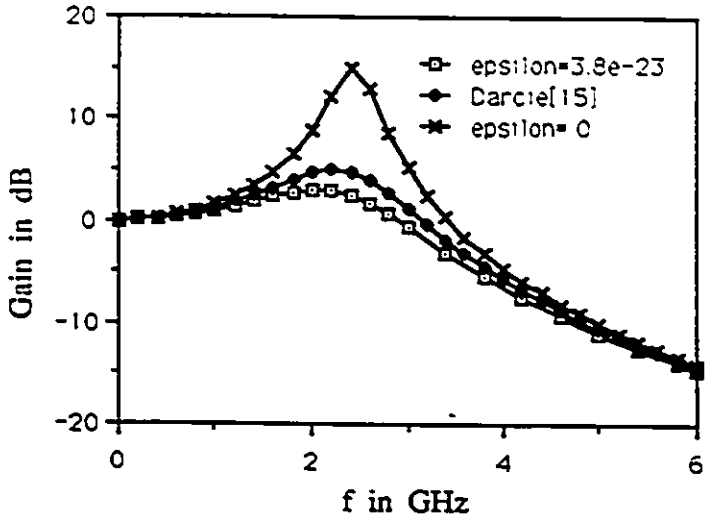

Fig. 19. Frequency response, $|H_1(\omega)|$, for d.c. bias=26.25 mA.

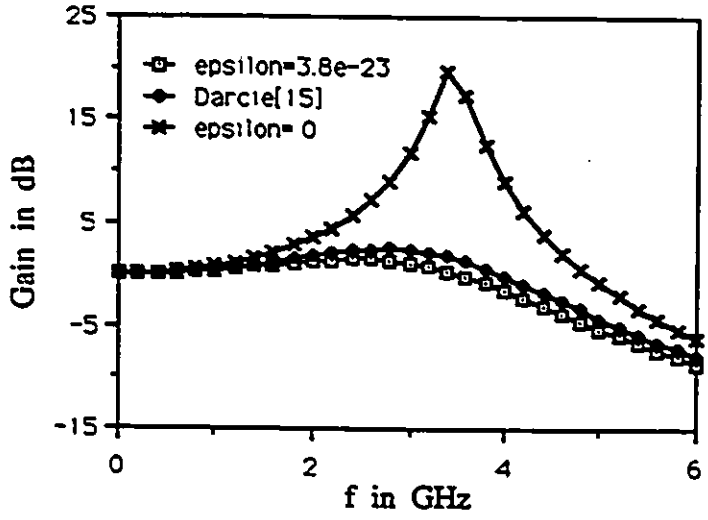

Fig. 20. Frequency response, $|H_1(\omega)|$, for d.c. bias=31.5 mA.

term ϵQ_o, there is no difference between the two curves. In equation (5.11), C is the intensity of the optical carrier, I is the amplitude of input current. Thus, the amplitude of the optical carrier is the magnitude of the input current times the system linear transfer function.

5.3.1 Second Harmonic Distortion

Let us now consider the output $q_2(t)$ of the system H_2 in Fig 17. Here H_2 is the second-order Volterra transfer function as calculated for the laser in chapter 4. The output of the system is (detailed calculation is given in Appendix D)

$$q_2(t) = \frac{I^2}{4} Re[H_2(\omega,\omega)e^{j2\omega t}] + \frac{I^2}{4} Re[H_2(\omega,-\omega)] \tag{5.13}$$

The response of the second-order system to a sinusoidal signal of input frequency ω is, therefore, a sinusoid of frequency 2ω plus a constant term at zero frequency which we neglect. The first term in equation (5.13) is the sinusoid with amplitude $\frac{I^2}{4}|H_2(\omega,\omega)|$. The value of the constant is given by the second term in equation (5.13). However, in the calculation of harmonic distortion we are interested only on the first term which is the second harmonic term. Comparing this with equation (5.9) we find the magnitude of second harmonic distortion

$$2HD = \frac{I^2}{4}|H_2(\omega,\omega)| \tag{5.14}$$

It is seen from the above equation that, the second harmonic distortion is completely dependent on signal frequency and proportional to the square of the input signal amplitude. If we now take the ratio of equation (5.14) to equation (5.11), it will give the distortion relative to the fundamental carrier amplitude. Thus,

$$\frac{2HD}{C} = \frac{|H_2(\omega,\omega)|}{4|H_1(\omega)|} I \tag{5.15}$$

The optical modulation depth (OMD) is defined [15] as the ratio of the peak light intensity C of the carrier to the steady state value Q_o. In terms of the electrical quantities

and the laser transfer function this can be expressed as follows. We will denote OMD by m. Therefore,

$$\begin{aligned} m &= \frac{C}{Q_o} \\ &= \frac{I|H_1(\omega)|}{(I_o - I_{th})|H_1(0)|} \end{aligned} \tag{5.16}$$

Where, I_o and I_{th} are the bias and threshold currents of the device. Since Hs are already expressed in terms of output-to-input transfer functions Gs therefore, using equations (4.15), (4.20) and (5.16) equation (5.15) can be expressed in terms of Gs as

$$\frac{2HD}{C} = \frac{m(I_o - I_{th})|G_2(\omega,\omega)|}{4|G_1(0)G_1(2\omega)|} \tag{5.17}$$

In chapter 4 we have expressed all these Gs in terms of the laser parameters. Thus, distortion is expressed in terms of the laser parameters, carrier frequency and optical modulation depth. We have plotted the distortion at bias current of 36.75 mA for the laser of Table 5.1 in Fig 21. Here an optical modulation depth of 0.4 is considered. For the purpose of comparison we took the second harmonic distortion expression given by equation (1.1) and plotted it in the same graph. An excellent agreement is observed between our result and Darcie's result. Darcie[15] had compared his result with the experimental result where he had found a close agreement. Thus, our theoretical model (5.17) for the second harmonic distortion agrees with experimental result.

We have also plotted equation (5.17) based on the simplified analysis discussed in section 3.3.1 and with the parameters given in equation (B.21). Excellent agreement is observed between this curve and exact analysis curve. The transfer-function-based model of equation (5.17) can be easily converted to device-parameter-based model of equation (1.1) using simplified analysis technique. This means that our assumptions for the simplified analysis are quite reasonable.

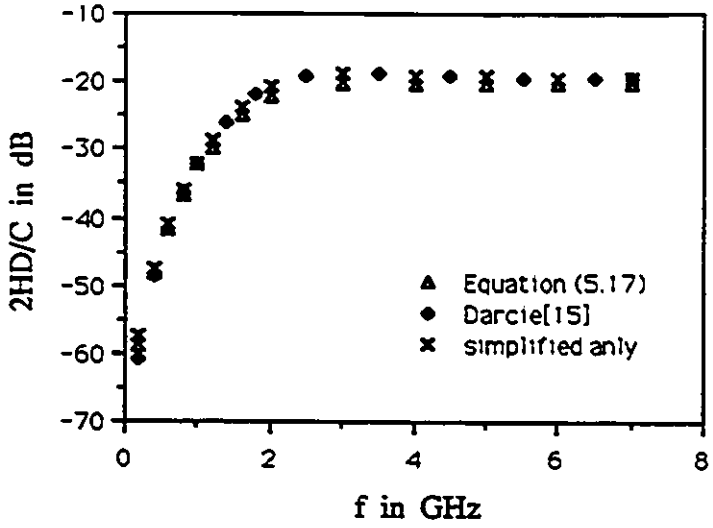

Fig. 21. Variation of second harmonic distortion with frequency for m =0.4 and bias=36.75 mA.

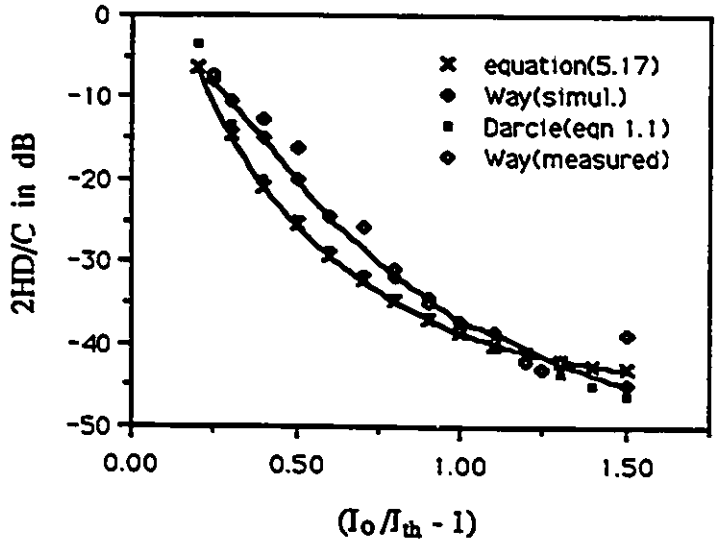

Fig. 22. Variation of 2HD with d.c. bias. The carrier is at 1 GHz with a peak amplitude of 5.6 mA.

W.I.Way of reference [16] has performed his simulation for the same laser using the software package SPICE. In Fig 22 we have plotted the second harmonic distortion as a function of bias current. Way's results are also shown in the same plot. The agreement is very good.

5.3.2 Third Harmonic Distortion

Now we consider the output $q_3(t)$ of the system H_3 in Fig 17. The calculation is done in Appendix D and the response is given by

$$q_3(t) = (\frac{I^3}{24})Re[H_3(\omega,\omega,\omega)e^{j3\omega t}] + (\frac{I^3}{8})Re[H_3(\omega,\omega,-\omega)e^{j\omega t}] \tag{5.18}$$

The response $q_3(t)$ consists of a third harmonic and a first harmonic of the input frequency ω. The amplitude and phase of the third harmonic is seen to be determined by the third order Volterra transfer function H_3 at a point where all of its arguments are equal to ω. Similarly, the first harmonic is also determined by the third order transfer function at a point where two of its arguments are equal to ω and one is equal to $(-\omega)$. The magnitude of the third harmonic term is $(\frac{I^3}{24})|H_3(\omega,\omega,\omega)|$ which we called $3HD$ in equation (5.9). Thus,

$$3HD = \frac{I^3}{24}|H_3(\omega,\omega,\omega)| \tag{5.19}$$

Therefore, the third harmonic distortion is dependent on the carrier frequency and proportional to the third power of the input signal amplitude. Taking the ratio of equations (5.19) to (5.11) we can obtain the relative third harmonic distortion

$$\frac{3HD}{C} = \frac{|H_3(\omega,\omega,\omega)|}{24|H_1(\omega)|}I^2 \tag{5.20}$$

Using the definition of OMD as given in (5.16) we can write

$$\frac{3HD}{C} = \frac{m^2(I_o - I_{th})^2|H_3(\omega,\omega,\omega)|}{24|H_1(\omega)|^3}|H_1(0)|^2 \tag{5.21}$$

We know that $H_1(0)$ is just the inverse of $G_1(0)$ and H_3 is expressed in terms of Gs in equation (4.24). With these relations the above equation becomes,

$$\frac{3HD}{C} = \frac{m^2(I_o - I_{th})^2}{24|G_1(0)|^2|G_1(3\omega)|}[G_3(\omega,\omega,\omega) - 3\frac{G_2(\omega,\omega)G_2(\omega,2\omega)}{G_1(2\omega)}] \qquad (5.22)$$

In this way we have expressed the distortion in terms of carrier frequency, OMD and the laser output-to-input transfer function, Gs. For a bias current of 36.75 mA and an optical modulation depth of 0.4, we have plotted $3HD$ as a function of frequency in Fig 23. In the same graph we have also shown Darcie's[3] results obtained from the expression (1.2). Here again an excellent agreement is observed between the two results. If we analyze the $2HD$ and $3HD$ graphs in Fig 21 and Fig 23 a few conclusions can be drawn. In the low frequency region, distortion increases as the frequency increases. But after a certain frequency range both second harmonic- and third harmonic distortion reach a steady state value which is almost independent of frequency. This means that for a fixed OMD, in the high frequency region harmonic distortion is dependent only on the laser parameters. The variation of $3HD$ with d.c. bias is shown in Fig 24.

Simplification of equation (5.22) using the parameters given in equation (B.21) of Appendix B gives simple expression for $3HD$ as

$$\frac{3HD}{C} = \frac{3}{2}m^2\frac{[\{(\frac{\omega}{\omega_r})^4 + \frac{1}{2}(\frac{\omega}{\omega_r})^2\}^2 + (\frac{\epsilon\omega^2}{g\omega_r^2})^2]^{\frac{1}{2}}}{|G'(2\omega)G'(3\omega)|} \qquad (5.23)$$

In which $G'(\omega) = 1 - \frac{\omega^2}{\omega_r^2} + j\frac{\epsilon}{g}\omega$. The term $(\frac{\epsilon\omega^2}{g\omega_r^2})^2$ is smaller then the other term in the numerator and it can be omitted. Therefore, equation (5.23) coincides with equation (1.2). To see the effect of gain compression, ϵ, on distortion we have plotted $2HD$ for three values of ϵ in Fig 25. It is seen that distortion decreases as ϵ increases. Therefore, for superior distortion characteristics higher values of ϵ is desired. However, device gain is compressed more with higher values of ϵ. Fig 26 shows the variation of $2HD$ with optical modulation depth. Here the curves are plotted for three values of m. Clearly, distortion increases with increasing values of m as it showed.

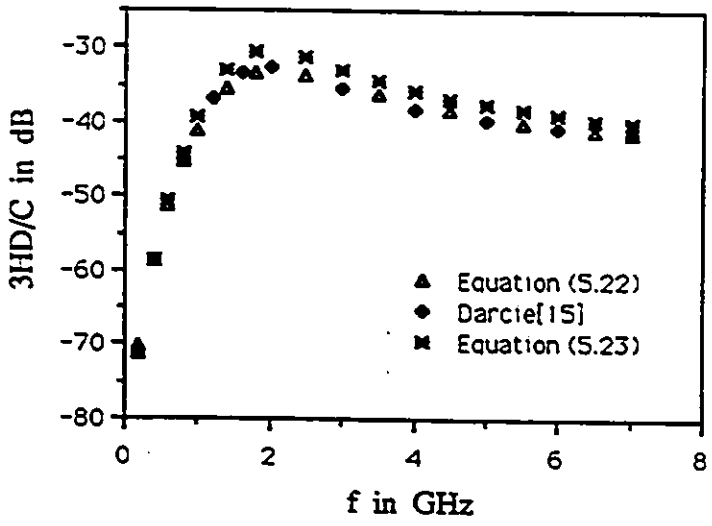

Fig. 23. Variation of third harmonic distortion with frequency for $m = 0.4$ and $I_o = 36.75$ mA.

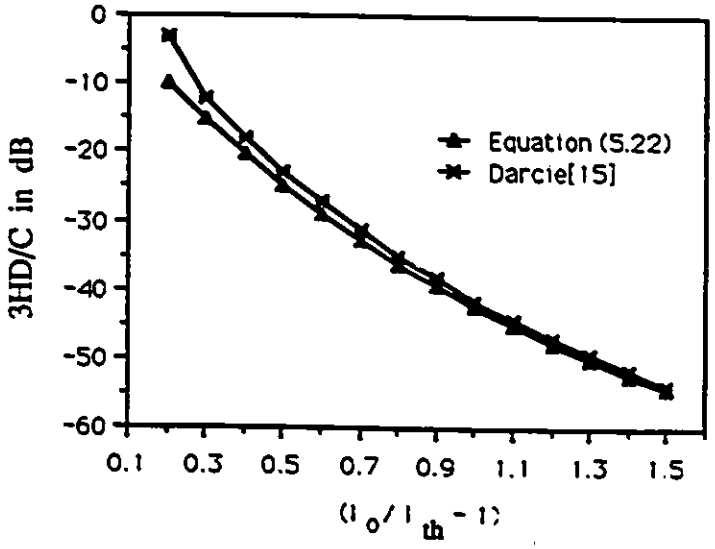

Fig. 24. Variation of third harmonic distortion with d.c. bias. The carrier is at 2 GHz with a peak amplitude of 5.6 mA.

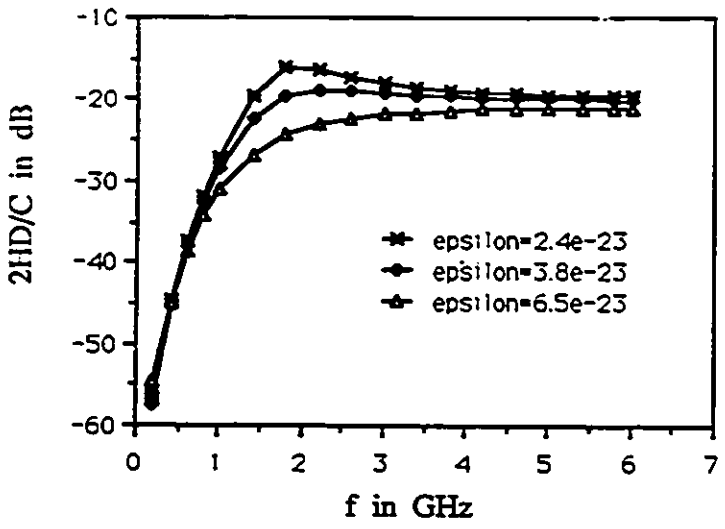

Fig. 25. Variation of second harmonic distortion with frequency for different values of ϵ, $m = 0.4$ and $I_o = 31.5$ mA.

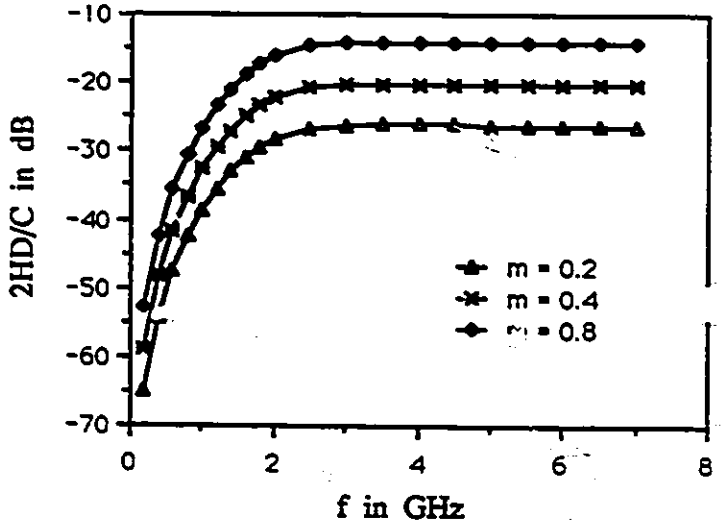

Fig. 26. Variation of second harmonic distortion with frequency for different values of m $I_o = 36.75$ mA and $\epsilon = 3.8X10^{-23}$.

5.3.3 A Comparison With A. Czylwik's [17] Analysis

Andreas Czylwik [17] analyzed nonlinearities of semiconductor laser applying Volterra series to the single-mode rate equations. He used Volterra series directly to solve the equations and carried out the analysis in the frequency domain using Fourier transform. Although he was able to derive the Volterra kernels for the laser, the laser parameters such as ϵ, the gain compression (extremely important in the nonlinearity analysis), Γ, the optical confinement coefficient were not considered in his analysis. Moreover he did not deal with the intermodulation distortion, another important factor in the subcarrier multiplexing multichannel transmission systems. Although he expressed the harmonic distortions in terms of transfer functions, the results remained unsimplified, computation is not simple and the effects of optical modulation depth, relaxation oscillation frequency and laser parameters on distortion are not clear from the distortion expressions.

Our approach of Volterra series analysis is quite different. We used, first, an output-to-input approach to the rate equations and expressed the drive current $i(t)$ of the laser as a function of photon density $q(t)$. By doing this we eliminated the carrier density $n(t)$ from the rate equations which reduces the number of parameters in the distortion calculation. We calculated the output-to-input transfer functions from the system equation using harmonic input method [30]. Using inverse technique [31], we then calculated the forward transfer functions from output-to-input transfer functions.

The presence of gain compression term ϵ in the rate equations increases, extremely, the complexity of the analysis. Therefore, direct solution of the rate equations is very difficult. However, the output-to-input approach reduces such complexities in the analysis. After simplification, the distortion expressions of our analysis become simple, the number of parameters is greatly reduced and the computation is also simpler.

We have compared our analysis with Czylwik's [17] results for $H_1(\omega)$, $2HD$ and $3HD$ using our exact equations (5.12), (5.17) and (5.22) and the laser parameters as given in [17].

An excellent agreement is observed between the results. In this comparison we have used the more accurate value of Q_o as obtained from

$$I_o = V'[\frac{N_o}{\tau_{sp}} + (\frac{1}{\Gamma} + \frac{1}{a\tau_{sp}})(\frac{Q_o}{\tau_p} - \frac{\Gamma\beta N_o}{\tau_{sp}})]$$

where,

$$a = \Gamma(gQ_o + \frac{\beta}{\tau_{sp}} - \epsilon g Q_o^2)$$

because the laser[17] characteristic is very much sensitive to Q_o. However, in this thesis, we have used Q_o as given by equation (3.8) for simplicity, which was recommanded by Tucker [25] and was also used by Darcie [15].

5.4 Analysis of Intermodulation Noise

In analog multichannel transmission the generation of intermodulation noise originating from the interference between different channels causes serious signal degradation. In simulation or in experiment, it is very easy to observe the effect of intermodulation products in the frequency plot or on the spectrum analyzer. But in theory it is extremely difficult to analyze the IMD effect for more than two input carriers and for higher-order products. We start our analysis with two input (to the laser) carriers at frequencies ω_1 and ω_2 of equal amplitudes and observe the two tone third-order intermodulation products at frequencies $(2\omega_1 - \omega_2)$ and $(2\omega_2 - \omega_1)$. Let

$$i(t) = I\cos\omega_1 t + I\cos\omega_2 t \tag{5.24}$$

With (5.24) as the input, we have calculated intermodulation distortions using Volterra series and Volterra transfer functions. Two-tone IMD is a third-order effect and the quantities that give these distortion terms are shown in Appendix E. From equation (E.12)

$$\tilde{q}_3(t) = \frac{I^3}{8}Re[H_3(\omega_1, \omega_1, -\omega_2)e^{j(2\omega_1-\omega_2)t}] + \frac{I^3}{8}Re[H_3(-\omega_1, \omega_2, \omega_2)e^{j(2\omega_2-\omega_1)t}] \tag{5.25}$$

In the above equation, $\eta_3(t)$ is the (fractional) output of the lower box H_3 in Fig 17 for the input (5.24). The first term on the right hand side is a sinusoid with frequency $(2\omega_1 - \omega_2)$ and amplitude $\frac{I^3}{8}H_3(\omega_1, \omega_1, -\omega_2)$ and the second term is also a sinusoid of frequency $(2\omega_2 - \omega_1)$ and its amplitude is $\frac{I^3}{8}H_3(-\omega_1, \omega_2, \omega_2)$. Although we do not have any input sinusoid of frequency $(2\omega_1 - \omega_2)$ or $(2\omega_2 - \omega_1)$, such frequency components appeared in the output signal because of interference of two carriers. In fact, there are many other frequency components appear in the output signal. Since we are interested only in the third-order IMD therefore, we will consider only the above two components. Both of them are third-order intermodulation products. Now, if we compare the above equation with equation (5.9), we can write the magnitude of the intermodulation distortion at frequency $(2\omega_1 - \omega_2)$ as

$$IMD = \frac{I^3}{8}|H_3(\omega_1, \omega_1, -\omega_2)| \tag{5.26}$$

In a similar way as $2HD$ and $3HD$, we can express the intermodulation distortion relative to the fundamental amplitude. For the purpose of calculation we consider IMD at $\omega_1 = \omega_2 = \omega$. Therefore,

$$\frac{IMD}{C} = \frac{m^2(I_o - I_{th})^2|H_3(\omega, \omega, -\omega)|}{8|H_1(\omega)|^3}|H_1(0)|^2 \tag{5.27}$$

In terms of Gs this can be written as follows.

$$\frac{IMD}{C} = \frac{m^2(I_o - I_{th})^2}{8|G_1(0)|^3|G_1(\omega)G_1(2\omega)|}\eta \tag{5.28}$$

where,

$$\begin{aligned}\eta = {} & G_3(\omega, \omega, -\omega)G_1(0)G_1(2\omega) - 2G_2(\omega, -\omega)G_2(\omega, 0)G_1(2\omega) \\ & -G_2(\omega, \omega)G_2(-\omega, 2\omega)G_1(0)\end{aligned} \tag{5.29}$$

Therefore, two-tone third-order relative IMD is also proportional to the square of OMD. We have plotted equation (5.28) in Fig 27 for a bias of 36.75 mA and $m = 0.4$. Here

also distortion increases with increasing frequency and it reaches a constant level at higher frequencies. Darcie's[15] IMD equation (1.3), we also plotted in the same graph where he has a null at 3 GHz. This is because of the fact that in the calculation of IMD from (1.3), the contribution from imaginary part is very small which does not give the accurate device performance for lasers with large ϵ. However, we have found that the imaginary part contributes a significant amount to the calculation of IMD. Here our IMD model disagrees with Darcie's model. In order to see this difference more directly we have made a few reasonable assumptions. Starting with the simplified analysis as discussed in section 3.3.1 (Parameters as given in Appendix B equation (B.21)), we went through the detailed calculations in Appendix F and finally we expressed intermodulation distortion directly in terms of laser parameters. Thus,

$$\frac{IMD}{C} = \frac{1}{2}m^2 \frac{[\{(\frac{\omega}{\omega_r})^4 - \frac{1}{2}(\frac{\omega}{\omega_r})^2\}^2 + \{\frac{\omega\gamma}{g\omega_r^2}\}^2]^{\frac{1}{2}}}{|G_1'(\omega)G_1'(2\omega)|} \tag{5.30}$$

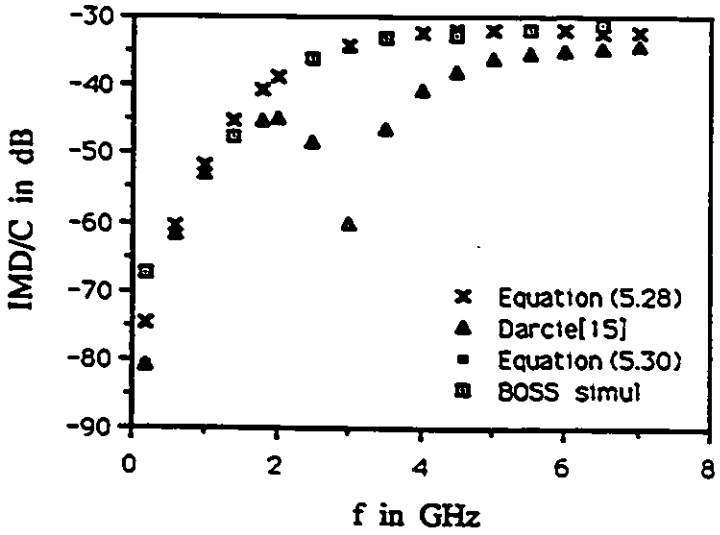

Fig. 27. Two-tone third order IMD at $m = 0.4$ and bias=36.75 mA.

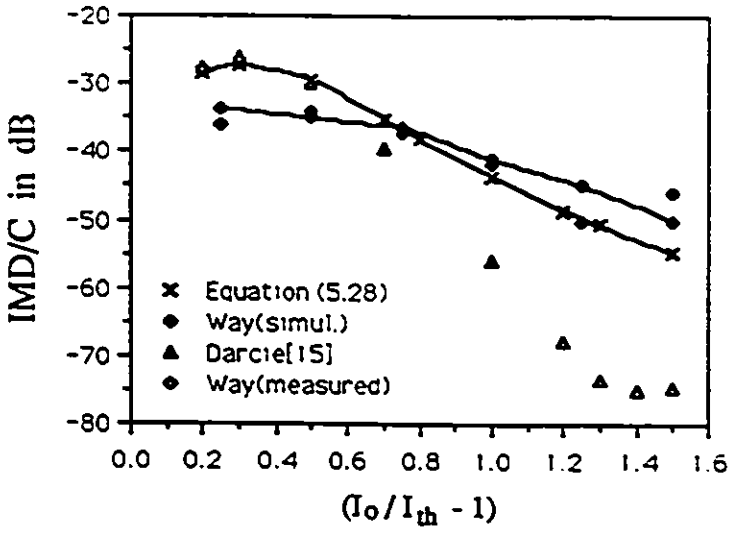

Fig. 28. Variation of IMD with bias current at $f = 4$ GHz.

where,

$$G_1'(\omega) = 1 - \frac{\omega^2}{\omega_r^2} + j\frac{\epsilon}{g}\omega \ ,$$

which gives almost the same result as (5.28). This differs from equation (1.3) in that m is the modulation depth per carrier and $\frac{\omega^2}{\omega_r^2}\tau_p$ is replaced with $\frac{\omega^2\epsilon}{\omega_r^2 g}$. This term in the numerator is the contribution from the imaginary part of η, of equation (5.29), and is completely dependent on device gain g and gain compression ϵ. Therefore, in addition to the optical modulation depth m and relaxation oscillation frequency ω_r, the parameters g and ϵ are necessary for the characterization of IMD. Equation (5.30) is also plotted in Fig 27 where it coincides with the exact analysis curve. The data points obtained with BOSS simulation model of the laser [35] developed by our colleague P. Neusy are also shown in the same plot. Our theoretical IMD along with Way's simulated and measured results is shown in Fig 28 where our results are closely matched with way's results except a 7~9 dB difference in the lower bias region. Significant difference between Darcie's results and measured results

can be observed as the bias level increases. Using a smaller value of gain compression ($\epsilon = 8.0X10^{-24}$), we calculated IMD with equation (5.30) and also with Darcie's equation (1.3). This is plotted in Fig 29. No difference is seen between the graphs which means that both the IMD models coincide for devices with small ϵ. However, our IMD model is more general and is true for all devices with any value of ϵ. Fig 30 is a plot showing the variation of IMD with modulation depth m.

In Fig 29 the two peaks (one at $\frac{\omega_r}{2}$, one at ω_r) and the null at 3 GHz are significant. The two peaks are related to the gain compression term ϵ. A laser with uniform electron distribution ($\epsilon = 0$) has zero diffusion damping and a high gain at the resonance frequency ω_r. In equation (5.30), when $\epsilon = 0$, the denominator $|G_1'(\omega)G_1'(2\omega)|$ has two nulls one at $\frac{\omega_r}{2}$ and the other at ω_r, the numerator has a null at $\frac{\omega_r}{\sqrt{2}}$ and a null at zero frequency. At high frequencies, the numerator term increases with frequency. The combined effect of the numerator and the denominator results a IMD as shown in Fig 29. For small values of ϵ, IMD shows similar peaks and nulls. With increasing values of ϵ the nulls of the numerator and the denominator terms decrease. At higher ϵ these nulls vanish.

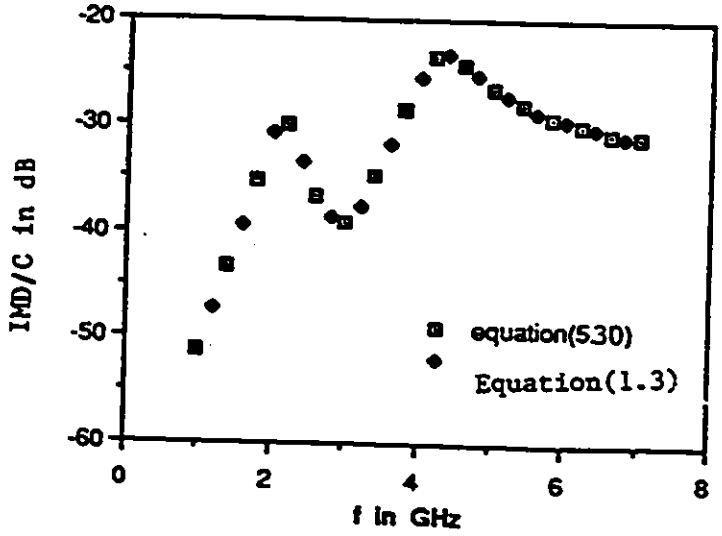

Fig. 29. IMD for $\epsilon = 8.0X10^{-24}$, $m = 0.4$ and bias=36.75 mA.

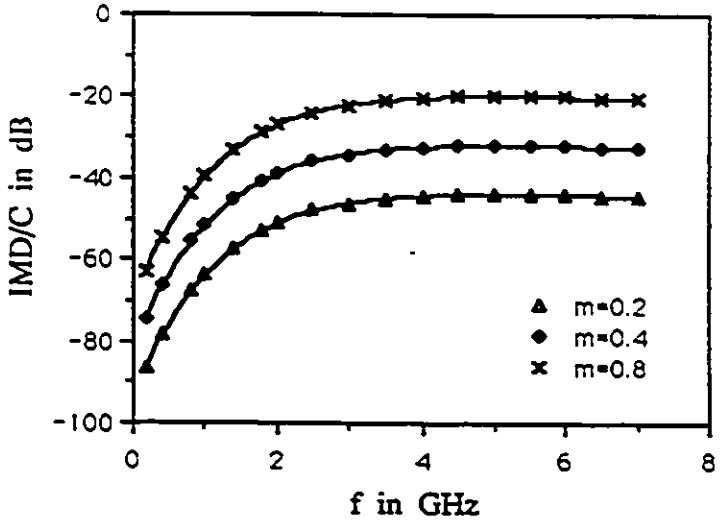

Fig. 30. Variation of IMD with modulation depth, $\epsilon = 3.8X10^{-23}$ and bias=36.75 mA.

For Ortel SL-620 laser, the value of ϵ is very high ($\epsilon = 3.8X10^{-23}$) and the actual intermodulation characteristic is as shown in Fig 27 without any null.

5.5 Intermodulation Spectra

The Mircea-Sinnreich equation expresses the power spectrum of output of a system in terms of the power spectrum of input. If $S_q(\omega)$ and $S_i(\omega)$ are the spectrums of photon density and current respectively then the Mircea-Sinnreich equation for the two-sided power spectrum can be written as[30]

$$\begin{aligned} S_q(\omega) &= < q(t) >^2 \delta(\omega) \\ &\quad + S_i(\omega)|H_1(\omega) + \frac{1}{2}\int_{-\infty}^{\infty} S_i(\omega_1) H_3(\omega, \omega_1, -\omega_1) d\omega_1|^2 \\ &\quad + \frac{1}{2!}\int_{-\infty}^{\infty} S_i(\omega_1) S_i(\omega - \omega_1)|H_2(\omega_1, \omega - \omega_1)|^2 d\omega_1 \\ &\quad + \frac{1}{3!}\int_{-\infty}^{\infty}\int_{-\infty}^{\infty} S_i(\omega_1) S_i(\omega_2) S_i(\omega - \omega_1 - \omega_2) \cdot \end{aligned}$$

$$|H_3(\omega_1, \omega_2, \omega - \omega_1 - \omega_2)|^2 d\omega_1 d\omega_2 \tag{5.31}$$

where $< q(t) >$ is the average value of $q(t)$ and $\delta(\omega)$ is a unit impulse function. In the above equation we have considered terms up to the third order. H_1, H_2 and H_3 are the linear, second- and third-order forward transfer functions, respectively. Since H's are known therefore, laser output spectra can be determined when the input spectra is known. In the right-hand side of the equation, there exists the d.c. term, the linear, second-order and third-order terms. We write the equation again as

$$S_q(\omega) = S_{q_0}(\omega) + S_{q_1}(\omega) + S_{q_2}(\omega) + S_{q_3}(\omega) \tag{5.32}$$

where

$$S_{q_1}(\omega) = S_i(\omega)|H_1(\omega) + \frac{1}{2}\int_{-\infty}^{\infty} S_i(\omega_1) H_3(\omega, \omega_1, -\omega_1) d\omega_1|^2 \tag{5.33}$$

is the fundamental output spectrum. In equation (5.33) the term $\frac{1}{2}\int_{-\infty}^{\infty} S_i(\omega_1) H_3(\omega, \omega_1, -\omega_1) d\omega_1$ appeared in addition to the term $H_1(\omega)$ is because of the contribution from the third-order system H_3 which is, in fact, extremely small compared to $H_1(\omega)$. If we neglect this term the output-input spectral relation becomes

$$S_{q_1}(\omega) = |H_1(\omega)|^2 S_i(\omega) \tag{5.34}$$

which is well known for any linear system. It is shown in the Fig 31 below.

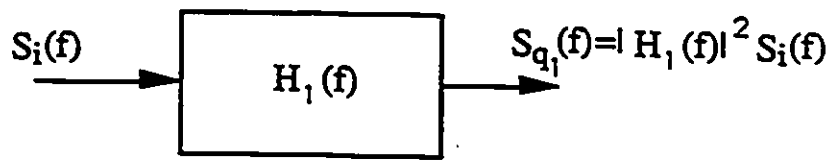

Fig. 31. Input-Output spectral relationship of a linear system.

From (5.31) and (5.32)

$$S_{q_2}(\omega) = \frac{1}{2!}\int_{-\infty}^{\infty} S_i(\omega_1)S_i(\omega-\omega_1)|H_2(\omega_1,\omega-\omega_1)|^2 d\omega_1 \tag{5.35}$$

Using equations (4.11), (4.12) and (4.20) one can write

$$\begin{aligned} S_{q_2}(\omega) &= \frac{(2L-N\omega^2)^2+(M\omega)^2}{2|G_1(\omega)|^2}\int_{-\infty}^{\infty}\frac{S_i(\omega_1)}{|G_1(\omega_1)|^2}\frac{S_i(\omega-\omega_1)}{|G_1(\omega-\omega_1)|^2}d\omega_1 \\ &= \frac{(2L-N\omega^2)^2+(M\omega)^2}{2|G_1(\omega)|^2}\int_{-\infty}^{\infty} S_{q_1}(\omega_1)S_{q_1}(\omega-\omega_1)d\omega_1 \\ &= \frac{(2L-N\omega^2)^2+(M\omega)^2}{2|G_1(\omega)|^2}[S_{q_1}(\omega) * S_{q_1}(\omega)] \end{aligned} \tag{5.36}$$

Similarly, with little assumption it can be shown that

$$\begin{aligned} S_{q_3}(\omega) &= \frac{(6R-2G\omega^2)^2+(2S\omega)^2}{6|G_1(\omega)|^2}\int_{-\infty}^{\infty}\int_{-\infty}^{\infty} S_{q_1}(\omega_1)S_{q_1}(\omega_2)S_{q_1}(\omega-\omega_1-\omega_2)d\omega_1 d\omega_2 \\ &= \frac{(6R-2G\omega^2)^2+(2S\omega)^2}{6|G_1(\omega)|^2}[S_{q_1}(\omega) * S_{q_1}(\omega) * S_{q_1}(\omega)] \end{aligned} \tag{5.37}$$

The terms $S_{q_2}(\omega)$ and $S_{q_3}(\omega)$ appeared in the output, in equation (5.32), are due to the system nonlinearity. $S_{q_2}(\omega)$ is seen to be proportional to the convolution of the fundamental output spectrum $S_{q_1}(\omega)$ with itself and $S_{q_3}(\omega)$ is proportional to the double convolution of $S_{q_1}(\omega)$ with itself. If we calculate each of these terms separately we can predict the amount of distortion introduced in the output of the system.

Let the injection current to the laser be

$$i(t) = I_o + I_m\sum_{k=1}^{N_1} cos(\omega_k t + \theta_k) \tag{5.38}$$

where I_m is the modulating current amplitude from each carrier (assuming all carriers with same amplitude), N_1 is the total number of channels, ω_k and θ_k are the carrier frequency and phase of the kth channel respectively. Using laser d.c. and threshold currents and OMD one can express I_m as

$$I_m = \frac{m(I_o - I_{th})|G_1(\omega)|}{|G_1(0)|} \tag{5.39}$$

If all the carrier amplitudes are the same, then the total power is given by[34] $P_t = N_1 \frac{I_o^2}{2}$ and the two sided power spectrum is $S_i(\omega) = \frac{P_t}{2\delta f}$. Where δf is the difference between the upper and the lower frequency limits of the spectrum. Since the fundamental output spectrum can be obtained from $S_i(\omega)$ using equation (5.34) therefore,

$$S_{q_1}(\omega) = \frac{N_1 m^2 (I_o - I_{th})^2}{4\delta f |G_1(0)|^2} \tag{5.40}$$

Equations (5.36) and (5.37) are the general equations which can be used in any system with different modulation schemes like AM, FM, QAM etc. for the calculation of distortion when the power spectrum $S_{q_1}(\omega)$ is known. The amplitude modulated vestigial-sideband (AM-VSB) signal format is very attractive for multichannel TV distribution because of the bandwidth efficiency although it requires a high signal-to-noise ratio [4],[8], [11]. A 40 dB SNR is generally considered to correspond to a good quality of signal. Today's CATV system uses AM-VSB format of signal transmission and the N_1 channels are transmitted in the frequency band ranging from 50 MHz to 500 MHz [8], [10]. A 6 MHz bandwidth is usually allocated for each channel. One common way to measure second- and third-order effects is to consider input tones of equal amplitudes and assume the input spectrum is flat [8].

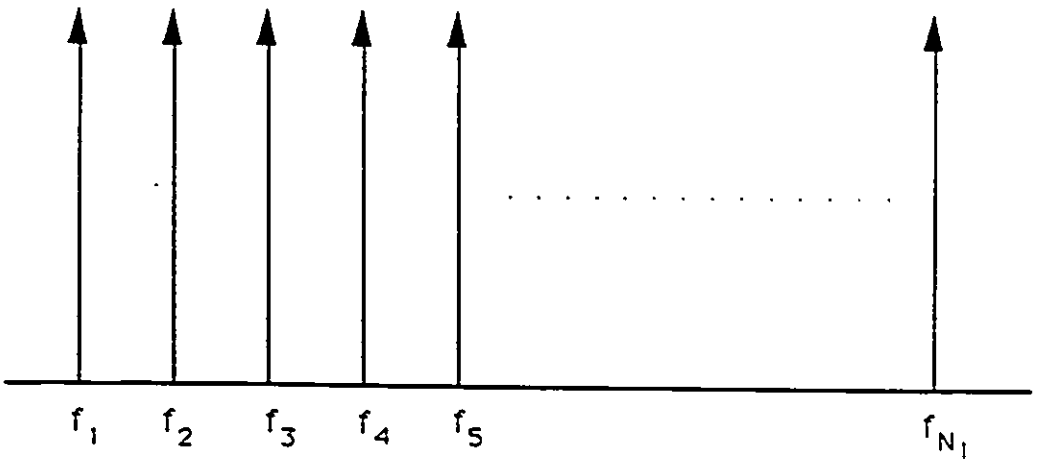

Fig. 32. FDM carriers of equal amplitudes from N_1 TV-channels

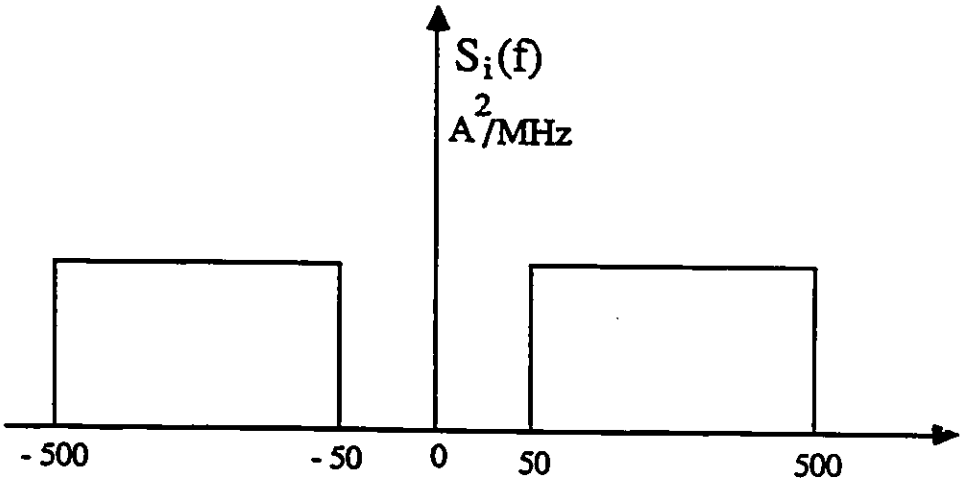

Fig. 33. Two-sided power spectrum of CATV system.

We wrote a computer program (program 'spectra' in Appendix) that calculates the relative (to the fundamental) second order- and third order distortions $\frac{S_{q_2}(\omega)}{S_{q_1}(\omega)}$ and $\frac{S_{q_3}(\omega)}{S_{q_1}(\omega)}$. The inputs to the program are the laser parameters, optical modulation depth, number of channels and the frequency limits of the bounded spectrum $S_{q_1}(\omega)$. Laser parameters D, E, F, L, M, N, R, S, and G are defined in Appendex B and can be calculated using Table 5.1. We calculated these parameters with a bias current of 36.75 mA. The number of channels N_1, optical modulation depth m and the lower and upper frequency range f_1 and f_2 (depending on the spectrum) can be varied in the main program. We considered the 50-500 MHz spectrum of Fig. 33 and 75 channels considering a channel spacing of 6 MHz. The power ratio of $\frac{S_{q_2}(\omega)}{S_{q_1}(\omega)}$ and $\frac{S_{q_3}(\omega)}{S_{q_1}(\omega)}$ are shown in Fig 34 and Fig 35 respectively. As we can see, distortion increases with increasing frequency and optical modulation depth. Keeping the OMD low, a superior distortion performance can be achieved. If we observe the above plots we see that even in the high frequency range the SNR is more than 40 dB i.e., with this particular laser a good quality of signal can be achieved, although there are some other sources of noise from transmitting end to the receiving end.

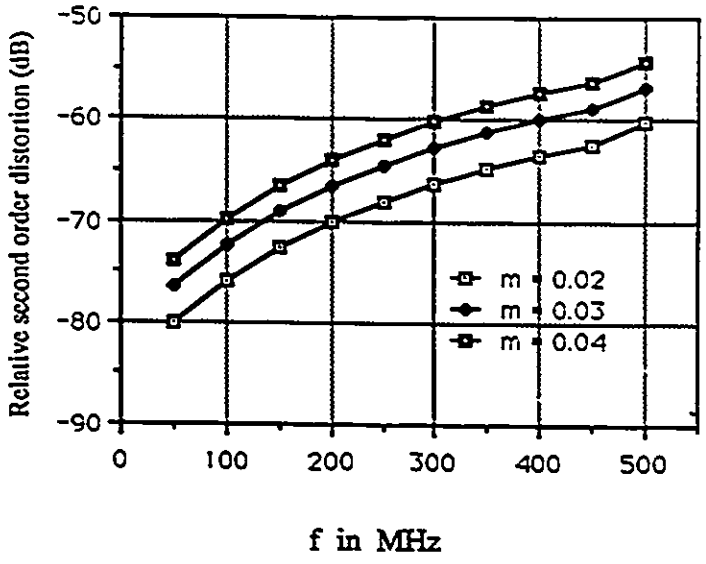

Fig. 34. Power ratio of $S_{q_2}(\omega)$ to $S_{q_1}(\omega)$ for a 75-channel system.

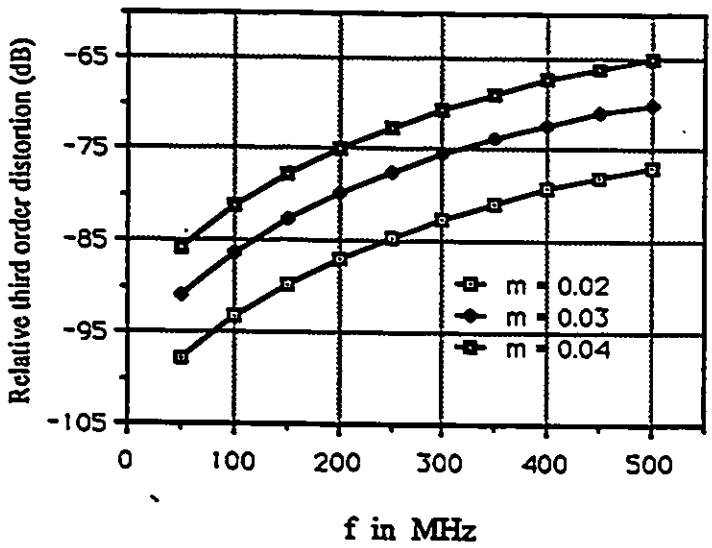

Fig. 35. Power ratio of $S_{q_3}(\omega)$ to $S_{q_1}(\omega)$ for a 75-channel system.

Chapter 6

CONCLUSIONS

6.1 Discussion

In this thesis, the nonlinear models for semiconductor laser have been investigated. While the large bandwidth of the lasers are attractive for broadband distribution on fibers, signal degradation resulting from laser nonlinearity limits their use for multichannel transmission in subcarrier multiplexing system. Harmonic and intermodulation distortions of the laser are two important parameters in determining the performance of wideband optical communications. In this thesis, we have made an attempt to analyze the nonlinearity of semiconductor lasers. Such an analysis helps to understand how the nonlinearity originates and how their effect can be reduced to improve device performance.

Since, the single-mode rate equations completely describe the characteristic of the laser diode through current injection, spontaneous emission and stimulated emission terms, we have started our analysis with the classic rate equations. The large-signal-model of rate equations contains a gain compression parameter, ϵ, which is very important in the nonlinearity analysis. In the analysis, an output-to-input approach was used where the injected current $i(t)$ to the laser was expressed as a function of photon density $q(t)$ and Volterra series was applied to the rate equations. With the use of harmonic input method, as rec-

ommended in [30], the Volterra transfer functions from output-to-input were first calculated for the laser. Then forward transfer functions were calculated from output-to-input transfer functions. Using these transfer functions and Volterra series the nonlinearity has been analyzed. Theoretical nonlinear models for harmonic and intermodulation distortions have been developed in terms of laser parameters, optical modulation depth and carrier frequency. Variations of distortion level with frequency and bias were shown graphically. Comparison of results with previous theoretical, simulation and experimental results were shown. An excellent agreement was found for the second and third harmonic distortion between our results and previous Darcie's[15] as well as Czylwik's [17] results. For the intermodulation distortion, we obtained a new model which corrects Darcie's equation (1.3). Comparison of two models show that Darcie's model for IMD is true for those devices which have small gain compression coefficient. However, our IMD model is very general and is true for all devices with any value of ϵ. The advantage of our approach is that it offers a more general analysis framework and an accurate rapid evaluation of the device performance. The output-to-input Volterra transfer functions play an important role throughout the analysis. Once these transfer functions are known, they can be used to analyze the system performance using the technique of this thesis. In the previous perturbation analysis, the analytical approach and also the Volterra kernels (for the laser) are unknown. The analytical technique of this thesis offers a valuable tool for the performance analysis of future broadband optical communications.

6.2 Further Suggestions

The single-mode rate equations describe the characteristics of the laser in the active region. Therefore, our analysis provides a solution that gives nonlinear behavior in the active region. However, in subcarrier multiplexing systems intermodulation products originate from two distinct nonlinear effects[3]. The first is the intrinsic nonlinearities cause by the mixing of electrons and photons in the laser cavity. Such effects are described by the rate equations

and therefore our analysis provides solution for intrinsic nonlinearities.

The other source of nonlinearity is the leakage current of the semiconductor laser diode[10] which causes sublinearity of the light-current characteristics. Such nonlinearities, which are not described by the rate equations, introduce second and third order distortions in the optical output. Applying the techniques, as we used in this thesis, such nonlinearities can be modeled.

Experimental work has to be performed for the measurement two tone intermodulation distortion using devices with gain compression ranging from very small to very large.

Our work can also be extended to solve multimode rate equations of the laser for nonlinear distortion.

Appendix A

Output-to-Input Equation

We recall the rate equations from section(3.1)

$$\frac{dN}{dt} = \frac{I_a}{V'} - \frac{N}{\tau_{sp}} - g(N - N_o)(1 - \epsilon Q)Q \tag{A.1}$$

$$\frac{dQ}{dt} = \Gamma g(N - N_o)(1 - \epsilon Q)Q - \frac{Q}{\tau_p} + \Gamma\beta\frac{N}{\tau_{sp}} \tag{A.2}$$

From equation (A.2) we can express the carrier density N as a function of photon density Q. Therefore,

$$\frac{dQ}{dt} = \{\Gamma g(1 - \epsilon Q)Q + \frac{\Gamma\beta}{\tau_{sp}}\}N - \Gamma g(1 - \epsilon Q)QN_o - \frac{Q}{\tau_p} \tag{A.3}$$

$$N = \frac{\frac{dQ}{dt} + \frac{Q}{\tau_p} + \Gamma g(1 - \epsilon Q)QN_o}{\Gamma g(1 - \epsilon Q)Q + \frac{\Gamma\beta}{\tau_{sp}}} \tag{A.4}$$

Now we add and subtract the term $\frac{\Gamma\beta N_o}{\tau_{sp}}$ in the numerator.

$$N = \frac{\frac{dQ}{dt} + \frac{Q}{\tau_p} + \{\Gamma g(1 - \epsilon Q)QN_o + \frac{\Gamma\beta N_o}{\tau_{sp}}\} - \frac{\Gamma\beta N_o}{\tau_{sp}}}{\Gamma g(1 - \epsilon Q)Q + \frac{\Gamma\beta}{\tau_{sp}}}$$

$$N = N_o + \frac{\frac{dQ}{dt} + \frac{Q}{\tau_p} - \frac{\Gamma\beta N_o}{\tau_{sp}}}{\Gamma g(1-\epsilon Q)Q + \frac{\Gamma\beta}{\tau_{sp}}} \tag{A.5}$$

From equation (A.1) we can write,

$$\frac{I_a}{V'} = \frac{N - N_o + N_o}{\tau_{sp}} + g(N - N_o)(1 - \epsilon Q)Q + \frac{dN}{dt}$$

Substituting equation (A.5) for N we obtain the current I_a as a function of photon density Q as

$$\begin{aligned} \frac{I_a}{V'} &= \frac{N_o}{\tau_{sp}} + [\frac{1}{\tau_{sp}} + g(1-\epsilon Q)Q]\frac{[\frac{dQ}{dt} + \frac{Q}{\tau_p} - \frac{\Gamma\beta N_o}{\tau_{sp}}]}{[\Gamma g(1-\epsilon Q)Q + \frac{\Gamma\beta}{\tau_{sp}}]} \\ &\quad + \frac{d}{dt}\{[\frac{dQ}{dt} + \frac{Q}{\tau_p} - \frac{\Gamma\beta N_o}{\tau_{sp}}]/[\Gamma g(1-\epsilon Q)Q + \frac{\Gamma\beta}{\tau_{sp}}]\} \end{aligned} \tag{A.6}$$

Appendix B

Derivation of Equation (3.6)

We recall equation (A.6) from Appendix A

$$\frac{I_a}{V'} = \frac{N_o}{\tau_{sp}} + [\frac{1}{\tau_{sp}} + g(1-\epsilon Q)Q]\frac{[\frac{dQ}{dt} + \frac{Q}{\tau_p} - \frac{\Gamma\beta N_o}{\tau_{sp}}]}{[\Gamma g(1-\epsilon Q)Q + \frac{\Gamma\beta}{\tau_{sp}}]} + \frac{d}{dt}\{[\frac{dQ}{dt} + \frac{Q}{\tau_p} - \frac{\Gamma\beta N_o}{\tau_{sp}}]/[\Gamma g(1-\epsilon Q)Q + \frac{\Gamma\beta}{\tau_{sp}}]\} \quad \text{(B.1)}$$

$$\frac{I_a}{V'} = \frac{N_o}{\tau_{sp}} + [\frac{\frac{1}{\tau_{sp}}}{\Gamma g(1-\epsilon Q)Q + \frac{\Gamma\beta}{\tau_{sp}}} + \frac{g(1-\epsilon Q)Q}{\Gamma g(1-\epsilon Q)Q + \frac{\Gamma\beta}{\tau_{sp}}}] \cdot [\frac{dQ}{dt} + \frac{Q}{\tau_p} - \frac{\Gamma\beta N_o}{\tau_{sp}}] + \frac{d}{dt}[\frac{\frac{dQ}{dt} + \frac{Q}{\tau_p} - \frac{\Gamma\beta N_o}{\tau_{sp}}}{\Gamma g(1-\epsilon Q)Q + \frac{\Gamma\beta}{\tau_{sp}}}] \quad \text{(B.2)}$$

Now, in the denominator of the second term within the first squared bracket, the term containing beta is very small which is due to the insignificant contribution of spontaneous emission into the lasing mode. If we neglect this term then the above equation reduces to

$$\frac{I_a}{V'} = \frac{N_o}{\tau_{sp}} + [\frac{\frac{1}{\tau_{sp}}}{\Gamma g(1-\epsilon Q)Q + \frac{\Gamma\beta}{\tau_{sp}}} + \frac{1}{\Gamma}][\frac{dQ}{dt} + \frac{Q}{\tau_p} - \frac{\Gamma\beta N_o}{\tau_{sp}}] + \frac{d}{dt}[\frac{\frac{dQ}{dt} + \frac{Q}{\tau_p} - \frac{\Gamma\beta N_o}{\tau_{sp}}}{\Gamma g(1-\epsilon Q)Q + \frac{\Gamma\beta}{\tau_{sp}}}] \quad \text{(B.3)}$$

We have mentioned before, Q and I_a can be expressed as the sum of steady state and time varying quantities, $Q = Q_o + q(t)$ and $I_a = I_o + i(t)$. Now,

$$\Gamma g(1-\epsilon Q)Q + \frac{\Gamma\beta}{\tau_{sp}} = \Gamma(gQ - \epsilon gQ^2 + \frac{\beta}{\tau_{sp}})$$

$$
\begin{aligned}
&= \Gamma[gQ_o + gq(t) - \epsilon g\{Q_o + q(t)\}^2 + \frac{\beta}{\tau_{sp}}] \\
&= \Gamma(gQ_o + gq - \epsilon gQ_o^2 - 2\epsilon gQ_o q - \epsilon gq^2 + \frac{\beta}{\tau_{sp}}) \\
&= \Gamma(gQ_o + \frac{\beta}{\tau_{sp}} - \epsilon gQ_o^2) + \Gamma(g - 2\epsilon gQ_o)q - \Gamma\epsilon gq^2 \\
&= a + bq(t) + cq^2(t) \\
&= a[1 + \{\frac{b}{a}q(t) + \frac{c}{a}q^2(t)\}] \qquad \text{(B.4)}
\end{aligned}
$$

Where, we have defined

$$
\begin{aligned}
a &= \Gamma(gQ_o + \frac{\beta}{\tau_{sp}} - \epsilon gQ_o^2) \\
b &= \Gamma(g - 2\epsilon gQ_o) \\
c &= -\Gamma\epsilon g \qquad \text{(B.5)}
\end{aligned}
$$

Now,

$$
\frac{1}{\Gamma g(1-\epsilon Q)Q + \frac{\Gamma\beta}{\tau_{sp}}} = \frac{1}{a[1 + \{\frac{b}{a}q(t) + \frac{c}{a}q^2(t)\}]} \qquad \text{(B.6)}
$$

In the above equation the denominator terms containing $q(t)$ are very complicated. Here, we expand these terms with Taylor series for analysis. Thus

$$
\begin{aligned}
\frac{1}{\Gamma g(1-\epsilon Q)Q + \frac{\Gamma\beta}{\tau_{sp}}} &= \frac{1}{a}[1 - (\frac{b}{a}q + \frac{c}{a}q^2) + (\frac{b}{a}q + \frac{c}{a}q^2)^2 - (\frac{b}{a}q + \frac{c}{a}q^2)^3 + ... - ...] \\
&= \frac{1}{a} - \frac{b}{a^2}q + (\frac{b^2}{a^3} - \frac{c}{a^2})q^2 + (\frac{2bc}{a^3} - \frac{b^3}{a^4})q^3 \\
&= \frac{1}{a} - \frac{b}{a^2}q(t) + \theta q^2(t) + \gamma q^3(t) \qquad \text{(B.7)}
\end{aligned}
$$

Where,

$$
\begin{aligned}
\theta &= \frac{b^2}{a^3} - \frac{c}{a^2} \\
\gamma &= \frac{2bc}{a^3} - \frac{b^3}{a^4} \qquad \text{(B.8)}
\end{aligned}
$$

As Q_o is the d.c component therefore, $\frac{dQ}{dt} = \frac{dq(t)}{dt}$. Now using equation (B.7) equation (B.3) becomes

$$
\frac{I_o + i(t)}{V'} = \frac{N_o}{\tau_{sp}} + [\frac{1}{\Gamma} + \frac{1}{\tau_{sp}}(\frac{1}{a} - \frac{b}{a^2}q + \theta q^2 + \gamma q^3)][\frac{dq}{dt} + \frac{Q_o + q}{\tau_p} - \frac{\Gamma\beta N_o}{\tau_{sp}}]
$$

$$
\begin{aligned}
&\frac{d}{dt}[\frac{dq}{dt}+\frac{Q_o+q}{\tau_p}-\frac{\Gamma\beta N_o}{\tau_{sp}}](\frac{1}{a}-\frac{b}{a^2}q+\theta q^2+\gamma q^3)\\
=\;&\frac{N_o}{\tau_{sp}}+[\frac{1}{\Gamma}+\frac{1}{a\tau_{sp}}-\frac{b}{a^2\tau_{sp}}q+\frac{\theta}{\tau_{sp}}q^2+\frac{\gamma}{\tau_{sp}}q^3][\frac{dq}{dt}+\frac{Q_o}{\tau_p}+\frac{q}{\tau_p}-\frac{\Gamma\beta N_o}{\tau_{sp}}]\\
&+[\frac{dq}{dt}+\frac{Q_o}{\tau_p}+\frac{q}{\tau_p}-\frac{\Gamma\beta N_o}{\tau_{sp}}][-\frac{b}{a^2}\frac{dq}{dt}+2\theta q\frac{dq}{dt}+3\gamma q^2\frac{dq}{dt}]\\
&+(\frac{1}{a}-\frac{b}{a^2}q+\theta q^2+\gamma q^3)[\frac{d^2q}{dt^2}+\frac{1}{\tau_p}\frac{dq}{dt}]
\end{aligned}
\tag{B.9}
$$

From the above equation considering terms upto third order(i.e. terms upto third power of $q(t)$) we get

$$
\begin{aligned}
\frac{I_o+i(t)}{V'} =\;&\frac{N_o}{\tau_{sp}}+(\frac{1}{\Gamma}+\frac{1}{a\tau_{sp}})\frac{dq}{dt}+(\frac{1}{\Gamma}+\frac{1}{a\tau_{sp}})(\frac{Q_o}{\tau_p}-\frac{\Gamma\beta N_o}{\tau_{sp}})+(\frac{1}{\Gamma}+\frac{1}{a\tau_{sp}})\frac{1}{\tau_p}q\\
&-\frac{b}{a^2\tau_{sp}}(\frac{Q_o}{\tau_p}-\frac{\Gamma\beta N_o}{\tau_{sp}})q-\frac{b}{a^2\tau_{sp}\tau_p}q^2-\frac{b}{a^2\tau_{sp}}q\frac{dq}{dt}+\frac{\theta}{\tau_{sp}\tau_p}q^3\\
&+\frac{\theta}{\tau_{sp}}(\frac{Q_o}{\tau_p}-\frac{\Gamma\beta N_o}{\tau_{sp}})q^2+\frac{\theta}{\tau_{sp}}q^2\frac{dq}{dt}+\frac{\gamma}{\tau_{sp}}(\frac{Q_o}{\tau_p}-\frac{\Gamma\beta N_o}{\tau_{sp}})q^3-\frac{b}{a^2}(\frac{dq}{dt})^2\\
&-\frac{b}{a^2\tau_p}q(\frac{dq}{dt})-\frac{b}{a^2}(\frac{Q_o}{\tau_p}-\frac{\Gamma\beta N_o}{\tau_{sp}})\frac{dq}{dt}+2\theta q(\frac{dq}{dt})^2+\frac{2\theta}{\tau_p}q^2\frac{dq}{dt}\\
&+2\theta(\frac{Q_o}{\tau_p}-\frac{\Gamma\beta N_o}{\tau_{sp}})q\frac{dq}{dt}+3\gamma(\frac{Q_o}{\tau_p}-\frac{\Gamma\beta N_o}{\tau_{sp}})q^2\frac{dq}{dt}+\frac{1}{a}\frac{d^2q}{dt^2}\\
&-\frac{b}{a^2}q\frac{d^2q}{dt^2}+\theta q^2\frac{d^2q}{dt^2}+\frac{1}{a\tau_p}\frac{dq}{dt}-\frac{b}{a^2\tau_p}q\frac{dq}{dt}+\frac{\theta}{\tau_p}q^2\frac{dq}{dt}
\end{aligned}
\tag{B.10}
$$

$$
\begin{aligned}
\frac{i(t)}{V'} =\;&\frac{N_o}{\tau_{sp}}-\frac{I_o}{V'}+(\frac{1}{\Gamma}+\frac{1}{a\tau_{sp}})(\frac{Q_o}{\tau_p}-\frac{\Gamma\beta N_o}{\tau_{sp}})+\frac{1}{a}\frac{d^2q}{dt^2}\\
&+(\frac{1}{\Gamma}+\frac{1}{a\tau_{sp}}-\frac{bQ_o}{a^2\tau_p}+\frac{b\Gamma\beta N_o}{a^2\tau_{sp}}+\frac{1}{a\tau_p})\frac{dq}{dt}\\
&+(\frac{1}{\Gamma\tau_p}+\frac{1}{a\tau_{sp}\tau_p}-\frac{bQ_o}{a^2\tau_p\tau_{sp}}+\frac{b\Gamma\beta N_o}{a^2\tau_{sp}^2})q-\frac{b}{a^2}(\frac{dq}{dt})^2\\
&-(\frac{b}{a^2\tau_{sp}}+\frac{2b}{a^2\tau_p}+\frac{2\theta\Gamma\beta N_o}{\tau_{sp}}-\frac{2\theta Q_o}{\tau_p})q\frac{dq}{dt}-\frac{b}{a^2}q\frac{d^2q}{dt^2}\\
&-(\frac{b}{a^2\tau_p\tau_{sp}}-\frac{\theta Q_o}{\tau_p\tau_{sp}}+\frac{\theta\Gamma\beta N_o}{\tau_{sp}^2})q^2+2\theta q(\frac{dq}{dt})^2
\end{aligned}
$$

$$+(\frac{\theta}{\tau_{sp}}+\frac{3\theta}{\tau_p}+\frac{3\gamma Q_o}{\tau_p}-\frac{3\gamma\Gamma\beta N_o}{\tau_{sp}})q^2\frac{dq}{dt}+\theta q^2\frac{d^2q}{dt^2}$$
$$+(\frac{\theta}{\tau_{sp}\tau_p}+\frac{\gamma Q_o}{\tau_{sp}\tau_p}-\frac{\gamma\Gamma\beta N_o}{\tau_{sp}^2})q^3 \qquad \text{(B.11)}$$

From which we write,

$$\begin{aligned} i(t) &= A+\{Dq(t)+Eq'(t)+Fq''(t)\}-\{Lq^2(t)+Mq(t)q'(t) \\ &+Nq(t)q''(t)+Nq'^2(t)\}+\{Rq^3(t)+Sq^2(t)q'(t) \\ &+2Gq(t)q'^2(t)+Gq^2(t)q''(t)\}-\ldots\ldots+\ldots\ldots \end{aligned} \qquad \text{(B.12)}$$

where the coefficients $A, D, E, F, L, M, N, R, S, G$ all are expressed in terms of laser parameters and steady state photon density as follows(a,b and c are as defined in equation (B.5) and θ and Γ are as defined in equation (B.8)).

$$A = V'[\frac{N_o}{\tau_{sp}}-\frac{I_o}{V'}+(\frac{1}{\Gamma}+\frac{1}{a\tau_{sp}})(\frac{Q_o}{\tau_p}-\frac{\Gamma\beta N_o}{\tau_{sp}})]$$
$$D = V'[\frac{1}{\Gamma\tau_p}+\frac{1}{a\tau_p\tau_{sp}}-\frac{bQ_o}{a^2\tau_{sp}\tau_p}+\frac{b\Gamma\beta N_o}{a^2\tau_{sp}^2}]$$
$$E = V'[\frac{1}{\Gamma}+\frac{1}{a\tau_{sp}}-\frac{bQ_o}{a^2\tau_p}+\frac{b\Gamma\beta N_o}{a^2\tau_{sp}}+\frac{1}{a\tau_p}]$$
$$F = \frac{V'}{a}$$
$$L = V'[\frac{b}{a^2\tau_{sp}\tau_p}-\frac{\theta Q_o}{\tau_{sp}\tau_p}+\frac{\theta\Gamma\beta N_o}{\tau_{sp}^2}]$$
$$M = V'[\frac{b}{a^2\tau_{sp}}+\frac{2b}{a^2\tau_p}+\frac{2\theta\Gamma\beta N_o}{\tau_{sp}}-\frac{2\theta Q_o}{\tau_p}]$$
$$N = \frac{bV'}{a^2}$$
$$R = V'[\frac{\theta}{\tau_{sp}\tau_p}+\frac{\gamma Q_o}{\tau_{sp}\tau_p}-\frac{\gamma\Gamma\beta N_o}{\tau_{sp}^2}]$$
$$S = V'[\frac{\theta}{\tau_{sp}}+\frac{3\theta}{\tau_p}+\frac{3\gamma Q_o}{\tau_p}-\frac{3\gamma\Gamma\beta N_o}{\tau_{sp}}]$$
$$G = V'\theta \qquad \text{(B.13)}$$

B.1 Simplified Calculation

We recall equation (3.7)

$$\frac{I_a - I_{th}}{V'} = \frac{1}{\Gamma}\frac{dQ}{dt} + \frac{Q}{\Gamma\tau_p} + \frac{d}{dt}\{\frac{(\frac{dQ}{dt} + \frac{Q}{\tau_p})}{\Gamma g(1-\epsilon Q)Q}\} \tag{B.14}$$

Substituting $Q = Q_o + q(t)$, $\frac{dQ}{dt} = \frac{dq(t)}{dt}$, $I_a = I_o + i(t)$ we have,

$$\frac{I_o - I_{th} + i(t)}{V'} = \frac{1}{\Gamma}[\frac{dq}{dt} + \frac{Q_o + q}{\tau_p}] + \frac{d}{dt}[\frac{\frac{dq}{dt} + \frac{Q_o+q}{\tau_p}}{\Gamma g(1-\epsilon Q_o - \epsilon q)(Q_o + q)}] \tag{B.15}$$

For a typical device Q_o is of the order of $10^{21}\ m^{-3}$ and ϵ is of the order of 10^{-23}. These parameters give a value for ϵQ_o which is very small(~ 0.05) compared to 1. We have neglected the term ϵQ_o. Therefore,

$$\begin{aligned}\frac{I_o - I_{th} + i(t)}{V'} &= \frac{1}{\Gamma}[\frac{dq}{dt} + \frac{Q_o + q}{\tau_p}] + \frac{d}{dt}[\frac{\frac{dq}{dt} + \frac{Q_o+q}{\tau_p}}{\Gamma g(1-\epsilon q)(Q_o + q)}] \\ &= \frac{1}{\Gamma}\frac{dq}{dt} + \frac{Q_o + q}{\Gamma\tau_p} + \frac{d}{dt}[\frac{\frac{dq}{dt}}{\Gamma g(1-\epsilon q)(Q_o+q)} + \frac{1}{\Gamma g\tau_p(1-\epsilon q)}]\end{aligned} \tag{B.16}$$

Using Taylor series we expand above equation as follows

$$\begin{aligned}\frac{I_o - I_{th} + i(t)}{V'} &= \frac{1}{\Gamma}\frac{dq}{dt} + \frac{Q_o + q}{\Gamma\tau_p} + \frac{d}{dt}[\frac{dq}{dt}\frac{1}{\Gamma g Q_o}\{1 + \epsilon q + (\epsilon q)^2 + (\epsilon q)^3 + ...\}\cdot \\ &\quad \{1 - \frac{q}{Q_o} + (\frac{q}{Q_o})^2 - (\frac{q}{Q_o})^3 + ... - ... + ... - ...\}] \\ &\quad + \frac{d}{dt}[\frac{1}{\Gamma g\tau_p}\{1 + \epsilon q + (\epsilon q)^2 + (\epsilon q)^3 + ...\}] \\ &= \frac{1}{\Gamma}\frac{dq}{dt} + \frac{Q_o + q}{\Gamma\tau_p} + \frac{1}{\Gamma g Q_o}\frac{dq}{dt}[\epsilon\frac{dq}{dt} + 2\epsilon^2 q\frac{dq}{dt} + 3\epsilon^3 q^2\frac{dq}{dt} - \frac{1}{Q_o}\frac{dq}{dt} \\ &\quad - \frac{2\epsilon q}{Q_o}\frac{dq}{dt} + \frac{2q}{Q_o^2}\frac{dq}{dt} + ..] + \frac{1}{\Gamma g Q_o}\frac{d^2q}{dt^2}[1 + \epsilon q + (\epsilon q)^2 - \frac{q}{Q_o} - \frac{\epsilon q^2}{Q_o} \\ &\quad + (\frac{q}{Q_o})^2 + ...] + \frac{1}{\Gamma g\tau_p}[\epsilon\frac{dq}{dt} + 2\epsilon^2 q\frac{dq}{dt} + 3\epsilon^3 q^2\frac{dq}{dt} + ...]\end{aligned} \tag{B.17}$$

$$\frac{i(t)}{V'} = \frac{Q_o}{\Gamma\tau_p} - \frac{I_o - I_{th}}{V'} + \frac{1}{\Gamma}\frac{dq}{dt} + \frac{q}{\Gamma\tau_p} + \frac{1}{\Gamma g Q_o}\frac{dq}{dt}[(\epsilon - \frac{1}{Q_o})\frac{dq}{dt} + (2\epsilon^2 - \frac{2\epsilon}{Q_o} + \frac{2}{Q_o^2})q\frac{dq}{dt} + 3\epsilon^3 q^2\frac{dq}{dt}] + \frac{1}{\Gamma g Q_o}\frac{d^2q}{dt^2} + \frac{(\epsilon - \frac{1}{Q_o})}{\Gamma g Q_o}q\frac{d^2q}{dt^2} + \frac{(\epsilon^2 - \frac{\epsilon}{Q_o} + \frac{1}{Q_o^2})}{\Gamma g Q_o}q^2\frac{d^2q}{dt^2} + \frac{1}{\Gamma g\tau_p}[\epsilon\frac{dq}{dt} + 2\epsilon^2 q\frac{dq}{dt} + 3\epsilon^3 q^2\frac{dq}{dt}] \quad \text{(B.18)}$$

$$\begin{aligned}\frac{i(t)}{V'} &= \frac{Q_o}{\Gamma\tau_p} - \frac{I_o - I_{th}}{V'} + \frac{1}{\Gamma}[\frac{dq}{dt} + \frac{q}{\tau_p} + \frac{1}{gQ_o}\frac{d^2q}{dt^2} + \frac{\epsilon}{g\tau_p}\frac{dq}{dt}] \\ &\quad + \frac{1}{\Gamma}[\frac{1}{gQ_o}(\epsilon - \frac{1}{Q_o})\{(\frac{dq}{dt})^2 + q\frac{d^2q}{dt^2}\} + \frac{2\epsilon^2}{g\tau_p}q\frac{dq}{dt}] \\ &\quad + [\frac{2}{\Gamma g Q_o}(\epsilon^2 - \frac{\epsilon}{Q_o} + \frac{1}{Q_o^2})q(\frac{dq}{dt})^2 + \frac{1}{\Gamma g Q_o}(\epsilon^2 - \frac{\epsilon}{Q_o} \\ &\quad + \frac{1}{Q_o^2})q^2\frac{d^2q}{dt^2} + \frac{3\epsilon^3}{\Gamma g\tau_p}q^2\frac{dq}{dt}] \\ &= \frac{Q_o}{\Gamma\tau_p} - \frac{I_o - I_{th}}{V'} + \frac{1}{\Gamma g Q_o}\frac{d^2q}{dt^2} + \frac{1}{\Gamma}(1 + \frac{\epsilon}{g\tau_p})\frac{dq}{dt} + \frac{q}{\Gamma\tau_p} \\ &\quad \frac{(\epsilon Q_o - 1)}{\Gamma g Q_o^2}\{(\frac{dq}{dt})^2 + q\frac{d^2q}{dt^2}\} + \frac{2\epsilon^2}{\Gamma g\tau_p}q\frac{dq}{dt} + \frac{2}{\Gamma g Q_o^3}(\epsilon^2 Q_o^2 \\ &\quad - \epsilon Q_o + 1)\{q(\frac{dq}{dt})^2 + \frac{q^2}{2}\frac{d^2q}{dt^2}\} + \frac{3\epsilon^3}{\Gamma g\tau_p}q^2\frac{dq}{dt}\end{aligned} \quad \text{(B.19)}$$

We neglect the terms ϵQ_o and $(\epsilon Q_o)^2$. Also, we consider $(1 + \frac{\epsilon}{g\tau_p}) \simeq \frac{\epsilon}{g\tau_p}$ (because $\frac{\epsilon}{g\tau_p}$ is 10 to 20 times bigger than 1).

Therefore,

$$\begin{aligned}\frac{i(t)}{V'} &= \frac{Q_o}{\Gamma\tau_p} - \frac{I_o - I_{th}}{V'} + [\frac{1}{\Gamma g Q_o}\frac{d^2q}{dt^2} + \frac{\epsilon}{\Gamma g\tau_p}\frac{dq}{dt} + \frac{q}{\Gamma\tau_p}] \\ &\quad - [\frac{1}{\Gamma g Q_o^2}\{(\frac{dq}{dt})^2 + q\frac{d^2q}{dt^2}\} - \frac{2\epsilon^2}{\Gamma g\tau_p}q\frac{dq}{dt}] \\ &\quad + [\frac{2}{\Gamma g Q_o^3}q(\frac{dq}{dt})^2 + \frac{1}{\Gamma g Q_o^3}q^2\frac{d^2q}{dt^2} + \frac{3\epsilon^3}{\Gamma g\tau_p}q^2\frac{dq}{dt}]\end{aligned} \quad \text{(B.20)}$$

Now we write,

$$A_1 = V''(\frac{Q_o}{\Gamma\tau_p} - \frac{I_o - I_{th}}{V'})$$

$$D_1 = \frac{V'}{\Gamma\tau_p}$$

$$E_1 = \frac{\epsilon V'}{\Gamma g\tau_p}$$

$$F_1 = \frac{V'}{\Gamma g Q_o}$$

$$N_1 = \frac{V'}{\Gamma g Q_o^2}$$

$$M_1 = -\frac{2\epsilon^2 V'}{\Gamma g\tau_p}$$

$$G_1 = \frac{V'}{\Gamma g Q_o^3}$$

$$S_1 = \frac{3\epsilon^3 V'}{\Gamma g\tau_p} \qquad \text{(B.21)}$$

We can now write the equation for laser drive current as

$$\begin{aligned} i(t) = {} & A_1 + \{D_1 q(t) + E_1 q'(t) + F_1 q''(t)\} - \{M_1 q(t)q'(t) + N_1 q(t)q''(t) \\ & N_1 q'^2(t)\} + \{S_1 q^2(t)q'(t) + 2G_1 q(t)q'^2(t) + G_1 q^2(t)q''(t)\} - \ldots + \ldots \end{aligned} \qquad \text{(B.22)}$$

Appendix C

Calculation of Output-to-Input Transfer functions

We recall equation (3.6)

$$\begin{aligned} i(t) &= A + \{Dq(t) + Eq'(t) + Fq''(t)\} - \{Lq^2(t) + Mq(t)q'(t) \\ &\quad + Nq(t)q''(t) + Nq'^2(t)\} + \{Rq^3(t) + Sq^2(t)q'(t) \\ &\quad + 2Gq(t)q'^2(t) + Gq^2(t)q''(t)\} - ..... + ... \end{aligned} \tag{C.1}$$

For the calculation of linear transfer function $G_1(\omega_1)$ let $q(t) = e^{j\omega_1 t}$. We substitute this value of $q(t)$ in equation (C.1). Therefore,

$$i(t) = A + De^{j\omega_1 t} + j\omega_1 Ee^{j\omega_1 t} + (j\omega_1)^2 Fe^{j\omega_1 t} - Le^{j2\omega_1 t} - .... + ... \tag{C.2}$$

Taking the coefficients of $e^{j\omega_1 t}$ we obtain $G_1(\omega_1)$. Thus

$$G_1(\omega_1) = D + j\omega_1 E - \omega_1^2 F \tag{C.3}$$

Setting $q(t) = e^{j\omega_1 t} + e^{j\omega_2 t}$ in equation (C.1) and taking the coefficients of $e^{j(\omega_1+\omega_2)t}$ we get the second order transfer function $G_2(\omega_1, \omega_2)$. From equation (C.1) we can see that, when we expand the right hand side with $q(t) = e^{j\omega_1 t} + e^{j\omega_2 t}$ neither the linear terms ($q(t)$, $q'(t)$, $q''(t)$) give any term of the form $e^{j(\omega_1+\omega_2)t}$ nor the terms containing third power of $q(t)$. The only terms of interest are the second order terms. Therefore,

$$
\begin{aligned}
i(t) &= A + D(e^{j\omega_1 t} + e^{j\omega_2 t}) + \ldots - L(e^{j\omega_1 t} + e^{j\omega_2 t})^2 \\
&\quad -M(e^{j\omega_1 t} + e^{j\omega_2 t})(j\omega_1 e^{j\omega_1 t} + j\omega_2 e^{j\omega_2 t}) - N(e^{j\omega_1 t} + e^{j\omega_2 t})(-\omega_1^2 e^{j\omega_1 t} - \omega_2^2 e^{j\omega_2 t}) \\
&\quad -N(j\omega_1 e^{j\omega_1 t} + j\omega_2 e^{j\omega_2 t})^2 + R(e^{j\omega_1 t} + e^{j\omega_2 t})^3 + \ldots \qquad \text{(C.4)}
\end{aligned}
$$

The coefficients of $e^{j(\omega_1+\omega_2)t}$ are

$$
\begin{aligned}
G_2(\omega_1, \omega_2) &= -2L - M(j\omega_1 + j\omega_2) - N(-\omega_1^2 - \omega_2^2 - 2\omega_1\omega_2) \\
&= -2L - jM(\omega_1 + \omega_2) + N(\omega_1 + \omega_2)^2 \qquad \text{(C.5)}
\end{aligned}
$$

Similarly substituting $q(t) = e^{j\omega_1 t} + e^{j\omega_2 t} + e^{j\omega_3 t}$ in equation (C.1) and taking the coefficients of $e^{j(\omega_1+\omega_2+\omega_3)t}$ we obtain the third order transfer function $G_3(\omega_1, \omega_2, \omega_3)$. Note that only the terms containing third power of $q(t)$ are of interest. Thus,

$$
\begin{aligned}
i(t) &= A + \ldots\ldots - \ldots\ldots + R\{e^{j3\omega_1 t} + 3e^{j(2\omega_1+\omega_2)t} + \ldots + 6e^{j(\omega_1+\omega_2+\omega_3)t} + \ldots\} \\
&\quad +S[e^{j2\omega_1 t} + e^{j2\omega_2 t} + e^{j2\omega_3 t} + 2e^{j(\omega_1+\omega_2)t} + 2e^{j(\omega_2+\omega_3)t} + 2e^{j(\omega_3+\omega_1)t}] \cdot \\
&\quad [j\omega_1 e^{j\omega_1 t} + j\omega_2 e^{j\omega_2 t} + j\omega_3 e^{j\omega_3 t}] + 2G[e^{j\omega_1 t} + e^{j\omega_2 t} + e^{j\omega_3 t}][-\omega_1^2 e^{j2\omega_1 t} - \omega_2^2 e^{j2\omega_2 t} \\
&\quad -\omega_3^2 e^{j2\omega_3 t} - 2\omega_1\omega_2 e^{j(\omega_1+\omega_2)t} - 2\omega_2\omega_3 e^{j(\omega_2+\omega_3)t} - 2\omega_3\omega_1 e^{j(\omega_3+\omega_1)t}] \\
&\quad +G[e^{j2\omega_1 t} + e^{j2\omega_2 t} + e^{j2\omega_3 t} + 2e^{j(\omega_1+\omega_2)t} + 2e^{j(\omega_2+\omega_3)t} + 2e^{j(\omega_3+\omega_1)t}] \cdot \\
&\quad [-\omega_1^2 e^{j\omega_1 t} - \omega_2^2 e^{j\omega_2 t} - -\omega_3^2 e^{j\omega_3 t}] - \ldots + \ldots \qquad \text{(C.6)}
\end{aligned}
$$

Therefore,

$$
\begin{aligned}
G_3(\omega_1, \omega_2, \omega_3) &= 6R + jS(2\omega_1 + 2\omega_2 + 2\omega_3) + 2G(-2\omega_1\omega_3 - 2\omega_2\omega_3 - 2\omega_1\omega_2) \\
&\quad +G(-2\omega_1^3 - 2\omega_2^2 - 2\omega_3^2) \\
&= 6R + j2S(\omega_1 + \omega_2 + \omega_3) - 2G(\omega_1 + \omega_2 + \omega_3)^2 \qquad \text{(C.7)}
\end{aligned}
$$

Appendix D

Calculation of $q(t)$'s

D.1 Calculation of $q_1(t)$

The input to the laser is a single sinusoid

$$\begin{aligned} i(t) &= I\cos\omega t \\ &= \frac{I}{2}e^{j\omega t} + \frac{I}{2}e^{-j\omega t} \\ &= i_a(t) + i_b(t) \end{aligned} \tag{D.1}$$

Where

$$i_a(t) = \frac{I}{2}e^{j\omega t} \tag{D.2}$$

and

$$i_b(t) = \frac{I}{2}e^{-j\omega t} \tag{D.3}$$

We recall the Volterra series from chapter 4. Since we will write the series for the laser therefore, instead of $x(t)$ and $y(t)$ we will write the input and output as $i(t)$ and $q(t)$ respectively which are the current and photon density. As we are interested for the input to output nonlinearities, we will use, $h_n(u_1, ..., u_n)$, the forward kernel in place of $g_n(u_1, ..., u_n)$. Therefore,

$$q(t) = \sum_{n=1}^{\infty} \frac{1}{n!} \int_{-\infty}^{\infty} ... \int_{-\infty}^{\infty} h_n(u_1 ... u_n) \prod_{l=1}^{n} i(t - u_l) du_1 ... du_n \tag{D.4}$$

For $n = 1$ we get the first order quantity

$$\begin{aligned} q_1(t) &= \frac{\cdot}{1!}\int_{-\infty}^{\infty} h_1(u_1)i(t-u_1)du_1 \\ &= \mathbf{B_1}[i(t)] \\ &= \mathbf{B_1}[i_a(t)+i_b(t)] \\ &= \mathbf{B_1}[i_a(t)]+\mathbf{B_1}[i_b(t)] \end{aligned} \tag{D.5}$$

$\mathbf{B_1}$ is the first order Volterra operator. Now,

$$\begin{aligned} \mathbf{B_1}[i_a(t)] &= \int_{-\infty}^{\infty} h_1(u_1)i_a(t-u_1)du_1 \\ &= \int_{-\infty}^{\infty} h_1(u_1)\frac{I}{2}e^{j\omega(t-u_1)du_1} \\ &= \frac{I}{2}e^{j\omega t}\int_{-\infty}^{\infty} h_1(u_1)e^{-j\omega u_1}du_1 \\ &= \frac{I}{2}H_1(\omega)e^{j\omega t} \end{aligned} \tag{D.6}$$

Where $H_1(\omega)$ is the Fourier transform of the linear kernel $h_1(u_1)$ which is, in fact, the linear Volterra transfer function of the system. It is seen that when the input to the linear system is $i_a(t) = \frac{I}{2}e^{j\omega t}$, the output is just the transfer function times the input. Similarly,

$$\begin{aligned} \mathbf{B_1}[i_b(t)] &= \int_{-\infty}^{\infty} h_1(u_1)i_b(t-u_1)du_1 \\ &= \int_{-\infty}^{\infty} h_1(u_1)\frac{I}{2}e^{-j\omega(t-u_1)du_1} \\ &= \frac{I}{2}e^{-j\omega t}\int_{-\infty}^{\infty} h_1(u_1)e^{j\omega u_1}du_1 \\ &= \frac{I}{2}H_1(-\omega)e^{-j\omega t} \end{aligned} \tag{D.7}$$

Substituting equations (D.6) and (D.7) to equation (D.5) we get

$$\begin{aligned} q_1(t) &= \frac{I}{2}H_1(\omega)e^{j\omega t}+\frac{I}{2}H_1(-\omega)e^{-j\omega t} \\ &= 2(\frac{I}{2})Re\{H_1(\omega)e^{j\omega t}\} \\ &= I|H_1(\omega)|cos[\omega t+\theta(\omega)] \end{aligned} \tag{D.8}$$

In equation (D.8) 'Re' means "the real part of" and we have used the polar form of transfer function

$$H_1(\omega) = |H_1(\omega)|e^{j\theta(\omega)} \tag{D.9}$$

D.2 Calculation of $q_2(t)$

For $n = 2$ the Volterra series can be written from (D.4) as

$$\begin{aligned} q_2(t) &= \frac{1}{2!}\int_{-\infty}^{\infty}\int_{-\infty}^{\infty} h_2(u_1,u_2)i(t-u_1)i(t-u_2)du_1du_2 \\ &= \mathbf{B}_2[i(t)] \\ &= \mathbf{B}_2[i_a(t)+i_b(t)] \end{aligned} \tag{D.10}$$

Where $\mathbf{B}_2$ is the second order Volterra operator. Since it is not linear therefore, $\mathbf{B}_2[i_a(t) + i_b(t)]$ can not be written as the linear combination of $\mathbf{B}_2[i_a(t)]$ and $\mathbf{B}_2[i_b(t)]$. However it can be written as[5]

$$\mathbf{B}_2[i_a(t)+i_b(t)] = \mathbf{B}_2[i_a(t)] + \mathbf{B}_2\{i_a(t),i_b(t)\} + \mathbf{B}_2\{i_b(t),i_a(t)\} + \mathbf{B}_2[i_b(t)] \tag{D.11}$$

in that

$$\mathbf{B}_2\{i_a(t),i_b(t)\} = \frac{1}{2!}\int_{-\infty}^{\infty}\int_{-\infty}^{\infty} h_2(u_1,u_2)i_a(t-u_1)i_b(t-u_2)du_1du_2 \tag{D.12}$$

Now,

$$\begin{aligned} \mathbf{B}_2[i_a(t)] &= \frac{1}{2!}\int_{-\infty}^{\infty}\int_{-\infty}^{\infty} h_2(u_1,u_2)i_a(t-u_1)i_a(t-u_2)du_1du_2 \\ &= \frac{1}{2}\cdot\frac{I^2}{4}\int_{-\infty}^{\infty}\int_{-\infty}^{\infty} h_2(u_1,u_2)e^{j\omega(t-u_1)}e^{j\omega(t-u_2)}du_1du_2 \\ &= \frac{I^2}{8}e^{j2\omega t}\int_{-\infty}^{\infty}\int_{-\infty}^{\infty} h_2(u_1,u_2)e^{-j\omega u_1}e^{-j\omega u_2}du_1du_2 \\ &= \frac{I^2}{8}H_2(\omega,\omega)e^{j2\omega t} \end{aligned} \tag{D.13}$$

where $H_2(\omega,\omega)$ is the two dimentional Fourier transform of the second order Volterra kernel $h_2(u_1,u_2)$. Similarly

$$\begin{aligned}
\mathbf{B}_2[i_b(t)] &= \frac{1}{2!}\int_{-\infty}^{\infty}\int_{-\infty}^{\infty} h_2(u_1,u_2)i_b(t-u_1)i_b(t-u_2)du_1du_2 \\
&= \frac{1}{2}\cdot\frac{I^2}{4}\int_{-\infty}^{\infty}\int_{-\infty}^{\infty} h_2(u_1,u_2)e^{-j\omega(t-u_1)}e^{-j\omega(t-u_2)}du_1du_2 \\
&= \frac{I^2}{8}e^{-j2\omega t}\int_{-\infty}^{\infty}\int_{-\infty}^{\infty} h_2(u_1,u_2)e^{j\omega u_1}e^{j\omega u_2}du_1du_2 \\
&= \frac{I^2}{8}H_2(-\omega,-\omega)e^{-j2\omega t} \qquad \text{(D.14)}
\end{aligned}$$

$$\begin{aligned}
\mathbf{B}_2\{i_a(t),i_b(t)\} &= \frac{1}{2!}\int_{-\infty}^{\infty}\int_{-\infty}^{\infty} h_2(u_1,u_2)\frac{I}{2}e^{j\omega(t-u_1)}\frac{I}{2}e^{-j\omega(t-u_2)}du_1du_2 \\
&= \frac{I^2}{8}\int_{-\infty}^{\infty}\int_{-\infty}^{\infty} h_2(u_1,u_2)e^{-j\omega u_1}e^{j\omega u_2}du_1du_2 \\
&= \frac{I^2}{8}H_2(\omega,-\omega) \qquad \text{(D.15)}
\end{aligned}$$

Similarly,

$$\mathbf{B}_2\{i_b(t),i_a(t)\} = \frac{I^2}{8}H_2(-\omega,\omega) \qquad \text{(D.16)}$$

Adding equations (D.13) through (D.16) and using (D.10) and (D.11) we obtain

$$q_2(t) = \frac{I^2}{8}H_2(\omega,\omega)e^{j2\omega t} + \frac{I^2}{8}H_2(-\omega,-\omega)e^{-j2\omega t} + \frac{I^2}{8}H_2(\omega,-\omega) + \frac{I^2}{8}H_2(-\omega,\omega) \qquad \text{(D.17)}$$

The first two terms are the conjugates of each other, also the last two terms and therefore we can write

$$\begin{aligned}
q_2(t) &= \frac{I^2}{8}[H_2(\omega,\omega)e^{j2\omega t} + \{H_2(\omega,\omega)e^{j2\omega t}\}^* + H_2(\omega,-\omega) + \{H_2(\omega,-\omega)\}^*] \\
&= 2\frac{I^2}{8}Re[H_2(\omega,\omega)e^{j2\omega t}] + 2\frac{I^2}{8}Re[H_2(\omega,-\omega)] \qquad \text{(D.18)}
\end{aligned}$$

D.3 Calculation of $q_3(t)$

From (D.4) we can write for $n = 3$

$$\begin{aligned} q_3(t) &= \frac{1}{3!}\int_{-\infty}^{\infty}\int_{-\infty}^{\infty}\int_{-\infty}^{\infty} h_3(u_1,u_2,u_3)i(t-u_1)i(t-u_2)i(t-u_3)du_1du_2du_3 \\ &= \mathbf{B}_3[i(t)] \\ &= \mathbf{B}_3[i_a(t)+i_b(t)] \end{aligned} \tag{D.19}$$

Where $\mathbf{B}_3$ is the third order Volterra operator and its operation can be written as[5]

$$\begin{aligned} \mathbf{B}_3[i_a(t)+i_b(t)] &= \mathbf{B}_3[i_a(t)] + 3\mathbf{B}_3\{i_a(t),i_a(t),i_b(t)\} + 3\mathbf{B}_3\{i_a(t),i_b(t),i_b(t)\} \\ &\quad +\mathbf{B}_3[i_b(t)] \end{aligned} \tag{D.20}$$

in which

$$\mathbf{B}_3\{i_a(t),i_a(t),i_b(t)\} = \frac{1}{3!}\int_{-\infty}^{\infty}\int_{-\infty}^{\infty}\int_{-\infty}^{\infty} h_3(u_1,u_2,u_3)i_a(t-u_1)i_a(t-u_2)i_b(t-u_3)du_1du_2du_3 \tag{D.21}$$

Now,

$$\begin{aligned} \mathbf{B}_3[i_a(t)] &= (\frac{I}{2})^3\cdot\frac{1}{3!}\int_{-\infty}^{\infty}\int_{-\infty}^{\infty}\int_{-\infty}^{\infty} h_3(u_1,u_2,u_3)e^{j\omega(t-u_1)}e^{j\omega(t-u_2)}e^{j\omega(t-u_3)}du_1du_2du_3 \\ &= (\frac{I}{2})^3\cdot\frac{1}{3!}e^{j3\omega t}\int_{-\infty}^{\infty}\int_{-\infty}^{\infty}\int_{-\infty}^{\infty} h_3(u_1,u_2,u_3)e^{-j\omega(u_1+u_2+u_3)}du_1du_2du_3 \end{aligned} \tag{D.22}$$

The integral on the right hand side is the third order kernel transform evaluated at $\omega_1 = \omega_2 = \omega_3 = \omega$. Therefore,

$$\mathbf{B}_3[i_a(t)] = (\frac{I}{2})^3\cdot\frac{1}{3!}H_3(\omega,\omega,\omega)e^{j3\omega t} \tag{D.23}$$

Similarly,

$$\mathbf{B}_3[i_b(t)] = (\frac{I}{2})^3\cdot\frac{1}{3!}H_3(-\omega,-\omega,-\omega)e^{-j3\omega t} \tag{D.24}$$

It is seen that $B_3[i_a(t)]$ and $B_3[i_b(t)]$ are conjugates of each other and the sum of these two gives

$$B_3[i_a(t)] + B_3[i_b(t)] = 2 \cdot (\frac{I}{2})^3 \cdot \frac{1}{3!} Re[H_3(\omega,\omega,\omega)e^{j3\omega t}] \quad (D.25)$$

Now, the second term of (D.20) is

$$\begin{aligned} 3B_3\{i_a(t), i_a(t), i_b(t)\} &= 3(\frac{I}{2})^3 \cdot \frac{1}{3!} \int_{-\infty}^{\infty}\int_{-\infty}^{\infty}\int_{-\infty}^{\infty} h_3(u_1,u_2,u_3)e^{j\omega(t-u_1)}e^{j\omega(t-u_2)}e^{-j\omega(t-u_3)} \\ &= 3(\frac{I}{2})^3 \cdot \frac{1}{3!} e^{j\omega t} \int_{-\infty}^{\infty}\int_{-\infty}^{\infty}\int_{-\infty}^{\infty} h_3(u_1,u_2,u_3)e^{-j\omega(u_1+u_2-u_3)}du_1du_2du_3 \\ &= (\frac{I^3}{16})H_3(\omega,\omega,-\omega)e^{j\omega t} \end{aligned} \quad (D.26)$$

Similarly,

$$3B_3\{i_a(t), i_b(t), i_b(t)\} = (\frac{I^3}{16})H_3(-\omega,-\omega,\omega)e^{-j\omega t} \quad (D.27)$$

Equation (D.26) and (D.27) are conjugates of each other. Adding both we get

$$3B_3\{i_a(t), i_a(t), i_b(t)\} + 3B_3\{i_a(t), i_b(t), i_b(t)\} = 2(\frac{I^3}{16})Re[H_3(\omega,\omega,-\omega)e^{j\omega t}] \quad (D.28)$$

Adding equations (D.25) and (D.28) and using equations (D.19) and (D.20) we have the response

$$q_3(t) = (\frac{I^3}{24})Re[H_3(\omega,\omega,\omega)e^{j3\omega t}] + (\frac{I^3}{8})Re[H_3(\omega,\omega,-\omega)e^{j\omega t}] \quad (D.29)$$

From (5.22)

$$\begin{aligned} \frac{3HD}{C} &= \frac{m^2(I_o - I_{th})^2}{24|G_1(0)|^2|G_1(3\omega)|}|[G_3(\omega,\omega,\omega) - 3\frac{G_2(\omega,\omega)G_2(\omega,2\omega)}{G_1(2\omega)}]| \\ &= \frac{m^2(I_o - I_{th})^2}{24|G_1(0)|^2|G_1(3\omega)G_1(2\omega)|}|\xi| \end{aligned} \quad (D.30)$$

Where,

$$\xi = G_3(\omega,\omega,\omega)G_1(2\omega) - 3G_2(\omega,\omega)G_2(\omega,2\omega) \tag{D.31}$$

From Appendix C using (C.3), (C.5) and (C.7) we can write

$$\begin{aligned} G_3(\omega,\omega,\omega)G_1(2\omega) &= (6R + j6S\omega - 18G\omega^2)(D + j2E\omega - 4F\omega^2) \\ &= 6RD + j6DS\omega - 18DG\omega^2 + j12RE\omega - 12SE\omega^2 \\ &\quad -j36GE\omega^3 - 24RF\omega^2 - j24SF\omega^3 + 72GF\omega^4 \end{aligned} \tag{D.32}$$

$$\begin{aligned} 3G_2(\omega,\omega)G_2(\omega,2\omega) &= 3(-2L - j2M\omega + 4N\omega^2)(-2L - j3M\omega + 9N\omega^2) \\ &= 4L^2 - 26NL\omega^2 + j10ML\omega - j30MN\omega^3 - 6M^2\omega^2 + 36N^2\omega^4 \end{aligned} \tag{D.33}$$

Therefore,

$$\begin{aligned} \xi &= (72GF - 108N^2)\omega^4 - (18DG + 12SE + 24RF - 78NL - 18M^2)\omega^2 \\ &\quad +(6RD - 12L^2) + j[(6DS + 12RE - 30ML)\omega \\ &\quad +(90MN - 36GE - 24SF)\omega^3] \end{aligned} \tag{D.34}$$

Equation (D.30) along with (D.34) has been used in the computer program for the calculation of numerical results.

Appendix E

Calculation of IMD

The input to the laser are two equal amplitude sinusoids

$$\begin{aligned} i(t) &= I\,cos\omega_1 t + I\,cos\omega_2 t \\ &= \frac{I}{2}e^{j\omega_1 t} + \frac{I}{2}e^{-j\omega_1 t} + \frac{I}{2}e^{j\omega_2 t} + \frac{I}{2}e^{-j\omega_2 t} \\ &= i_a(t) + i_b(t) + i_c(t) + i_d(t) \end{aligned} \tag{E.1}$$

Where,

$$i_a(t) = \frac{I}{2}e^{j\omega_1 t} \tag{E.2}$$

$$i_b(t) = \frac{I}{2}e^{-j\omega_1 t} \tag{E.3}$$

$$i_c(t) = \frac{I}{2}e^{j\omega_2 t} \tag{E.4}$$

and

$$i_d(t) = \frac{I}{2}e^{-j\omega_2 t} \tag{E.5}$$

In a similar way as we have calculated in (D.8), the intensity of a single optical carrier at the output of the laser is

$$C = I|H_1(\omega)| \tag{E.6}$$

The two tone intermodulation product is a third order effect and therefore those terms are of interest which give the product terms $(2\omega_1 - \omega_2)$ and $(2\omega_2 - \omega_1)$ in the optical output. Only the third order Volterra operator $\mathbf{B_3}$ produces these quantities at the output of the system. We recall equation (D.19). For the input (E.1)

$$\begin{aligned} q_3(t) &= \frac{1}{3!}\int_{-\infty}^{\infty}\int_{-\infty}^{\infty}\int_{-\infty}^{\infty} h_3(u_1,u_2,u_3)i(t-u_1)i(t-u_2)i(t-u_3)du_1du_2du_3 \\ &= \mathbf{B_3}[i(t)] \\ &= \mathbf{B_3}[i_a(t)+i_b(t)+i_c(t)+i_d(t)] \end{aligned} \tag{E.7}$$

Since $\mathbf{B_3}$ is a third order operator we can write its operation as

$$\begin{aligned} \mathbf{B_3}[i_a(t)+i_b(t)+i_c(t)+i_d(t)] &= \mathbf{B_3}[i_a(t)]+\mathbf{B_3}[i_b(t)]+\mathbf{B_3}[i_c(t)]+\mathbf{B_3}[i_d(t)] \\ &\quad +3\mathbf{B_3}\{i_a(t),i_b(t),i_b(t)\}+3\mathbf{B_3}\{i_a(t),i_c(t),i_c(t)\} \\ &\quad +3\mathbf{B_3}\{i_a(t),i_d(t),i_d(t)\}+3\mathbf{B_3}\{i_a(t),i_a(t),i_b(t)\} \\ &\quad +3\mathbf{B_3}[i_a(t),i_a(t),i_c(t)]+3\mathbf{B_3}\{i_a(t),i_a(t),i_d(t)\} \\ &\quad +3\mathbf{B_3}\{i_b(t),i_b(t),i_c(t)\}+3\mathbf{B_3}\{i_b(t),i_b(t),i_d(t)\} \\ &\quad +3\mathbf{B_3}\{i_b(t),i_c(t),i_c(t)\}+3\mathbf{B_3}\{i_b(t),i_d(t),i_d(t)\} \\ &\quad +3\mathbf{B_3}\{i_c(t),i_d(t),i_d(t)\}+3\mathbf{B_3}\{i_c(t),i_c(t),i_d(t)\} \\ &\quad +6\mathbf{B_3}\{i_a(t),i_b(t),i_c(t)\}+6\mathbf{B_3}\{i_a(t),i_b(t),i_d(t)\} \\ &\quad +6\mathbf{B_3}\{i_a(t),i_c(t),i_d(t)\}+6\mathbf{B_3}\{i_b(t),i_c(t),i_d(t)\} \end{aligned}$$

Among these only the terms $3\mathbf{B_3}\{i_a(t),i_a(t),i_d(t)\}$ and $3\mathbf{B_3}\{i_b(t),i_b(t),i_c(t)\}$ produces frequency components at $(2\omega_1-\omega_2)$ and the terms $3\mathbf{B_3}\{i_b(t),i_c(t),i_c(t)\}$ and $3\mathbf{B_3}\{i_a(t),i_d(t),i_d(t)\}$ produces frequency components at $(2\omega_2-\omega_1)$.

$$3\mathbf{B_3}\{i_a(t),i_a(t),i_d(t)\} = 3(\frac{I}{2})^3\cdot\frac{1}{3!}\int_{-\infty}^{\infty}\int_{-\infty}^{\infty}\int_{-\infty}^{\infty} h_3(u_1,u_2,u_3)e^{j\omega_1(t-u_1)}e^{j\omega_1(t-u_2)}e^{-j\omega_2(t-u_3)}du_1du_2du$$

$$= \frac{I^3}{16} e^{j(2\omega_1-\omega_2)} \int_{-\infty}^{\infty}\int_{-\infty}^{\infty}\int_{-\infty}^{\infty} h_3(u_1,u_2,u_3) e^{-j(\omega_1 u_1+\omega_1 u_2-\omega_2 u_3)} du_1 du_2 du_3$$

$$= \frac{I^3}{16} H_3(\omega_1,\omega_1,-\omega_2) e^{j(2\omega_1-\omega_2)t} \qquad \text{(E.8}$$

Similarly

$$3B_3\{i_b(t),i_b(t),i_c(t)\} = \frac{I^3}{16} H_3(-\omega_1,-\omega_1,\omega_2) e^{-j(2\omega_1-\omega_2)t} \qquad \text{(E.9)}$$

$$3B_3\{i_b(t),i_c(t),i_c(t)\} = \frac{I^3}{16} H_3(-\omega_1,\omega_2,\omega_2) e^{j(2\omega_2-\omega_1)t} \qquad \text{(E.10)}$$

$$3B_3\{i_a(t),i_d(t),i_d(t)\} = \frac{I^3}{16} H_3(\omega_1,-\omega_2,-\omega_2) e^{-j(2\omega_2-\omega_1)t} \qquad \text{(E.11)}$$

Adding (E.8) through (E.11) we have

$$\begin{aligned} \tilde{q}_3(t) &= \frac{I^3}{16}[H_3(\omega_1,\omega_1,-\omega_2)e^{j(2\omega_1-\omega_2)t} + H_3(-\omega_1,-\omega_1,\omega_2)e^{-j(2\omega_1-\omega_2)t} \\ &\quad + H_3(-\omega_1,\omega_2,\omega_2)e^{j(2\omega_2-\omega_1)t} + H_3(\omega_1,-\omega_2,-\omega_2)e^{-j(2\omega_2-\omega_1)t}] \\ &= \frac{I^3}{16}[2Re\{H_3(\omega_1,\omega_1,-\omega_2)e^{j(2\omega_1-\omega_2)t}\} + 2Re\{H_3(-\omega_1,\omega_2,\omega_2)e^{j(2\omega_2-\omega_1)t}\} \\ &= \frac{I^3}{8} Re[H_3(\omega_1,\omega_1,-\omega_2)e^{j(2\omega_1-\omega_2)t}] + \frac{I^3}{8} Re[H_3(-\omega_1,\omega_2,\omega_2)e^{j(2\omega_2-\omega_1)t}] \end{aligned} \qquad \text{(E.12)}$$

Appendix F

Simplified Model for IMD

We recall equation (5.28)

$$\begin{aligned}\eta &= G_3(\omega,\omega,-\omega)G_1(0)G_1(2\omega) - 2G_2(\omega,-\omega)G_2(\omega,0)G_1(2\omega) \\ &\quad -G_2(\omega,\omega)G_2(-\omega,2\omega)G_1(0) \qquad \text{(F.1)}\end{aligned}$$

Now,

$$\begin{aligned}G_3(\omega,\omega,-\omega)G_1(0)G_1(2\omega) &= (6R+j2S\omega-2G\omega^2)(D+j2E\omega-4F\omega^2) \\ &= 6RD^2+j(2D^2S\omega+12RDE\omega-4DGE\omega^3-8DFS\omega^3) \\ &\quad -(2D^2G+4DSE+24RDF)\omega^2+8DFG\omega^4 \qquad \text{(F.2)}\end{aligned}$$

$$\begin{aligned}2G_2(\omega,-\omega)G_2(\omega,0)G_1(2\omega) &= 2(2L)(2L-N\omega^2+jM\omega)(D+j2E\omega-4F\omega^2) \\ &= 8DL^2-(4DNL+8MEL+32FL^2)\omega^2+16FLN\omega^4 \\ &\quad +j[(4DML+16EL^2)\omega-(8NEL+16FML)\omega^3] \qquad \text{(F.3)}\end{aligned}$$

$$\begin{aligned}G_2(\omega,\omega)G_2(-\omega,2\omega)G_1(0) &= \cdot(2L-4N\omega^2+j2M\omega)(2L-N\omega^2+jM\omega)\cdot D \\ &= 4DL^2-(10DLN+2DM^2)\omega^2+4DN^2\omega^4+j(6DML\omega-6DMN\omega^3) \\ &\qquad \text{(F.4)}\end{aligned}$$

and

$$\eta = [6RD^2 - 12DL^2 + (14DLN - 2D^2G - 4DSE - 24RDF + 8MEL + 32FL^2 + 2DM^2)\omega^2 + (8DFG - 16FLN - 4DN^2)\omega^4] + j[(2D^2S + 12RDE - 10DML - 16EL^2)\omega + (8NEL - 4DGE - 8DFS + 16FML + 6DMN)\omega^3] \quad (F.5)$$

This value of η has been used with equation (5.27) in numerical calculation. In the simplified analysis instead of A, D, E, ... etc. the constants are A_1, D_1, E_1, ... with $R_1 = 0$ and $L_1 = 0$ as given in Appendix B equation (B.21). Therefore,

$$\begin{aligned} \eta &= -(2D_1^2G_1 + 4D_1S_1E_1 - 2D_1M_1^2)\omega^2 + (8D_1F_1G_1 - 4D_1N_1^2)\omega^4 \\ &\quad + j[2D_1^2S_1\omega - (4D_1G_1E_1 + 8D_1F_1S_1 - 6D_1M_1N_1)\omega^3] \\ &= \alpha_1 + j\beta_1 \end{aligned} \quad (F.6)$$

$$\begin{aligned} \alpha_1 &= -(2D_1^2G_1 + 4D_1S_1E_1 - 2D_1M_1^2)\omega^2 + (8D_1F_1G_1 - 4D_1N_1^2)\omega^4 \\ &= -[2\frac{V'^2}{\Gamma^2\tau_p^2}\frac{V'}{\Gamma gQ_o^3} + 4\frac{V'}{\Gamma\tau_p}\frac{3\epsilon^3V'}{\Gamma g\tau_p}\frac{\epsilon V'}{\Gamma g\tau_p} - 2\frac{V'}{\Gamma\tau_p}\frac{4\epsilon^4V'^2}{\Gamma^2g^2\tau_p^2}]\omega^2 \\ &\quad + [8\frac{V'}{\Gamma\tau_p}\frac{V'}{\Gamma gQ_o}\frac{V'}{\Gamma gQ_o^3} - 4\frac{V'}{\Gamma\tau_p}\frac{V'^2}{\Gamma^2g^2Q_o^4}]\omega^4 \\ &= -[\frac{2V'^3}{\Gamma^3g\tau_p^2Q_o^3} + \frac{4\epsilon^4V'^3}{\Gamma^3g^2\tau_p^3}]\omega^2 + (\frac{4V'^3}{\Gamma^3g^2\tau_pQ_o^4})\omega^4 \end{aligned} \quad (F.7)$$

The second term within the first squared bracket is smaller than the first term so that we can neglect this term. Hence,

$$\alpha_1 = -(\frac{2V'^3}{\Gamma^3g\tau_p^2Q_o^3})\omega^2 + (\frac{4V'^3}{\Gamma^3g^2\tau_pQ_o^4})\omega^4 \quad (F.8)$$

$$\alpha_1(I_o - I_{th})^2 = -(\frac{2V'^3(I_o - I_{th})^2}{\Gamma^3g\tau_p^2Q_o^3})\omega^2 + (\frac{4V'^3(I_o - I_{th})^2}{\Gamma^3g^2\tau_pQ_o^4})\omega^4 \quad (F.9)$$

Steady state value of photon density Q_o is given by the relation

$$Q_o = \frac{\Gamma\tau_p(I_o - I_{th})}{V'} \quad (F.10)$$

Using this value of Q_o

$$\begin{aligned}\alpha_1(I_o - I_{th})^2 &= -[\frac{2V'^5}{\Gamma^5\tau_p^5}\frac{V'}{\Gamma g(I_o - I_{th})}]\omega^2 + [\frac{4V'^5}{\Gamma^5\tau_p^5}\frac{V'^2}{\Gamma^2 g^2(I_o - I_{th})^2}]\omega^4 \\ &= 4(\frac{V'}{\Gamma\tau_p})^5[(\frac{\omega}{\omega_r})^4 - \frac{1}{2}(\frac{\omega}{\omega_r})^2] \qquad \text{(F.11)}\end{aligned}$$

where $\omega_r^2 = \frac{\Gamma g(I_o - I_{th})}{V'}$ is the resonance frequency of the laser.

$$\beta_1 = 2D_1^2 S_1\omega - (4D_1G_1E_1 + 8D_1F_1S_1 - 6D_1M_1N_1)\omega^3 \qquad \text{(F.12)}$$

The terms $8D_1F_1S_1$ and $6D_1M_1N_1$ are extremely smaller than the term $4D_1G_1E_1$ so, we can neglect these two terms. Since at higher frequencies ω^3 is the dominant frequency component, we will proceed only with this term and omit the term containing ω. Therefore,

$$\begin{aligned}\beta_1 &= -(4D_1G_1E_1)\omega^3 \\ &= -4\frac{V'}{\Gamma\tau_p}\frac{V'}{\Gamma g Q_o^3}\frac{\epsilon V'}{\Gamma g\tau_p}\omega^3 \\ &= -\frac{4\epsilon V'^3}{\Gamma^3\tau_p^2 g^2 Q_o^3}\omega^3 \qquad \text{(F.13)}\end{aligned}$$

Using (F.10),

$$\begin{aligned}\beta_1(I_o - I_{th})^2 &= -\frac{4\epsilon V'^3(I_o - I_{th})^2 V'^5}{\Gamma^3 g^2\tau_p^2\Gamma^3\tau_p^3(I_o - I_{th})^3}\omega^3 \\ &= -\frac{4\epsilon V'^5}{\Gamma^5\tau_p^5 g}\frac{V'}{\Gamma g(I_o - I_{th}}\omega^3 \\ &= -\frac{4\epsilon}{g}(\frac{V'}{\Gamma\tau_p})^5\frac{\omega^3}{\omega_r^2} \qquad \text{(F.14)}\end{aligned}$$

Now, from equations (F.6), (F.11) and (F.14)

$$\eta(I_o - I_{th})^2 = 4(\frac{V'}{\Gamma\tau_p})^5[(\frac{\omega}{\omega_r})^4 - \frac{1}{2}(\frac{\omega}{\omega_r})^2 - j\frac{\epsilon}{g}\frac{\omega^3}{\omega_r^2}] \qquad \text{(F.15)}$$

Now, we recall equation (5.27), then we substitute (F.15) into that. It may be noted that $G_1(0) = D_1 = \frac{V'}{\Gamma\tau_p}$. Therefore,

$$\begin{aligned}\frac{IMD}{C} &= \frac{m^2(I_o - I_{th})^2|\eta|}{8|G_1(0)|^3|G_1(\omega)G_1(2\omega)|} \\ &= \frac{|m^2 4D_1^5[(\frac{\omega}{\omega_r})^4 - \frac{1}{2}(\frac{\omega}{\omega_r})^2 - j\frac{\epsilon}{g}\frac{\omega^3}{\omega_r^2}]|}{8D_1^3|G_1(\omega)G_1(2\omega)|} \qquad \text{(F.16)}\end{aligned}$$

From which we have the simplified model for intermodulation distortion

$$\frac{IMD}{C} = \frac{1}{2}m^2 \frac{[\{(\frac{\omega}{\omega_\tau})^4 - \frac{1}{2}(\frac{\omega}{\omega_\tau})^2\}^2 + \{\frac{\epsilon}{g}\frac{\omega^3}{\omega_\tau^2}\}^2]}{|G_1'(\omega)G_1'(2\omega)|} \tag{F.17}$$

Where,

$$G_1(\omega) = D_1 + jE_1\omega - F_1\omega^2 \tag{F.18}$$

and

$$\begin{aligned} G_1'(\omega) &= 1 + j\frac{E_1}{D_1}\omega - \frac{F_1}{D_1}\omega^2 \\ &= 1 + j\frac{\epsilon}{g}\omega - \frac{\omega^2}{\omega_\tau^2} \end{aligned} \tag{F.19}$$

Appendix G

Perturbation Analysis Technique of Rate Equations

The perturbation analysis of the rate equations has been indicated in the literature [3], [7]. The starting procedure of such analysis is outlined below.

We recall the rate equations

$$\frac{dN}{dt} = \frac{I_a}{V'} - \frac{N}{\tau_{sp}} - g(N - N_o)(1 - \epsilon Q)Q \tag{G.1}$$

$$\frac{dQ}{dt} = \Gamma g(N - N_o)(1 - \epsilon Q)Q - \frac{Q}{\tau_p} + \Gamma\beta\frac{N}{\tau_{sp}} \tag{G.2}$$

The quantities I_a, N and Q can be written as

$$I_a = i_o + i \tag{G.3}$$

$$N = n_o + n_1 + n_2 + n_3 + ... \tag{G.4}$$

$$Q = q_o + q_1 + q_2 + q_3 + ... \tag{G.5}$$

Where i_o, n_o and q_o are the d.c. quantities. The subscripts refer to the perturbation order and the terms of interest are up to the third order. The zero order quantities are time independent and others are time dependent. We can Substitute these to equations (G.1)

and (G.2). First we expand the term $g(N-N_o)(1-\epsilon Q)Q$. Let

$$\xi = g(N-N_o)(1-\epsilon Q)Q \tag{G.6}$$

$$\begin{aligned}
\xi &= g(n_o+n_1+n_2+n_3-N_o)(1-\epsilon q_o-\epsilon q_1-\epsilon q_2-\epsilon q_3)(q_o+q_1+q_2+q_3) \\
&= g(n_o-N_o+n_1+n_2+n_3)(q_o+q_1+q_2+q_3-\epsilon q_o^2--2\epsilon q_o q_2-2\epsilon q_o q_3 \\
&\quad 2\epsilon q_o q_1-2\epsilon q_1 q_2-\epsilon q_1^2) \\
&= g[N'q_o(1-\epsilon q_o)+\{N'(1-2\epsilon q_o)q_1+q_o(1-\epsilon q_o)n_1\}+\{N'(1-2\epsilon q_o)q_2- \\
&\quad N'\epsilon q_1^2+q_o(1-\epsilon q_o)n_2+(1-2\epsilon q_o)n_1q_1\}+\{N'(1-2\epsilon q_o)q_3-2N'\epsilon q_1q_2+ \\
&\quad q_o(1-\epsilon q_o)n_3+(1-2\epsilon q_o)n_2q_1+(1-2\epsilon q_o)n_1q_2-\epsilon n_1q_1^2\}]
\end{aligned} \tag{G.7}$$

Where, $N'=n_o-N_o$. Let us define $A=gq_o(1-\epsilon q_o)$ and $B=g(1-2\epsilon q_o)$. Therefore,

$$\begin{aligned}
\xi &= N'A+\{N'Bq_1+An_1\}+\{N'Bq_2-N'\epsilon q_1^2+An_2+Bn_1q_1\} \\
&\quad +\{N'Bq_3-2N'\epsilon q_1q_2+An_3+Bn_2q_1+Bn_1q_2-\epsilon n_1q_1^2\}]
\end{aligned} \tag{G.8}$$

Using equation (G.6), equations (G.1) and (G.2) can be written as

$$\frac{d(n_o+n_1+n_2+n_3)}{dt}=\frac{i_o+i}{V'}-\frac{n_o+n_1+n_2+n_3}{\tau_{sp}}-\xi \tag{G.9}$$

$$\frac{d(q_o+q_1+q_2+q_3)}{dt}=\Gamma\xi-\frac{q_o+q_1+q_2+q_3}{\tau_p}+\Gamma\beta\frac{n_o+n_1+n_2+n_3}{\tau_{sp}} \tag{G.10}$$

The steady state equations are

$$0=\frac{i_o}{V'}-\frac{n_o}{\tau_{sp}}-N'A \tag{G.11}$$

$$0=\Gamma N'A-\frac{q_o}{\tau_p}+\Gamma\beta\frac{n_o}{\tau_{sp}} \tag{G.12}$$

The first order equations are

$$\frac{dn_1}{dt}=\frac{i}{V'}-\frac{n_1}{\tau_{sp}}-N'Bq_1-An_1 \tag{G.13}$$

$$\frac{dq_1}{dt} = \Gamma N' B q_1 + \Gamma A n_1 - \frac{q_1}{\tau_p} + \Gamma\beta\frac{n_1}{\tau_{sp}} \tag{G.14}$$

The second order equations are

$$\frac{dn_2}{dt} = -\frac{n_2}{\tau_{sp}} - N' B q_2 + g\epsilon N' q_1^2 - A n_2 - B n_1 q_1 \tag{G.15}$$

$$\frac{dq_2}{dt} = \Gamma\{N' B q_2 - g\epsilon N' q_1^2 + A n_2 + B n_1 q_1\} - \frac{q_2}{\tau_p} + \Gamma\beta\frac{n_2}{\tau_{sp}} \tag{G.16}$$

The third order equations are

$$\frac{dn_3}{dt} = -\frac{n_3}{\tau_{sp}} - N' B q_3 + 2N'\epsilon q_1 q_2 - A n_3 - B n_2 q_1 - B n_1 q_2 + g\epsilon n_1 q_1^2 \tag{G.17}$$

$$\frac{dq_3}{dt} = \Gamma\{N' B q_3 - 2N'\epsilon q_1 q_2 + A n_3 + B n_2 q_1 + B n_1 q_2 - g\epsilon n_1 q_1^2\} - \frac{q_3}{\tau_p} + \Gamma\beta\frac{n_3}{\tau_{sp}} \tag{G.18}$$

Equations (G.13) and (G.14) can be used to solve the first order quantities n_1 and q_1. Here, i is the driving current. Similarly, equations (G.15) and (G.16) can be used to solve the second order quantities and so on.

```
program main(input,output);
var
 a,b,c,d,e,f,g,h,i,OMD,Ith,Q,w,b1,c1,theta,gamma,d1:double;
 e1,f1,l1,m1,n1, r1,s1,g1,f2,f3,w1,a1:double;
 h1, p1,p2,p3,p4,p5,k1,k2,k3,k4,k5,g4,r2,r3,r4.r5,r6:double;
begin
    a:=1.44E-35;                                          {a = V }
    b:=2e-12;                                             {b = tau_ph}
    c:=3.72e-9;                                           {c = tau_sp}
    d:=4.6e+24;                                           {d = No}
    e:=1e-12;                                             {e = g}
    f:=0.646;                                             {f = Gamma}
    g:=1e-03;                                             {g = beta}
    h:=3.8e-23;                                           {h = epsilon}
    OMD:=0.4;
    Ith:=21e-03;
    i:=36.75E-03;                                         {i = Idc}
    Q:=f*b*(i-Ith)/a;
    w:= f*(e*q+g/c-h*e*q*q);                              {w=a}
    b1:=f*e*(1-2*h*q);                                    {b1=b}
    c1:=-h*e*f;                                           {c1=c}
    theta:=b1*b1/(w*w*w)-c1/(w*w);
    gamma:=(2*b1*c1-b1*b1*b1/w)/(w*w*w);
    d1:=a*(1/(f*b)+1/(w*c*b)-b1*q/(w*w*b*c)+b1*f*g*d/(w*w*c*c));
    e1:=a*(1/f+1/(w*c)-b1*q/(w*w*b)+b1*f*g*d/(w*w*c)+1/(w*b));
    f1:=a/w;
    l1:=a*(b1/(w*w*c*b)-theta*q/(c*b)+theta*f*g*d/(c*c));
    m1:=a*(b1/(w*w*c)+2*b1/(w*w*b)+2*theta*f*g*d/c-2*theta*q/b);
    n1:=b1*a/w/w;
    r1:=a*(theta/(c*b)+gamma*q/(c*b)-gamma*f*g*d/(c*c));
    s1:=a*(theta/c+3*theta/b+3*gamma*q/b-3*gamma*f*g*d/c);
    g1:=theta*a;
    f3:=sqrt(e*Q/b)/2/(3.141592654);
    f2:=1e+09;                                            {f2 = frequency}
 repeat
    w1:=2*3.14159265 4*f2;                                {w1 = angular freq.}
{Calculation of H1(w)}
       p5:=sqrt(sqr(d1-f1*w1*w1)+sqr(e1*w1));             {p5 = G1(w)}
       a1:=sqrt(sqr(1-f1*w1*w1/d1)+sqr(e1*w1/d1));
       H1:=20.0*ln(a1)/ln(10.0);
     { OMD:=5.6E-03*d1/((i-Ith)*p5); }
 {Calculation of 2HD/C}
       p1:=sqrt(sqr(2*l1-4*n1*w1*w1)+sqr(2*m1*w1));    {p1 = G2(w,w)}
       p4:=sqrt(sqr(d1-4*f1*w1*w1)+sqr(2*e1*w1));      {p4 = G1(2w)}
       p2:=OMD*(i-Ith)*p1/(4*d1*p4);                   {p2 = 2HD/C}
       p3:=20*ln(p2)/ln(10);
  {Calculation of 3HD/C}
       k1: = sqr(w1*w1)*(72*g1*f1-108*n1*n1)-sqr(w1)*(12*s1*e1+18*d1*g1-
             18*m1*m1+ 24*r1*f1-78*n1*l1)+6*r1*d1-12*l1*l1;
```

```
        k2: = w1*w1*w1*(90*m1*n1-36*g1*e1-24*s1*f1)+w1*(6*d1*s1+12*r1*e1
            -30*m1*l1);
        k3:=sqrt(k1*k1+k2*k2);
        g4:=sqrt(sqr(d1-9*f1*w1*w1)+sqr(3*e1*w1));     {g4 = G(3w)}
        k4:=sqr(OMD*(i-Ith))*k3/(24*d1*d1*p4*g4);      {k4 = 3HD/C}
        k5:=20*ln(k4)/ln(10);
  {Calculation of IMD/C}
        r2:=6*r1*d1*d1-12*d1*l1*l1+w1*w1*(14*d1*n1*l1-2*d1*d1*g1
            -4*d1*s1*e1- 24*r1*d1*f1+8*m1*e1*l1+32*f1*l1*l1+2*d1*m1*m1)
            +sqr(w1*w1)*(8*d1*f1*g1-16*f1*l1*n1-4*d1*n1*n1);
        r3:=w1*(2*d1*d1*s1+12*r1*d1*e1-10*d1*m1*l1-16*e1*l1*l1)+w1*w1*w1*(
            8*n1*e1*l1-4*d1*g1*e1-8*d1*f1*s1+16*f1*m1*l1+6*d1*m1*n1);
        r4:=sqrt(r2*r2+r3*r3);
        r5:=sqr(OMD*(i-Ith))*r4/(8*d1*d1*d1*p4*p5);     {r5 = IMD/C}
        r6:=20*ln(r5)/ln(10);
        writeln('f=',f2,    'value=',r6);
        f2:=f2+0.2e+09;
   until f2 >5e+09;
end.
```

```
program Darcie(input,output);
type real=double;
var
   V,Tph,Tsp,No,g,gamma,beta,epsilon,Idc,OMD,Ith,Q,fr,f:real;
   g1,k8,g2,g3, HD2,HD3,u1,u2,u3,u4,u5,u6,u7,IMD:real;
begin
    V:=1.44E-35;
    Tph:=2e-12;
    Tsp:=3.72e-9;
    No:=4.6e+24;
    g:=1e-12;
    gamma:=0.646;
    beta:=1e-03;
    epsilon:=8e-24;
    Idc:=36.75e-03;
    OMD:=0.4;
    Ith:=21e-03;
    f:=1e+09;
repeat
    Q:=gamma*Tph*(Idc-Ith)/V;
    fr:=sqrt(g*Q/Tph)/(2*3.141592654);
    g1:=sqrt(sqr(sqr(f/fr)-1)+sqr(2*3.141592654*epsilon*f/g));      {g1=g(f)}
    k8:=20*ln(g1)/ln(10);
   { OMD:=5.6e-03/(Idc-Ith)/g1;}
{Calculation of 2HD/C}
    g2:=sqrt(sqr(sqr(2*f/fr)-1)+sqr(2*3.141592654*epsilon*2*f/g));  {g2=g(2f)}
    g3:=sqrt(sqr(sqr(3*f/fr)-1)+sqr(2*3.141592654*epsilon*3*f/g));  {g3=g(3f)}
    u2:=OMD*f*f/(fr*fr*g2);                                         {u2=2HD/C}
    HD2:=20*ln(u2)/ln(10);
{Calculation of 3HD/C}
    u1:=sqr(sqr(f/fr))+0.5*sqr(f/fr);
    u3:=1.5*sqr(OMD)*u1/(g2*g3);                                    {u3=3HD/C}
    HD3:=20*ln(u3)/ln(10);
{Calculation of IMD/C }
    u4:=sqr(sqr(f/fr))-0.5*sqr(f/fr);
    u5:=2*3.141592654*f*f*f*epsilon/(g*fr*fr);
    u6:=sqrt(u4*u4+u5*u5);
    u7:=0.5*sqr(OMD)*u6/(g1*g2);                                    {u7=IMD/C}
    IMD:=20*ln(u7)/ln(10);
    writeln('f=',f,'value=',IMD);
    f:=f+0.2e+09;
 until f>7e+09;
 end.
```

```
program Simplified(input,output);
var
   a,b,c,d,e,f,g,h,i,Ith,OMD,Q,d1,e1,f1,g1:double;
   l1,m1,n1,r1,s1,f2,w1,u1,u2,u3,u4,u5,v1,v2,v3,v4,v5,v6,v7:double;
   p1,p2,p3,p4,p5,p6,wr,r2,r3,r4,r5,r6,r7,r8:double;
begin
    a{V}:=1.44E-35;
    b{Tph}:=2e-12;
    d{No}:=4.6e+24;
    e{g}:=1e-12;
    f{gamma}:=0.646;
    g{beta}:=0;
    h{epsilon}:=8e-24;
    Ith:=21e-03;
    i{Idc}:=36.75e-03;
    Q:=f*b*(i-Ith)/a;
    OMD:=0.4;
    d1:=a/f/b;
    e1:=a*h/f/e/b;
    f1:=a/(f*e*Q);
    l1:=0;
    n1:=a/(f*e*q*q);
    m1:=-2*h*h*a/(f*e*b);
    r1:=0;
    s1:=3*h*h*h*a/(f*e*b);
    g1:=n1/q;
    f2:=1E+09;
 repeat
    w1:=2*3.141592654*f2;
{Calculation of 2HD/C}
    u5:=sqrt(sqr(d1-f1*w1*w1)+sqr(w1*e1));                    {u5:=G(f)}
  { OMD:=(5.6E-03)*d1/(i-Ith)/u5;}
    u1:=sqrt(sqr(2*l1-4*n1*w1*w1)+4*sqr(m1*w1));
    u2:=sqrt(sqr(d1-4*f1*w1*w1)+sqr(2*w1*e1));                {u2=G(2f)}
    u3:=OMD*(i-Ith)*u1/(u2*4*d1);
    u4:=20*ln(u3)/ln(10);
{Calculation of 3HD/C}
    v1:=sqr(w1*w1)*(72*g1*f1-108*n1*n1)-(12*s1*e1+18*d1*g1+24*r1*f1
    -78*n1*l1-18*m1*m1)*w1*w1+6*r1*d1-12*l1*l1;
    v2:=w1*w1*w1*(90*m1*n1-36*g1*e1-24*s1*f1)+w1*(6*d1*s1+12*r1*e1-30*m1*l1);
    v3:=sqrt(v1*v1+v2*v2);
    v4:=sqrt(sqr(d1-4*f1*w1*w1)+4*e1*e1*w1*w1);               {v4=G(2f)}
    v5:=sqrt(sqr(d1-9*f1*w1*w1)+sqr(3*w1*e1));                {v5=G(3f)}
    v6:=sqr(OMD*(i-Ith))*v3/(24*d1*d1*v4*v5);
    v7:=20*ln(v6)/ln(10);
{Calculation of IMD/C}
    wr:=sqrt(e*Q/b);
    r2:=sqr(sqr(w1/wr))-0.5*sqr(w1/wr);
```

```
    r3:=h*w1*w1*w1/(e*wr*wr);
    r4:=sqrt(r2*r2+r3*r3);
    r5:=sqrt(sqr(1-w1*w1/wr/wr)+sqr(h*w1/e));
    r6:=sqrt(sqr(1-4*w1*w1/wr/wr)+sqr(2*h*w1/e));
    r7:=0.5*sqr(OMD)*r4/(r5*r6);
    r8:=20*ln(r7)/ln(10);
    writeln('f=',f2  ,'  ''value=',r8);
    f2:=f2+0.2e+09;
 until f2>7E+09;
end.
```

Outline of the program 'spectra'

This program calculates $S_{q_2}(\omega)$ and $S_{q_3}(\omega)$ of equations (5.35) and (5.36) and then takes the ratio $\frac{S_{q_2}(\omega)}{S_{q_1}(\omega)}$, $\frac{S_{q_3}(\omega)}{S_{q_1}(\omega)}$ and expresses them in decibels (dB). First, the laser parameters V, Tph (τ_{ph}) , Tsp (τ_{sp}), g, Gamma (Γ), beta (β), epsilon (ϵ), N_o, I_{th}, I_o are entered in the program as inputs. Q is the steady state photon density as defined in equation (3.8). a, b and c are the constants as defined in equation (B.5) and theta (θ), gamma1 (γ) are as defined in equation (B.8). The other constants (defined laser parameters) D, E, F3 (F), L, M, N, R, S and G4 (G) are as given in equation (B.13). For any particular laser, all the parameters are fixed. The only parameter can be varied is the bias current I_o.

The number of channels N_1, optical modulation depth (OMD) and the lower and upper frequency ranges f_1 and f_2 of the fundamental input spectrum are entered in the program as inputs. The fundamental output spectrum of the laser, as defined in equation (5.39), is $S_{q_1}(\omega) = \frac{N_1(OMD)^2(I_o-I_{th})^2}{4\delta f|G_1(0)|^2}$, which we consider as $\frac{K_1}{2\delta f}$ Where, $K_1 = \frac{N_1(OMD)^2(I_o-I_{th})^2}{2\delta f D^2}$, $G_1(0) = D$ and $\delta f = f_2 - f_1$. The spectrum $S_{q_1}(\omega)$ (two sided) of Fig 31 is defined in 'Function Sq' of the program. If a different shape of the spectrum is used it has to be defined properly in 'Function Sq'. 'Function convol2' calculates the convolution $[S_{q_1}(\omega) * S_{q_1}(\omega)]$ and 'Function convol3' calculates the convolution $[S_{q_1}(\omega) * S_{q_1}(\omega) * S_{q_1}(\omega)]$. Since the two sided spectrum $S_{q_1}(\omega)$ ranges from $-f_2$ to f_2, the convolution $[S_{q_1}(\omega) * S_{q_1}(\omega)]$ will range from $-2f_2$ to $2f_2$ and the double convolution $[S_{q_1}(\omega) * S_{q_1}(\omega) * S_{q_1}(\omega)]$ will range from $-3f_2$ to $3f_2$. These frequency ranges are defined properly in appropriate 'Function's. For example, the convolution $[S_{q_1}(\omega) * S_{q_1}(\omega)]$ of the spectrum of Fig 31 ranges from -1000 MHz to 1000 MHz and in 'Function convol2' we have set the discreate frequency range f_4 from -1002 to 1002. Similarly, in 'Function convol3' we set the frequency range K_2 from -1502 to 1502. For a spectrum with different frequency limits these ranges have to be changed. In both 'Function convol2' and 'Function convol3' T is the sampling interval which is needed for the discreate approximation of the continuous convolution.

Within the 'repeat' loop in the main program we defined G1 which is $|G_1(\omega)|^2$, the output-to-input linear transfer function of the laser. a2 is the quantity $|S_{q_2}(\omega)|$ and b3 is the quantity $|S_{q_3}(\omega)|$. a3 and b3 are the ratio $\frac{S_{q_2}(\omega)}{S_{q_1}(\omega)}$ and $\frac{S_{q_3}(\omega)}{S_{q_1}(\omega)}$ respectively.

```
program Spectra(input,output);
{Calculates intermodulation spectra}
var
  V,Tph,Tsp,g,Gamma,beta,epsilon,No,Ith,Io,Q:double;
  a,b,c,theta,gamma1,D,E,F3,L,M,N,R,S,G4,N1,OMD:double;
  f1,f2,df,K1,f,w,G1,G2,G3,a1,a2,a3,a4,b1,b2,b3,b4:double;

Function Sq(f:double):double;
  begin
     if (abs(f) >=50.0) and (abs(f) <=500.0) then Sq:=K1/(2*df)
     else
        Sq:=0;
  end;

Function convol2(f:double):double;
  const
     T:integer = 4;
  var
     f4: double;
     x:  double;
  begin
     x:=0;
     f4:=-1000-T/2;
     repeat
       x:=x+Sq(f4)*Sq(f-f4)*T;
       f4:=f4+T;
     until f4>1000+T/2;
     convol2:=x;
  end;

Function convol3(f:double):double;
  const
     T:integer = 4;
   Var
      k2:double;
      x:double;
    begin
      x:=0;
      k2:=-1500.0-T/2;
      repeat
         x:=x+convol2(K2)*Sq(f-k2)*T;
         k2:=k2+T;
         until k2>1500.0+T/2;
       convol3:=x;
    end;

BEGIN
  V:=1.44E-35;
  Tph:=2E-12;
  Tsp:=3.72E-09;
```

```
   g:=1E-12;
   Gamma:=0.646;
   beta:=1E-03;
   epsilon:=3.8E-23;
   No:=4.6E+24;
   Ith:=21E-03;                    {Ith = Threshold current}
   Io:=36.75E-03;                  {Io = Laser bias current}
   Q:=Gamma*Tph*(Io-Ith)/V;        {Q = Steady state photon density}
   a:=Gamma*(g*Q+beta/Tsp-epsilon*g*Q*Q);
   b:=Gamma*g*(1-2*epsilon*Q);
   c:=-epsilon*g*Gamma;
   theta:=b*b/(a*a*a)-c/(a*a);
   gamma1:=(2*b*c-b*b*b/a)/(a*a*a);     {gamma1 = defined const gamma}
   D:=V*(1/(Gamma*Tph)+1/(a*Tsp*Tph)-b*Q/(a*a*Tph*Tsp)+b*Gamma*beta*
      No/(a*a*Tsp*Tsp));
   E:=V*(1/Gamma+1/(a*Tsp)-b*Q/(a*a*Tph)+b*Gamma*beta*No/(a*a*Tsp)
      +1/(a*Tph));
   F3:=V/a;              {F3 = defined const F}
   L:=V*(b/(a*a*Tsp*Tph)-theta*Q/(Tsp*Tph)+theta*Gamma*beta*No/(Tsp*Tsp));
   M:=V*(b/(a*a*Tsp)+2*b/(a*a*Tph)+2*theta*Gamma*beta*No/Tsp-2*theta*Q/Tph);
   N:=b*V/(a*a);
   R:=V*(theta/(Tsp*Tph)+gamma1*Q/(Tsp*Tph)-gamma1*Gamma*beta*No/(Tsp*Tsp));
   S:=V*(theta/Tsp+3*theta/Tph+3*gamma1*Q/Tph-3*gamma1*Gamma*beta*No/Tsp);
   G4:=theta*V;    {G4 = defined const G}
   writeln('enter number of channels, OMD per carrier');
   readln(N1, OMD);
   writeln('lower and upper frequency limits of Sq1(w) in MHz');
   readln(f1, f2);
   df:= f2-f1;
   K1:=N1*sqr(OMD*15.75e-03)/(2*D*D);

   f:=50.0;
repeat
   w:=2*3.141592654*f*1e+06;
   G1:=sqr(D-w*w*F3)+sqr(w*E);              {G1= sqr(G1(w))}
   G2:=sqr(2*L-N*w*w)+sqr(M*w);             {G2= sqr(G2(w,w))}
   G3:=sqr(3*R-2*G*w*w)+sqr(2*S*w);         {G3=sqr(G3(w1,w2,w-w1-w2))}
   a1:=G2/(2*G1);
   a2:=a1*convol2(f);                       {a2=Sq2(w)}
   a3:=a2/Sq(f);                            {a3 =Sq2(w)/Sq1(w) }
   a4:=10*ln(a3)/ln(10);
   b1:=G3/(6*G1);
   b2:=b1*convol3(f);                       {b2 = Sq3(w)}
   b3:=b2/Sq(f);                            {b3 = Sq3(w)/Sq1(w) }
   b4:=10*ln(b3)/ln(10);
   writeln('at frequency =',f ,'s3=',a4);

   f:=f+50.0;
until f>500.0
END.
```

Bibliography

[1] R.Olshansky, P. Hill and V.Lanzisera,"High-speed InGaAsP Lasers for SCM Optical fiber systems". OPTOELECTRONICS-Devices and Technologies, vol.3, No.2, pp.143-153, Dec 1988.

[2] T.E.Darcie and G.E.Bodeep, "Lightwave Multichannel Analog AM Video Distribution Systems", ICC.1989, pp.32.4.1-32.4.4

[3] R.Olshansky, Vincent A. Lanzisera and P.M.Hill, "Subcarrier Multiplexing Lightwave Systems for Broadband Distribution", IEEE Journal of Lightwave Technology, vol.7,No.9, pp.13291342, Sept. 1989.

[4] W. I. Way, "Subcarrier Multiplexed Lightwave System Design Considerations for Subcriber Loop Applications", J. of Lightwave Technology, vol. 7, No. 11, pp. 1806-1818, Nov 1989.

[5] W.I.Way *et. al.*, "Application of Travelling-wave Laser Amplifier in Subcarrier Multiplexed Lightwave Systems", ICC'89, 32.2.1-32.2.9.

[6] T.K.Biswas and W.F.McGee, "Analytical Predictions of Intermodulation Noise of Semiconductor Laser Diode", Canadian Conference on Electrical and Computer Engineering, pp 23.4.1-23.4.4, Sept 1990.

[7] Herman Gysel, "Composite Triplebeat and Noise in a Fiber Optic Link Using Laser Diodes", 1988 NCTA Technical Papers, pp. 94-101.

[8] T.E.Darcie, J.Lipson, C.B.Roxlo and C.J.McGrath, "Fiber Optic Device Technology for Broadband Analog Video Systems", IEEE Lightwave Communication Systems, Vol.1, No.1, pp.46-52, Feb 1990.

[9] R. Olshansky, "Microwave Subcarrier Multiplexing: New Approach to Wideband Lightwave Systems", IEEE Circuits and Devices Magazine, Nov 1988, pp. 8-14.

[10] S. Huang *et. al.*, "Frequency-Dependent Distortions of Composite Triple Beat in Lightwave CATV Transmission Systems", IEEE J. on Selected Areas in Communications, vol. 8, No. 7, pp. 1365-1368, Sept 1990.

[11] W.I.Way *et. al.*, "Multichannel AM-VSB Television Signal Transmission Using an Erbium-Doped Optical Fiber Amplifier", IEEE Photonics Technology Letters, vol. 1, No. 10, pp. 343-345, Oct 1989.

[12] Y.Yamamoto, "AM and FM Quantum Noise in Semiconductor Lasers-Part I: Theoretical Analysis", IEEE J. of Quantum Electronics, vol. QE-19, No. 1, pp. 34-46, Jan 1983.

[13] Kristian Stubkjaer and Magnus Danielsen, "Nonlinearities of GaAlAs Lasers-Harmonic Distortion",IEEE Journal of Quantum Electronics, vol. QE-16, No.5,pp.531-537, May 1980.

[14] K.Y.Lau and A.Yariv, "Intermodulation distortion in a directly modulated semiconductor injection laser", Appl. Phys Lett. vol.45, pp.1034-1036, No. 10, Nov 1984.

[15] T.E.Darcie, R.S.Tucker and G.J.Sullivan,"Intermodulation and Harmonic Distortion in InGaAsP Lasers" Electron. Lett., vol.21, No.16, pp. 665-666, Aug 1985. and "Errata" Electron. Lett. vol.22, No.11, pp.619, May 1986.

[16] W.I.Way,"Large Signal Nonlinear Distortion Prediction for a Single-Mode Laser Diode Under Microwave Intensity Modulation". IEEE Journal of Lightwave Technology, vol. LT-5. No.3,pp.305-315, March 1987.

[17] Andreas Czylwik, "Nonlinear System Modeling of Semiconductor Lasers Based on Volterra Series", Journal of Optical Communications, 7(1986) 3, 104-114.

[18] John M. Senior, "Optical fiber Communications", London:Prentice-Hall International, Inc. 1985.

[19] Stewart E. Miller, and Ivan P. Kaminow, "Optical fiber Telecommunications II". New York: Academic Press, Inc. 1988.

[20] Michael K. Branoski, "Fundamentals of Optical fiber Communications", New York: Academic Press, Inc. 1981.

[21] Gred Keiser, "Optical Fiber Communications", New York: McGraw-Hill Inc. 1983.

[22] H.Kressel and J.K.Bulter, "Semiconductor Lasers and Heterojunction LED's", New York: Academic Press 1977.

[23] R.S.Tucker, D.J.Pope, "Circuit Modelling of the Effect of Diffusion on Damping in a Narrow-Stripe Semiconductor Laser", IEEE J.Quantum Electron., Vol.QE-19, No.7, pp.1179-1183, July 1983.

[24] C. Harder, J. Katz, S. Margalit, J. Shacham and A. Yariv, " Noise Equivalent Circuit of a Semiconductor Laser Diode", IEEE J. of Quantum Electronics, vol. QE-18, No. 3, pp. 333-337, March 1982.

[25] Rodney S.Tucker, "High-Frequency Characteristics of Directly Modulated InGaAsP Ridge Waveguide and Buried Heterostructure Lasers", IEEE Journal of Lightwave technology, vol.LT-2, No.4, pp.385-393, Aug 1984.

[26] P. Neusy, W.F. McGee, "Effects of Laser Nonlinearities on TV Distribution using Subcarrier Multiplexing". Canadian Conference on Electrical and Computer Engineering, vol.2, pp. 833-836, Sept 1989.

[27] S.Narayanan, "Transistor Distortion Analysis Using Volterra Series Representation",Bell system technical journal, May-June 1967, pp.991-1024.

[28] J.Waddington and F.Fallside, "Analysis of Nonlinear Differential Equations by the Volterra Series", Int.J.Control, 1966, Vol.3, No.1,pp.1-15.

[29] S.Benedetto, E.Biglieri and R.Daffara, "Modelling and Performance Evaluation of Nonlinear Satellite Links - A Volterra Series Approach", IEEE Transactions on Aerospace and Electronic Systems, Vol.AES-15,No.4, pp.494-507, July 1979.

[30] Edward Bedrosian and Stephen O. Rice, "The Output Properties of Volterra Systems(Nonlinear Systems with Memory) Driven by Harmonic and Gaussian Inputs". Proceedings of the IEEE, vol.59, No.12,pp.1688-1707, Dec 1971.

[31] M.Schetzen,"The Volterra and Wiener Theories of Nonlinear Systems", New York: Wiley 1980.

[32] S.J.Wang and N.K.Dutta, "Intermodulation and Harmonic Distortion in GaInAsP Distributed Feedback Lasers", Electronics Letters, vol. 25, No. 13, pp. 850-852, June 1989.

[33] S.J. wang *et. al.*, "Temperature Dependence of The Second Harmonic Distortion of Buried Heterostructure DFB Lasers", Electronics Letters, vol. 26, No. 14, pp. 1095-1097, July 1990.

[34] B.P.Lathi, "Modern Digital and Analog Communication Systems", New York: CBS College Publishing, 1983.

[35] P.C.Neusy, "Subcarrier Multiplexing for Fiber-Based Video Distribution: A Performance Study", M.A.Sc. thesis, Dept. of Electrical Engineering, University of Ottawa, June 1990.

[36] Frederick H.Moon, "Distortion in CATV Signals - An Overview", TENCON 1987, Seoul pp.38.7.1-38.7.6